

DEVELOPMENT OF NEXT GENERATION CARPET
BACKINGS FOR FACILE RECYCLABILITY

A Thesis
Presented to
The Academic Faculty

By

Anthony Cascio

In Partial Fulfillment
of the Requirements for the Degree
Master of Science in Polymers in the
School of Polymer, Textile and Fiber Engineering

Georgia Institute of Technology

August 2006

DEVELOPMENT OF NEXT GENERATION CARPET
BACKINGS FOR FACILE RECYCLABILITY

Approved by:

Dr. Fred L. Cook, Advisor
School of Polymer, Textile and Fiber
Engineering
Georgia Institute of Technology

Dr. Mary Lynn Realff
School of Polymer, Textile and Fiber
Engineering
Georgia Institute of Technology

Dr. John D. Muzzy
School of Chemical and Biomolecular
Engineering
Georgia Institute of Technology

Date Approved: June 27, 2006

Dr. Radhakrishnaiah Parachuru
School of Polymer, Textile and Fiber
Engineering
Georgia Institute of Technology

ACKNOWLEDGEMENTS

The research could not have been possible without the guidance and support from my thesis advisor, Dr. Fred Cook, and thesis committee members Dr. John Muzzy, Dr. Radhakrishnaiah Parachuru and Dr. Mary Lynn Realff. I would like to thank David Hartman from Owens Corning Corp., Greg Fowler and Allen Battenhoff from Shaw Industries, Inc., and Rich Simmons from Georgia Composites, Inc., for their time, use of facilities, and support towards my research. I am also grateful to the CCACTI organization that funded my research.

Thanks also go to undergraduate students Chuck Kahng and Joey Yu who assisted me in conducting experiments and research toward the thesis goals. Finally I want to thank my family, who have supported and encouraged me through my undergraduate and graduate years here at Georgia Tech.

TABLE OF CONTENTS

ACKNOWLEDGEMENTS	iii
LIST OF TABLES	vii
LIST OF FIGURES	viii
LIST OF SYMBOLS	xi
SUMMARY	xii
CHAPTER 1: OVERVIEW	1
CHAPTER 2: INTRODUCTION AND LITERARY SEARCH	3
2.1 The History of Carpet in the U. S.	3
2.1.1 Woven Carpet.....	3
2.1.2 Tufting as a Process	4
2.1.3 Tufted Carpet.....	5
2.2 Current Generic Broadloom Carpet Construction.....	6
2.2.1 Carpet Tufting Process.....	7
2.2.2 Carpet Dyeing Processes	8
2.2.3 Application of Latex and Secondary Backing	9
2.3 Post Consumer Carpet and Recycling	9
2.4 Current Carpet Recycling Methods	12
2.5 New Carpet Construction.....	13
CHAPTER 3: MECHANICAL AND THERMAL PROPERTIES OF DEVELOPED CARPET BACKINGS	17
3.1 Introduction of Carpet Components.....	18
3.1.1 Backings	18
3.1.2 Elvamide® Resins.....	19
3.2 Physical Characteristics of Materials.....	22
3.2.1 Breaking Strength	22
3.2.2 Delamination Strength	22
3.2.3 Air Permeability	23
3.2.4 Tuft Bind Strength	24
3.2.5 Microscopy.....	24
3.3 Thermal Characteristics of Materials.....	24
3.3.1 Radiant Panel Flammability Test	24
3.3.2 Ignition Characteristics	25
3.3.2.1 ASTM Method.....	25
3.3.2.2 British Standard Method.....	25
3.3.3 Thermal Transmittance	26

3.4 Results and Discussion.....	27
3.4.1 Tuft Bind Strengths	27
3.4.2 Delamination of Elvamide® Resin Film from Tufted Backings.....	28
3.4.3 Carpet Flammability Results	29
3.4.3.1 Radiant Panel Flammability Test Results	29
3.4.3.2 Hot Metal Nut Test Results	36
3.4.3.3 Discussion of Carpet Flammability Results.....	41
3.4.4 Tensile Properties of Carpets	42
3.4.5 Tensile Properties of Glass Mats	45

CHAPTER 4: ANALYZING THE TUFTING PROPERTIES OF PRIMARY CARPETBACKING SYSTEMS.....

4.1 Introduction.....	49
4.1.1 Composite Primary Backings	49
4.1.2 Composite Backing Break Down	49
4.2 Backing Modifications	53
4.2.1 Thermal Consolidation.....	53
4.2.2 Tufting of Backings	53
4.3 Qualitative and Quantitative Analyses of Composite Backing Carpets	54
4.3.1 Microscopy.....	54
4.3.2 Thermal Analysis	54
4.3.3 Developed Needle Force Test Apparatus.....	55
4.4 Results and Discussion.....	60
4.4.1 Tuft Measurements	60
4.4.1.1 Penetration Force Analysis	60
4.4.1.2 Withdrawal Force Analysis	63
4.4.1.3 Damage Determination.....	64
4.4.2 Glass Mat Analysis	66
4.4.3 Determination of Consolidation Parameters	69
4.4.3.1 Determination of Consolidation Time.....	69
4.4.3.2 Determination of Consolidation Temperature	73
4.4.4 Consolidation of Composite Backings <i>A</i> , <i>B</i> and <i>C</i>	77
4.4.5 Tuft Bind Strength Versus Yarn Denier of Mended Primary Backings	78
4.4.6 Validation of Test Method.....	80
4.4.6.1 Tuft Needle Penetration Force Correlated with Damaged Area.....	80
4.4.6.2 Tuft Bind Strength Versus Needle Withdrawal Force.....	80

CHAPTER 5: DYEING OF TUFTED CARPET AND COMPOSITE BACKINGS

5.1 Introduction to Dyeing	86
5.1.1 Atmospheric Batch Dyeing of Carpet	86
5.1.2 Continuous Dyeing of Carpet	87
5.1.3 Nylon and Acid Dyes.....	87
5.2 Tufted Carpet Dyeing Procedures.....	88

5.2.1 Beaker Dyeing of Developed Carpet Constructions	88
5.2.2 Pressure Dyeing of Developed Carpet Constructions	88
5.2.3 Pad-Steam Dyeing of Developed Carpet Constructions	89
5.3 Determination of Dye Exhaustion	91
5.3.1 Lambert-Beer Law	91
5.3.2 Spectrophotometer	92
5.4 Evaluation of Carpet Coloration by C. I. Acid Red 361 Dye	93
5.4.1 Determination of Absorptivity Constant, a	93
5.4.2 Exhaustion	97
5.5 Dyeing Results and Discussions	97
5.5.1 Batch Dyeing of Glass-Based Primary Carpet Backings	97
5.5.2 Exhaustion Behavior of Glass-Based Composite Primary Backings	98
5.5.3 Batch Dyeing of Tufted Carpet	98
5.5.3.1 Dye Exhaustion Versus Temperature	100
5.5.3.2 Plasticized Flow Of Elvamide® 8063 Resin Film	101
5.5.3.3 Tuft Bind Strengths of Dyed, Developed Carpets	105
5.5.3.4 Instantaneous Versus Rise To Boil Carpet Dyeing Techniques	107
5.5.3.5 Exhaust Batch Dyeing of Cut Pile, Glass Mat Backing Carpet ..	109
5.5.4 Continuous Dyeing of PP Backing Carpets	109
5.5.5 Dyeing of Carpet Made From Composite Backing <i>C</i>	117
5.5.6 Elvamide® 8063 Resin Versus Nylon 6 Resin	119
CHAPTER 6: CONCLUSIONS AND RECOMMENDATIONS	123
6.1 Conclusions of Glass Backing Carpet	123
6.1.1 Primary Backing Conclusions	123
6.1.2 Original Glass Carpet Conclusions	124
6.1.3 Composite Glass Backing Conclusions	126
6.1.3 Dyeing Conclusions	128
6.2 Conclusions of PP Carpet	130
6.3 Recommendations	131
6.3.1 Glass Carpet	131
6.3.2 PP Carpet	134
6.3.3 Future Work	135
REFERENCES	137

LIST OF TABLES

Table 3.1	Thermal Properties of DuPont Elvamide® Resins 8063 and 8201	21
Table 3.2	Tuft Bind Strengths of Loop Pile Carpet Samples.....	28
Table 3.3	Delamination Strength of Resin from Carpets	29
Table 3.4	Carpet Classification Based on Critical Radiant Flux.....	35
Table 3.5	Impregnation Factors for Glass Mats	43
Table 4.1	Glass Composite Backing Descriptions	50
Table 4.2	Standard Deviation of Needle Forces Versus Consolidation Temperature.....	75
Table 4.3	Needle Force Measurements of Consolidated Composite Backings <i>A, B, and C</i>	78

LIST OF FIGURES

Figure 2.1	Schematic of the Structure of Conventional Tufted Carpet.....	10
Figure 3.1	DSC of Elvamide® 8063	20
Figure 3.2	DSC of Elvamide® 8201	20
Figure 3.3	Schematic for Extrusion of Resin and Merger of Secondary Backing.....	21
Figure 3.4	Burn Times of Radiant Panel Flammability Samples.....	31
Figure 3.5	Burn Distances of Radiant Panel Flammability Samples	31
Figure 3.6	Critical Radiant Flux of Radiant Panel Flammability Samples.....	32
Figure 3.7	Rate of Burn of Radiant Panel Flammability Samples	32
Figure 3.8	Radiant Panel Flammability Carpet Test Samples.....	33
Figure 3.9	Burn Radiuses of Samples Using the Hot Metal Nut Method.....	37
Figure 3.10	Burn Rate of Samples using Hot Metal Nut Method	37
Figure 3.11	The Hot Metal Nut Test Samples	39
Figure 3.12	Microscopy Images at 4x Magnification of Hot Metal Nut Method Samples.....	40
Figure 3.13	Intrinsic Thermal Transmittance of Varying Glass Mats.....	43
Figure 3.14	Breaking Force of Carpet Made from the Glass Backing with Elvamide® 8063 Resin, Machine Direction	44
Figure 3.15	Breaking Force of Carpet Made from the Glass Backing with Elvamide® 8063 Resin, Cross Machine Direction	44
Figure 3.16	Breakage Force in Machine Direction of Glass Mats varying with Percent Binder, Weight, and Staple Length	46
Figure 3.17	Breakage Force in Cross Machine Direction of Glass Mats varying with Percent Binder, Weight, and Staple Length	46

Figure 4.1	Apparatus to Measure and Hold the Primary Carpet Backing along with the Tufting Needle (Not to Size)	56
Figure 4.2	Measurements of the Tufting Forces Acting on the Tufting Needle	59
Figure 4.3	Bare Needle Tufting Forces of Carpet Backings: Back Tuft	61
Figure 4.4	Bare Needle Tufting Forces of Carpet Backings: Face Tuft	61
Figure 4.5	Reductions in Tufting Forces From Initial Penetration and Second Penetration Cycles	65
Figure 4.6	Needle Penetration Forces of Bare Glass Mats	67
Figure 4.7	Needle Withdrawal Forces of Bare Glass Mats	67
Figure 4.8	DSC of Nylon 6 Film Removed from Backing 3893	70
Figure 4.9	Delamination Force of Nylon 6 Film from Glass Veil in Backing 3893	70
Figure 4.10	Microscopy Images of Backing 3893 at 4x Magnification After Several Consolidation Temperatures	72
Figure 4.11	Needle Penetration and Withdrawal Forces of Thermally Consolidated Backing C	74
Figure 4.12	Microscopy Images of Thermally Consolidated Backing C	75
Figure 4.13	Tuft Bind Strengths of Hand-Tufted Composite Glass Backings	79
Figure 4.14	Microscopy Images of Backings After Tufting Needle Penetration	81
Figure 4.15	Damaged Area on Backing Versus Reduction in Tuft Penetration	82
Figure 4.16	Tuft Bind Strength Versus Tuft Needle Withdrawal Force	84
Figure 4.17	Tuft Bind Strength Versus Tuft Needle Penetration Force	84
Figure 5.1	Simplified Schematic of the Spectrophotometer	94
Figure 5.2	Absorbance Versus Wavelength for C. I. Acid Red 361 Dye	96
Figure 5.3	Dye Concentrations Versus Absorbance for C.I. Acid Red 361 Dye	96
Figure 5.4	Images of Glass-Based Primary Carpet Backings	99

Figure 5.5	Dye Exhaustion Analyses of the Various Composite Glass Backings.....	99
Figure 5.6	Dyeing Analyses of C. I. Acid Red 361 Dye Applied to Cut Loop, PP Backing Carpet with 6 oz./yd. ² of Applied Elvamide® 8063 Resin	102
Figure 5.7	Microscopy Images of Dyed, Cut Pile, PP Carpet with 6 oz./yd. ² of Applied Elvamide® 8063 Resin at 4x Magnification.....	103
Figure 5.8	Tuft Bind Strengths of Dyed, Cut Pile, PP Carpet with 6 oz./yd. ² of Applied Elvamide® 8063 Resin Colored in an Instantaneous Exposure Mode	106
Figure 5.9	Tuft Bind Strengths of Dyed, Cut Pile, PP Carpet with 6 oz./yd. ² of Applied Elvamide® 8063 Resin Colored by Several Techniques	106
Figure 5.10	Tuft Bind Strengths of Dyed, Cut Pile, Bare Glass Mat Backing Carpets with 6 oz./yd. ² of Applied Elvamide® 8063 Resin Colored by Several Procedures	110
Figure 5.11	Microscopy Images of Dyed, Cut Pile, Bare Glass Mat Backing Carpets with 6 oz./yd. ² of Applied Elvamide® 8063 Resin at 4x Magnification	111
Figure 5.12	Tuft Bind Strengths of Cut Pile, PP Backing Carpet with 6 oz./yd. ² of Applied Elvamide® 8063 Resin Colored by Pad-Steam Process	113
Figure 5.13	Microscopy Images of Dyed, Cut Pile, PP Carpet with 6 oz./yd. ² of Applied Elvamide 8063 Resin at 4x Magnification.....	115
Figure 5.14	Tuft Bind Strengths of Dyed Consolidated Backing C and PP Backing Carpets.....	118
Figure 5.15	Tuft Bind Strengths of Cut Pile, Bare Glass Mat Carpets Consolidated with Applied Nylon 6 and Elvamide® 8063 Nylon Resins.....	121

LIST OF SYMBOLS

U_1	combined intrinsic thermal transmittance of the backing plus the air	27
P	power lost from the test plate	27
A	area of the test plate	27
T_P	test plate temperature	27
T_A	air temperature	27
U_2	intrinsic thermal transmittance of just the backing alone	27
U_{bp}	intrinsic thermal transmittance of the bare plate	27
D	percent difference between forces	57
F_0	first recorded cyclic force	57
F_n	next recorded cyclic force	57
A	absorbance of the dye liquor	91
a	absorptivity constant of the dye molecule	91
b	path length of the sample	91
c	concentration of the dye liquor	91
T	transmittance	93
P_o	power of the radiation before entering the sample	93
P	power of the radiation leaving the sample	93
% E	dye bath exhaustion	97
C_o	initial concentration of dye bath	97
C	concentration of dye bath at a desired time	97

SUMMARY

The current carpet construction is a sandwich composite containing both thermoplastic and thermoset polymeric components as well as calcium carbonate particles. Due to the combination of components used and its impact on separation schemes in recycling pathways, as well as on manufacturing processes, the current carpet construction leads to an abundant amount of solid waste entering landfills each year. The mass of post-consumer and manufacturing carpet waste entering U. S. landfills is ~4.5-5 billion pounds per year, or ~15-20 pounds per person. Of that total mass, only 150 million pounds of post consumer carpet are recycled each year due to the geographically-dilute nature of the post-consumer carpet waste stream and the preparation/recycling cost factors of the current generic broadloom construction [1, 2].

To combat these recycling problems, new carpet constructions were designed and developed to be easily recycled. The new broadloom carpet construction, according to industry constrictions, must maintain nearly all of the current carpet formation processes to minimize capital investment in converting existing manufacturing lines. The new construction must also at least meet the current construction's physical performance on the floor and overall cost characteristics.

The research focused on creating the next generation of broadloom carpet that consisted of backings made from either nonwoven glass mats or the traditional woven polypropylene (PP) primary backing. The developed carpet constructions, while still

utilizing the traditional nylon face yarn, substituted nylon resins for the conventional calcium carbonate-filled SBR latex to consolidate the final structures, lock in the nylon yarn tufts and incorporate the secondary backing.

On tufting the developed bare glass mat backing, fractured fiber “fly” was generated which posed a potential problem for plant workers handling and tufting the construction, thus supporting the need for entrapment of the glass component. In preliminary studies with bare glass mat and PP backing carpets, the flammability and mechanical properties of the alternative broadloom constructions were measured. With the flammability tests, the constructions based on the traditional primary PP backing gave good performances, while the glass based primary backing carpets performed below the PP backing carpets. The lower flammability results of the glass mat backing carpets were attributed to three causes: the high percentage of polymeric acrylic binder (~20% by weight) used to bind the glass nonwoven mat; the thermal transmittance characteristics of E-glass fiber; and the open structure of the nonwoven glass mat backing.

Mechanical tests of the developed carpet constructions revealed higher strength characteristics for the PP backing construction. The tuft bind strength of the straight loop pile, PP backing carpet peaked at 4.43 lbf. with 9 oz./yd.² of applied Elvamide® 8201 resin, while that of the bare glass mat backing carpet peaked at 4.17 lbf. with 6 oz./yd.² of applied Elvamide® 8063 resin. However, neither of the initial developed constructions reached the tuft bind strength of 7.6 lbf. exhibited by a similar, conventional straight-loop carpet construction.

The deficiencies in “fly” generation on tufting, flammability and mechanical properties exhibited by the bare glass mat backing carpet constructions were addressed by

the design of a series of composite glass backings made from a nonwoven glass mat core with: a lower percentage (~10%) of acrylic binder; encasement by nylon 6 layers (a film or nonwoven veils) on one or both sides of the core and the construction bound together by monofilament yarn stitching; and use of a smaller-diameter (12 microns), flexible E-glass fiber that was less susceptible to brittle fracture on tufting. Higher tufting needle forces of penetration were exhibited by the composite backings compared to the traditional woven PP tape primary backing. For the withdrawal force of the tufting needle from the glass composite backings, the results varied, with some composite constructions showing higher forces than the traditional PP primary backing and some lower. The composite glass/nylon backing constructions suffered more “hole damage” upon initial needle penetration than did the standard woven PP tape primary backing. The latter exhibited a loss of ~30% of cyclic needle penetration force and ~ 12% of cyclic needle withdrawal force. By contrast, the composite glass/nylon backings showed a loss of ~60-75% of needle cyclic penetration force and ~20-30% of needle cyclic withdrawal force.

Dyeing of the new carpet constructions by a simulated industrial exhaust batch process showed that for any construction containing a resin layer, as the temperature of the dyebath increased above 80°C or the time spent at the dyeing hold temperature was increased, the tuft bind strength increased over un-dyed carpet. When the developed carpet constructions underwent a pad-steam dyeing process, as long as the dye pad bath was at a temperature >65°C and the padded carpet was steamed for at least 4 minutes, the tuft bind strength increased. In summary, dyeing of the developed carpet constructions

under industrial process conditions and after the application of the resin resulted in increased tuft bind strengths.

The increase in the tuft bind strength was attributed to water-induced plasticized flow of the nylon resin film at higher dyeing temperatures. Plasticized flow is the induction/onset of segmental mobility of polymer chains in the amorphous (unordered) regions of the solid-state structure [3]. Through aqueous dyeing, water entered the nylon resin film in the amorphous regions, breaking the hydrogen bonds between nylon polymer chains. The breakage of these hydrogen bonds caused the free volume of the polymer network to increase and the resulting wet glass transition temperature to lower. When less-crystalline Elvamide® nylon copolymer comprised the resin layer, the higher the extent of induced plasticized flow, the greater the degree of curling and loss of dimensional stability observed in the dyed carpet samples. When more-crystalline nylon 6 resin replaced the Elvamide®, no curling was observed under the dyeing conditions.

CHAPTER 1

OVERVIEW

The overall goal of the research was to develop the next generation, generic construction of broadloom carpet that will compete on both a performance and cost basis with the current construction while avoiding the major recycling disadvantages of the latter. The new construction was designed to maintain nearly all of the current carpet formation processes to minimize capital investment in converting existing manufacturing lines. A major industry constriction was that the new construction must at least meet the current construction's physical performance on the floor and overall cost characteristics.

The work related to this goal is presented in Chapters 3, 4, and 5. In Chapter 3, the alternative broadloom carpet constructions, made from either the traditional PP primary backing or a bare nonwoven glass mat, were tested for their flammability parameters as well as their mechanical properties. The flammability tests that were conducted were the Radiant Panel Flammability Test and the Hot Metal Nut Test. For the study of mechanical properties, the delamination force to separate the nylon resin layer from the primary backing was measured along with the tuft bind strength and tensile properties of both the carpet and the backing samples.

Based on the results presented in Chapter 3, several glass composite backings were designed with the intent to overcome and improve upon defects or problems

associated with the initial bare nonwoven glass mat backing utilized in the research. In Chapter 4, the newly designed backings were tested in order to gain information of whether the overall design changes to the glass backings displayed any improvements. To test these new primary backings without undergoing the tufting process, a test procedure was developed which characterized the backings based on the penetration of a tufting needle into the backing, the resistance of the needle being withdrawn from the backing, and the subsequent damage caused to the backing by the tufting process. To test the effects of yarns used in tufting, yarns of varying denier were mended into the backings and the tuft bind strengths were measured. Also in this chapter, since the new backing designs utilized pre-formed nylon layer components, i.e., a nonwoven or a film, the effects of carrying the structures through a preliminary thermal consolidation stage were studied. The data presented in Chapter 4 led to the actual pilot machine tufting of two composite glass primary backings.

In Chapter 5, the dyeing of the composite backings and the carpet samples were studied. The samples were submitted to several simulated dyeing processes in which dyeing parameters (duration, temperature, etc.) were varied. Dyed samples were then analyzed to approach an ideal dyeing situation based on dye exhaustion and tuft bind strength for the carpet samples. Finally, the research was summarized and conclusions and recommendations were presented in Chapter 6.

CHAPTER 2

INTRODUCTION AND LITERARY SEARCH

2.1 The History of Carpet in the U. S.

2.1.1 Woven Carpet

Not until the mid-eighteenth century did the hand-woven carpet industry experience revolutionary technological advancement with the invention of the power loom for weaving carpets made possible by Erasmus Bigelow [4, 5]. His steam powered loom doubled carpet production in the first year after its creation and tripled it by 1850 [6]. The carpet industry in the U. S. began in 1879 with the first woven carpet mill in Philadelphia, PA.

In 1878, four brothers from the Shuttleworth family brought 14 second hand looms from England to Amsterdam, New York. By 1908, the firm introduced a new carpet, Karnak [4, 7]. The introduction of this carpet became such a success that weavers worked four and five years without changing either the color or pattern on their looms [7]. In 1920, the brothers merged with the nearby companies of McCleary, Wallin and Crouse to form Mohawk Carpet Mills, Inc, today the world's largest floor covering manufacturer and distributor [7]. Shaw Industries, Inc. of Dalton, GA is the largest carpet manufacturer in the world.

2.1.2 Tufting as a Process

The process of tufting yarn loops into a flat fabric base was begun around the turn of the century by a Dalton, GA woman named Catherine Evans Whitener. In trying to recreate a quilt pattern, she sewed thick cotton yarns with a running stitch into unbleached muslin, and then clipped the ends so they would fluff out [4]. Catherine's sewing process later became known as tufting. The unique quilts, eventually dubbed chenille bedspreads, generated sufficient demand that they led to the creation of a small cottage business, and Catherine sold her first bedspread in 1900 at a then-lofty price of \$2.50. Soon, other Dalton area women and their entire families were working hard to hand-tuft the spreads for 10 to 25 cents per unit. Through the early twentieth century, the Dalton area struggled so much with the existing cotton mills and steel manufacturing plants that the growing chenille bedspread manufacturing industry played a large role in helping the local families survive the depression [4, 8].

With all these families and emerging companies creating chenille bedspreads, by the 1930's more than 10,000 employees were producing tufted bedspreads in the Dalton area, all by hand. Keeping up with the exponentially-increasing demand for chenille bedspreads led to the development of the first mechanized tufting machine, credited to Glen Looper Foundry of Dalton. The new mechanized tufter used a modified single needle commercial Singer sewing machine that would tuft the thick yarn into unbleached muslin without tearing the fabric, and containing an attached knife that would cut the loop [4, 8]. The machine, dramatically increasing the production rate of the bedspreads, produced 99% of all tufted bedspreads by 1941 [8]. Machines quickly developed into

four, then eight, then twenty-four and more needles to make the parallel rows of tufting known as chenille [4].

2.1.3 Tufted Carpet

Not until after World War II did the carpet industry experience a tremendous expansion due to the desire for color, beauty and aesthetics in the U. S. populace that only a soft, fiber-based floor covering could generate. First, the government allowed the E. I. DuPont Co. to re-introduce nylon 6,6 fiber products back into the U. S. marketplace, it having commandeered all nylon production for war needs from 1941-5. Nylon from its introduction was much cheaper than the preferred carpet fiber at the time, wool, and had vastly superior physical, wear and flammability properties than the commodity carpet fiber, cotton. At this same time, it was found that carpets could be made more cheaply by tufting rather weaving, and that they offered improved aesthetic properties [4, 8]. In looking for experienced tufters, entrepreneur carpet manufacturers looked to Dalton, GA and the chenille bedspread industry. Building on the industrial platform, infrastructure and trained workers that the chenille bedspread industry provided, the machine tufted carpet industry grew at an extremely rapid rate in the 1950-70 period.

Machinery was developed for making tufted chenille throw rugs, and over time this allowed for the creation of larger rugs and eventually broadloom carpet. At the same time, machinery changed and developments of new fibers accelerated the growth of broadloom carpet [4, 8]. “Until about 1954, cotton was virtually the only fiber used in tufted products. Wool and manmade fibers (polyester, nylon, rayon, and acrylics) were gradually introduced by textile men in Dalton [4].” Nylon, first introduced in 1947, grew

steadily to dominate the market, followed by polyester in 1965 and later the olefin fiber, polypropylene [4]. The use of synthetic fibers allowed for a more economical carpet to be produced with more durable and luxurious properties.

The tufted carpet industry is today a vital part of Georgia's economy. To quote, "Georgia's carpet manufacturers are responsible for 74 percent of total U.S. carpet production, and 44 percent of world carpet production. Moreover, 80% of the U.S. carpet market is supplied by mills located within a 65-mile radius of Dalton, including Whitfield, Gordon, Catoosa, Murray, and Bartow counties. Georgia's 174 carpet manufacturing plants employ over 50,000 people and indirectly provide for over 30,000 additional employees *via* their suppliers. Finally, over 75 percent of the yarn used by the carpet industry is produced in Georgia [8]."

2.2 Current Generic Broadloom Carpet Construction

Today estimates show that over 90% of wall-to-wall broadloom carpet is tufted in the U. S. (over 1.3 million square meters [9, 10]), leaving an estimate of 10% woven carpet produce (89 thousand square meters [9]). The current tufted carpet construction is a "sandwich" composite containing both thermoplastic and thermoset components. Thermoplastics are polymers that can be processed repeatedly by cyclic heating and cooling. A thermoset polymer, however, once formed cannot be re-melted and processed again [11]. In a typical broadloom carpet, approximately 50% by weight of the construction is face fiber yarns, most often either nylon 6 or 6,6 (~80% of production, [12]). Today, nylon carpet production is ~evenly divided between the 6 and 6,6 varieties. The remaining ~20% of U. S. carpet production contains polyester, polypropylene or

wool (woven only) are used, depending on the end use and aesthetic preferences. The carpet also contains ~10% polypropylene tape/fiber contained in the primary and secondary backings [12]. A typical primary backing in which yarn is tufted into consists of a woven polypropylene tape that has 15 picks per inch. The main purpose of the primary backing is to hold the tufted yarns during the carpet manufacturing process, giving the structure initial three-dimensional stability. The secondary backing, typically a polypropylene scrim, serves to enhance dimensional stability, strength, and stretch resistance of the final carpet, and as an attachment layer of the carpet to the floor via tack strips around the edges of the room [13-16]. A 9% by weight styrene-butadiene rubber (SBR) latex adhesive, filled at a 35% by weight level with powdered calcium carbonate, is applied as a water-based foam to the tufted back side of the primary backing, i.e., the side opposite that of the face yarn tufts [12]. The latex adheres the secondary backing to the tufted carpet and “locks” the tufts into the overall construction [13-16].

2.2.1 Carpet Tufting Process

Typical broadloom carpet manufacturing begins with the tufting of the face yarns into the primary backing. Tufted carpet is produced on machines similar to sewing machines in which several hundred needles stitch hundreds of rows of pile yarn through the primary backing forming the tufts of one of two types. If the penetrating yarn is caught by loopers and pulled through the primary backing to a set length, the construction is called loop-pile carpet. If in addition the tufts are cut at their maximum length blades that operate in tandem with the loopers, the construction is termed cut-pile carpet [13]. The tufted yarns can vary in fiber type, denier, ply, twist, nature (e.g., staple or bulk

continuous filament, or BCF) and pretreatments. Depending on the desired effect, several different yarns can be used to tuft a single broadloom style of carpet, such as denier and ply to give a specific texture. The tufting needle bars can move horizontally to achieve patterns when using different predyed yarns, or remain stationary to give a straight loop carpet.

2.2.2 Carpet Dyeing Processes

Once the primary backing has been tufted, the “greige” broadloom carpet is today most often colored via a continuous dyeing process. If the yarns used are not predyed, the open-width carpet is fed through a Kuester’s Fluid Dyer® applicator which distributes dye liquor through a slot and uniformly across the width of the pile surface via a metering pump arrangement [17]. If nylon 6 or 6,6 face yarn is used in the construction, then the dye liquor will likely contain colorants in the Colour Index Acid Dye Class [17-19].

Once the dye has been applied to the yarn, the carpet is then fed through a festoon steamer fed by saturated steam (~220F) to mass transport and “fix” the dye to the fibers. The steaming process lasts long enough to effect complete penetration of the dye into the fibers and throughout the carpet face structure (achieving side-to-side and end-to-end “level”), usually accomplished in a 2.5-3 minute time period because if steaming prolonged, damage to the carpet, set pile deformation, can result [17, 19]. After being steamed, the carpet goes through several washing baths to remove unfixed dye. If desired, stain blocking, fluorocarbon, and other finishing treatments are generally applied

wet-on-wet as the carpet exits the dye line washers [13, 17]. The carpet is then carried through a final wash and dried in preparation for the latex application.

2.2.3 Application of Latex and Secondary Backing

As the final step in manufacturing, the dyed/dried carpet is fed through a foam latex applicator to apply SBR latex filled with powdered calcium carbonate to the non-pile side (back) of the primary backing and “back-tufts” of yarn. The PP scrim secondary backing is then added to the carpet in the merge to form the final “sandwich” composite of the generic construction. The carpet then proceeds through several heating zones to cure the latex and insure the binding of the secondary backing to the primary backing and the “lock-in” of the back-tufts of yarn. Once the carpet has been cured, it is inspected for color and construction quality assurance, cut to the desired length, rolled, packaged and shipped. A cross section of completed carpet manufactured by the conventional process is seen in Figure 2.1.

2.3 Post Consumer Carpet and Recycling

The Carpet America Recovery Effort (CARE) reports show that the annual amount of carpet being placed in landfills each year is increasing [20-22]. Projected data estimates 4.5 to 5 billion pounds of post consumer carpet placed in U. S. landfills each year [2, 20-22]. Of that volume, only a small fraction is being recycled, around 150 million pounds per year [2].

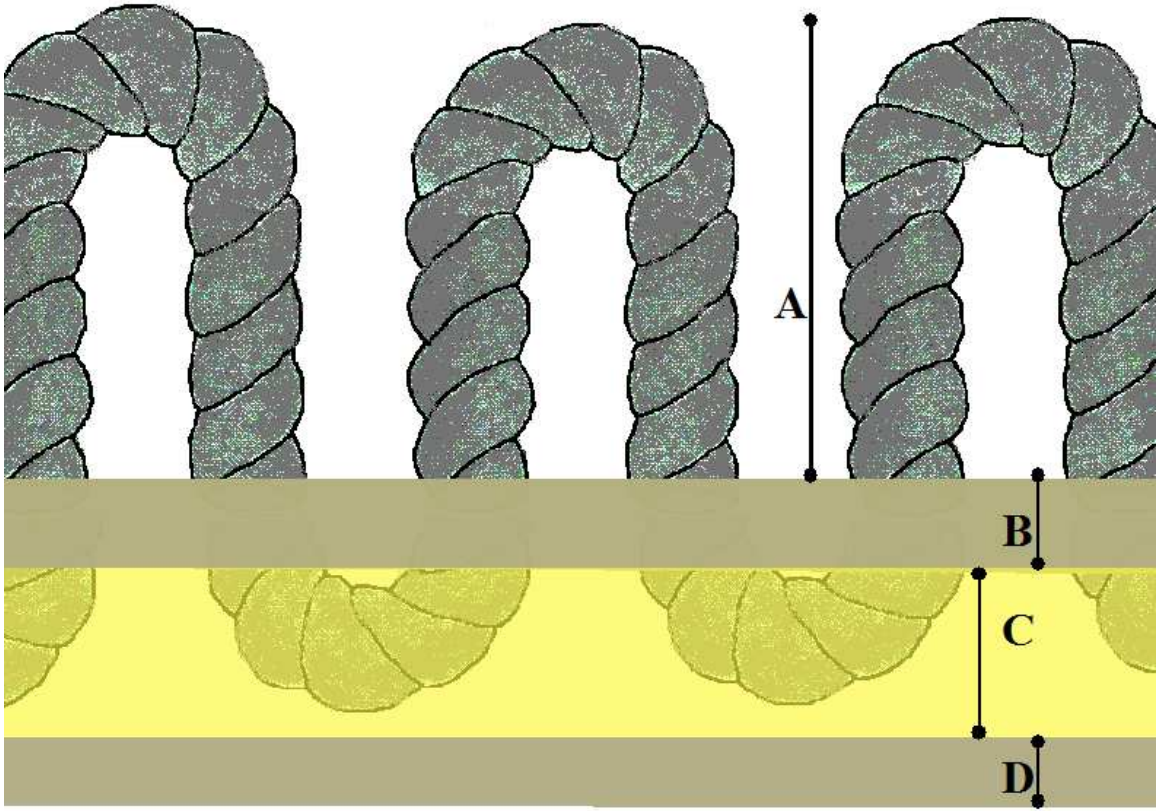


Figure 2.1: Schematic of the Structure of Conventional Tufted Carpet. **A** is the face tuft pile height, **B** is the PP primary backing, **C** is the calcium carbonate-filled SBR latex and **D** is the PP secondary backing.

To find a solution to this problem, a Memorandum of Understanding for Carpet Stewardship was created between a group of carpet companies represented by CRI/CARE and 17 states located mainly in the Upper Midwest and Northeast for the following goals to be met by 2012: Reuse 3-5% and recycle 20-25% of generated post consumer carpet [23]. With the deployment of these goals, the amount of carpet annually entering U. S. landfills will be reduced. However, the general problem of post consumer carpet disposal in the U. S. will still persist if a revolutionary solution cannot be found [23].

One of the key limiting factors in carpet recycling is the effective design and development of reverse production systems for collection and processing. A reverse production system can be comprised of chemical and material recycling functional elements [1]. Companies around the world are increasingly developing programs to take back post-consumer products for reuse, remanufacture, or recycling, due mainly to the adoption of "Extended Producer Responsibility" (EPR) policies in the leading industrialized countries. However, the U.S. remains unique among the industrialized countries in not having any national EPR mandates [24]. Companies such as Milliken Carpet, LaGrange, GA and Interface, Inc., Atlanta, GA have direct carpet reuse programs in which old carpet tiles are cleaned and refurbished [25]. Collins & Aikman Floorcoverings Inc. in Dalton, Georgia takes old carpet tiles with polyvinyl chloride (PVC) backing and extrudes it to produce new, 100 % recycled-content secondary backings for new carpet [26]. Other companies such as Atlanta-based Nycore, Inc. recycles post-consumer carpet into wood-replacement building materials, and Tie Tek,

LLC located in Houston manufactures railroad ties that contain used carpet materials [27].

2.4 Current Carpet Recycling Methods

The thermoplastic components of tufted carpet (nylon, polyester, or polypropylene face fiber, polypropylene primary and secondary backings) are easily recycled. However, they must first be separated and removed from the thermoset component of the conventional construction (SBR latex filled with calcium carbonate) [13, 28]. The thermoset component poses severe problems to recycling schemes, since no easy, economical pathway exists to fully separate the latex/filler from the construction so that the nylon and other polymers can be melted and extruded to new carpet fibers or other added-value products [13, 28].

The current construction is a major impediment to post-consumer carpet recycling into added-value products. The rigorous processes necessary to shred/grind/cut the composite to facilitate post-processing and/or component separation schemes are prohibitively expensive, allowing only components of carpets to be recycled (28, 29). The filled SBR latex is often mechanically pulverized, separated from the residual nylon/PP fiber mix and landfilled or incinerated. In recycling the thermoplastic components of the carpet, there are several methods which include reactive extrusion of the nylon face fiber [29, 30], depolymerization or conversion of thermoplastics [12, 31, 32], or mechanical separation of the face yarn and backings into their original materials [33]. Another option with post consumer carpet is utilization of the carpet fibers as reinforcement in concrete and soil. Tests show that with just a small percentage of fibers

for reinforcement, both compressive and tensile properties of concrete were increased [34]. Each of these processes still do not allow for 100% recycling of the carpet mass.

2.5 New Carpet Construction

To combat the recycling problems presented by the current generic carpet construction, new ones were designed and fabricated that were easily recycled. The next-generation broadloom carpet construction, according to industry constrictions, must be designed to maintain nearly all of the current broadloom generic carpet formation processes to minimize capital investment in converting existing manufacturing lines. The new construction must also at least meet the current construction's physical performance on the floor and overall cost of production characteristics. The research focused on creating the next generation of carpet constructions that consisted of primary backings made from nonwoven glass mats or the traditional woven polypropylene primary backing and tufted nylon face yarns. The filled thermoset SBR latex was eliminated from the carpet construction in lieu nylon resins to lock in the nylon yarn tufts and secure the secondary backing.

Woven PP tape was still used as one choice for the primary backing in the new carpet constructions, not only for its proven tufting properties and industrial acceptance but also because an extrusion-recycling scheme has been developed between nylon and PP melts. When melted, nylon and PP do not mix and bond well together without the use of a compatibilizer. In experiments conducted, the research showed that by blending the polymer melts with the compatibilizer maleated polypropylene, the tensile strength achieved of its extruded components were the same or higher than the tensile strength of

polypropylene [35, 36]. If desired, chopped glass fibers can also be added to the maleated PP, compatible PP-nylon melts for reinforcement [36].

Another recycling scheme could be employed if the final optimized construction incorporates only nylon and PP. Following the shredding/grinding of the composite carpet, a physical separation scheme utilizing the density differences between the two materials (PP = ~ 0.9 g/cc, nylon = ~ 1.2 g/cc) similar to that now utilized by the DuPont Co. in its post consumer carpet recycling scheme can be used to isolate the two material flow streams [36]. The isolated nylon and PP can then be re-extruded into products (new fiber, molding resin pellets, etc.).

E-glass fiber from Owens Corning's Advantex® line was chosen as an alternative primary carpet backing material not only for its easily-recycled configuration, but also for its improved dimensional stability over PP. Commodity fiber glass is also in the same approximate price range as PP fiber. The first advantage of the glass backing was its stability in wet dyeing/finishing processes. With the PP backing, the width of the conventional construction tends to deviate during wet processing due to the PP instability and tendency to shrink/relax under steam conditions, requiring wider lengths of PP to form a constant carpet width. Once the carpet is manufactured, the excess strips beyond the standard 12 or 15 foot width, called the selvedge, is cut off each width edge and land filled. Selvedge width usually varies from 1-3 inches on each side of the completed carpet, and alone contributes an estimated 40 M lbs./year of baled manufacturing waste to the Whitfield County, GA landfill. Since the glass fiber is impervious to water and steam, the nonwoven mat primary backing made from it should not deviate in its width during wet processing, potentially resulting in less waste in the carpet manufacturing process.

The other stability benefit of glass addresses installed carpet “creeping” over time on the floor. After stretching the traditional carpet in the installation process, the PP backing often relaxes/creeps, causing the carpet surface to become uneven. With the higher strength and rigid nature of glass compared to polymeric PP fiber, less “creep” with time of the glass-based carpet after stretching should lead to improved floor stability.

For recovery of post-consumer, glass-based carpets, a typical nitrogen-blanketed, melt zone, porous belt process can be utilized to melt the nylon face yarns and resin components (T_m 's 176-260°C) from the glass-based backings ($T_m > 650^\circ\text{C}$) [36]. The nylon melt stream, with added carbon black to generate a uniform color, can then be re-extruded into products (new fiber, RIM articles, molding resin pellets, etc.). The glass component exiting the process can either be re-melted and extruded into fibers for recycled products, or garneted/shredded and reformed directly into new fabric products (carpet backings, glass mats for composites, etc.) [36]. With glass-based carpet, the entire carpet can also be chopped up and melt extruded into molds to directly produce glass reinforced nylon composite structures [36-38].

Traditionally, nonwoven primary backings are not used in manufacturing broadloom carpet [13]. During the tufting process, nonwoven primary backings tend to scissor/rip, resulting in the partial two-dimensional failure of the backing, and the potentially generate particle “fly” due to brittle fracture of the fibers. Other problems such as the tufts become easily removed and a severe loss of tensile strength in the machine and cross machine direction have been linked to nonwoven primary backings. Nonwoven backing layers are used in carpet tiles and automotive carpets; however,

seldom are nonwoven primary backings carried through the severe tufting process [39-41], and woven PP tape is still the choice for primary backing choice for conventional tufted broadloom carpet. Despite these limitations and for economic and strength reasons, an acrylic-bound, nonwoven glass primary backing was chosen as the initial candidate for the new carpet constructions.

CHAPTER 3

MECHANICAL AND THERMAL PROPERTIES OF DEVELOPED CARPET BACKINGS

After the first stage of prototype backings (bare glass mat) and standard PP woven backing went through the tufting process and subsequent nylon copolymer resin application, the completed carpets underwent mechanical and flammability tests. The mechanical tests were used to characterize improvements found in the manufacturing process. With 24 total variations of the developed carpets, 12 for the bare glass mat construction and 12 for the PolyBac® polypropylene (PP) construction, the resulting data was vital in optimizing the glass-based backing and the performance properties of all the completed carpets.

Flammability tests, which were conducted at Shaw Ind., Dalton, GA and Georgia Tech, also aided in the elimination of certain carpet constructions. The flammability tests held a higher level of importance in timing of the research project, since if a carpet construction achieved a poor flammability rating, the proposed line could be eliminated from consideration, negating any further mechanical testing of that construction.

3.1 Introduction of Carpet Components

3.1.1 Backings

Two primary backings were used to make the first prototype carpets. The first primary backing was a BP polypropylene (PP) based product, PolyBac® 2205. PolyBac® 2205 was a 15 pick per inch woven PP tape (both warp and fill directions) primary carpet backing that will henceforth be referred to as the “PP backing.” A PP backing of this type is commonly used as the primary backing for yarn tufting in the manufacture of broadloom carpet.

The second primary backing was a bare, non-woven glass mat provided by Owens-Corning Fiberglass. The glass mat was based on extruded, 16 µm. E-glass filaments from the company’s Advantex© line of products that were chopped into one inch staple lengths. The staple glass fibers were then converted into the nonwoven glass mat via a standard wet-laid process [42]. To bind the glass mat, a 20% by weight polymeric acrylic binder of proprietary composition was applied to the construction and cured [42].

In conjunction with the GIT research team, BP Amoco tufted each primary backing, producing both straight and cut loop carpet samples. Yarn used to produce the straight loop carpets was predyed a wine shade, while the yarn for the cut loop carpets was undyed (white). Once tufted, Elvamide® resin was applied continuously at various loadings to the backs of the carpets via a melt slot extruder to lock in the tufts and consolidate the carpets.

In part of the lengths of primary backing constructions, a secondary backing was also applied in the carpet resin consolidation step to ascertain the ability of the nylon

copolymer to properly bind and lock the backing into the overall construction. The secondary backing was again a BP Amoco Polybac© PP product, consisting of a five pick per inch woven construction with PP tape in the warp direction and a staple PP yarn used as the filling.

3.1.2 Elvamide® Resins

To lock the tufts into the primary backing and to replicate the role of calcium carbonate-filled SBR latex in the conventional carpet construction, E. I. DuPont's Elvamide® line of multipolymer resins was used [43]. The two sub-lines of resins employed in the initial trials were 8063 and 8201, both of which were copolymers of nylon 6 and nylon 6,6. DuPont representatives indicated that Elvamide® 8201 also contained a third monomer of proprietary nature. Although the two resins did have slightly different mechanical properties, the main difference was in their thermal properties (see Figure 3.1, Figure 3.2, and Table 3.1). Elvamide® resins were used because they are both melt compatible with nylon 6 and nylon 6,6, which is important to the projected carpet recycling schemes detailed in Section 2.5.

The resins were applied at BP Amoco by means of a slot melt extruder with a dye temperature of 280°C (535°F), a die width of 10 mm, a nip pressure of 20 psi and a linear line speed of 10.6 m/min. (35 ft/min.). Once the resin extrusion occurred, the secondary backing was applied at the resin-tufted primary backing merge zone and while passing over a cooling drum. The application process for the resin and the PP secondary backing to the tufted primary backing is pictured in Figure 3.3.

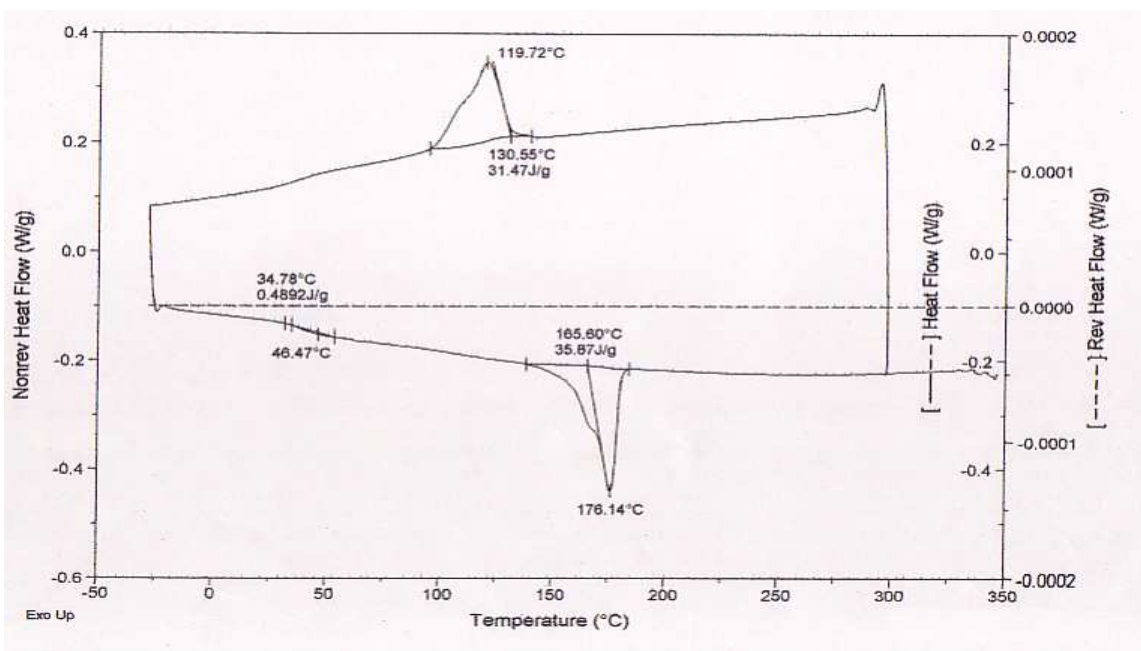


Figure 3.1: DSC of Elvamide® 8063.

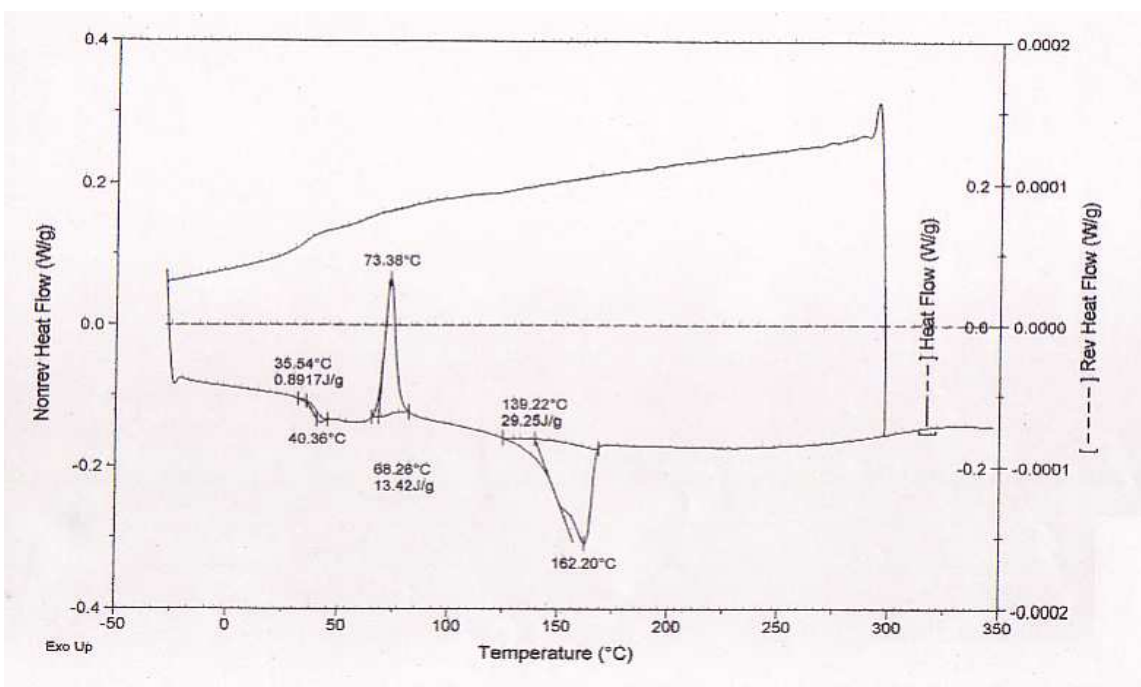


Figure 3.2: DSC of Elvamide® 8201.

Table 3.1: Thermal Properties of DuPont Elvamide® Resins 8063 and 8201.

Resin	Thermal Properties		
	Heat of Melting (J/g)	Melt Temperature (°C)	Crystallization Temperature (°C)
Elvamide® 8063	36	176	120
Elvamide® 8201	29	162	74

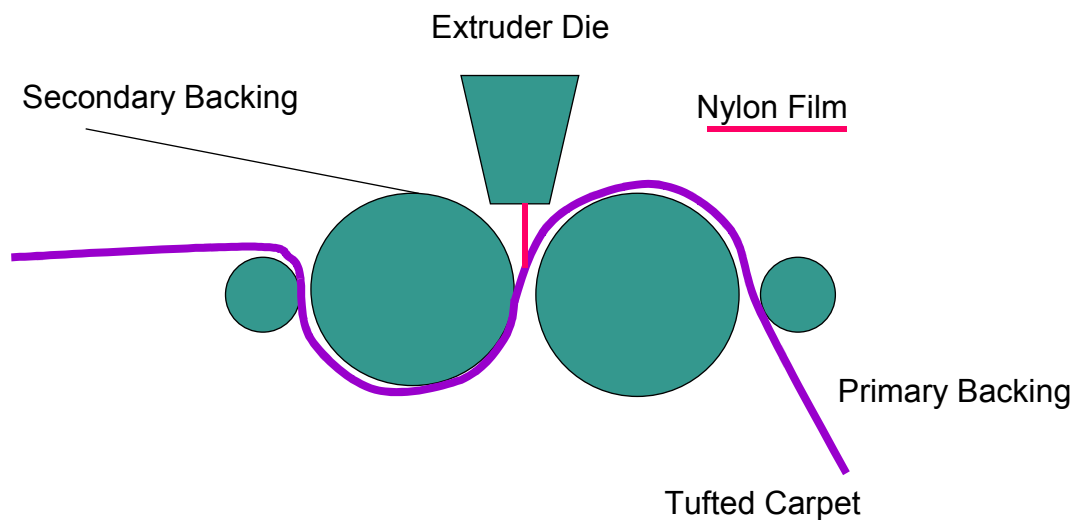


Figure 3.3: Schematic for Extrusion of Resin and Merger of Secondary Backing.
The left drum was cooled.

3.2 Physical Characterization of Materials

3.2.1 Breaking Strength

Breaking strength measurements of primary backing glass mats and completed carpets were conducted with the use of test method ASTM D 5035-95 [44]. Each sample was conditioned in accordance to ASTM methods [45]. Test specimens were prepared with a die cutter to a 2.5 cm x 15.25 cm (1 in. x 6 in.) dimension. Specimens were cut with their long dimension parallel either to the warp (machine) direction or to the filling (cross) direction for a total of 24 specimens, 12 in each direction.

Breakage strength was measured with an Instron 5567 Tensile Testing Machine fitted with a 10 kN load cell. Two pneumatic clamps were used to hold samples while the test was conducted. The gage length (distance between the clamps) was set to 75 ± 1 mm. (3 ± 0.05 in.). The Instron Tester was programmed to run at a rate of 300 mm/min. (12 in./min.). After the samples were mounted and locked in the clamps, the test was initiated and the breakage force was measured to occur between 10 and 90% of the full-scale force [15]. For each specimen, the ASTM D 5035-95 test procedure was followed to determine the breakage strength.

3.2.2 Delamination Strength

Resistance to delamination of the Elvamide® resin applied to the carpet backings were conducted with method ASTM 3936-97 [46]. Specimens were brought to standard moisture equilibrium in accordance to ASTM procedures [45], and then cut to a size of 5 cm x 20 cm (2 in. by 8 in.). Specimen size in the long direction was at least 150 mm (6 in.) due to the initial manual separation and the amount of material needed to conduct the

test. Manual separation was approximately 75 mm (3 in.), which allowed the other minimum 75 mm for data acquisition.

The delamination strength was measured via an Instron 5567 Tensile Testing Machine fitted with a 10 kN load cell. Two pneumatic clamps were used to hold the samples and the gage length was set to 25 ± 1 mm. The Instron Tester was programmed to run at a rate of 300 mm/min. (12 in./min.). To mount the specimens, the resin was placed in one of the clamps and the primary backing in the other. Specimens were then tested for the total length and the force versus elongation was measured. The data recorded consisted of a series of peaks, each represented the force at which the layers had separated, and troughs corresponded to the fall back of the force. After the initial peak was recorded and an additional 75 mm (3 in.) of the specimen had been delaminated, the test was stopped. The resistance to delamination was determined by dividing the average of the highest force peaks of each 12 mm interval (initial peak disregarded) by the specimen's width.

3.2.3 Air Permeability

Air Permeability was measured in accordance with ASTM D 737-04, and samples were prepared by ASTM standards [45, 47]. The instrument used, an Air Permeability Testing Apparatus, consisted of: a test head, which provided the circular test area; a clamp to secure the specimens; a pressure gauge to measure the drop in pressure across the specimen; and a flow meter which measured the air velocity through the test area. Test samples were approximately 30 cm x 30 cm, which was a larger area than the clamped surface.

3.2.4 Tuft Bind Strength

Carpet samples were prepared in accordance to ASTM practices to prepare textile samples [45]. The tuft bind strength was measured with a Tuft Withdrawal Tensometer, with maximum capability of 5 kg force. For samples that went above the instrument's limits, an Instron 5567 Tensile Testing Machine was used with a 10 kN load cell. The detailed test method procedure for tuft bind strength was followed according to ASTM *D* 1335-98 [48].

3.2.5 Microscopy

A Motic B3 Professional Series Optical Microscope with 4, 10, 40 and 100 magnification capabilities was used to study the morphology of the Elvamide® resins. Specimens were cut to 1 in. square samples to accommodate the microscope's stage. The microscope images were captured and measured using the Motic Images 2000 software and a notebook computer with USB 2.0 connectivity.

3.3 Thermal Characterization of Materials

3.3.1 Radiant Panel Flammability Test

Carpet samples were subjected to the Radiant Panel Flammability Test at Shaw Industries' Testing facility in Dalton, GA. Specimens were cut to a width of 200 mm (7.9 in.) and a length of 1000 mm (39.4 in.), and then bonded to a standard simulated concrete subfloor panel, pile side face up. The mounted specimens were conditioned and tested in accordance with ASTM E 648-04 [49]. The test required three assessments conducted for one sample. Specimens were placed in the Flooring Radiant Panel Tester

where they were subjected to radiant heat and ignition with an air-gas mixture. Burn distance, burn time and critical radiant flux were measured for the three specimens, which were then categorized as either a class one (pass), class two (marginal), or unclassified standing [50].

3.3.2 Ignition Characteristics

3.3.2.1 ASTM Method

Ignition characteristics of the carpets were tested in accordance with ASTM D 2859-04 and required eight specimens for one carpet sample group [51]. Specimens were cut into 230 mm (9 in.) squares and then preconditioned in accordance to the ASTM method to remove excess humidity [45]. The test procedure called for a prepared specimen to be placed pile side up in the specified test chamber where a steel frame the size of the sample was placed on top to hold it down. A methenamine tablet was then placed in the middle of the specimen and ignited by the touch of a match. Specimens were allowed to burn until they self extinguished or the burn reached the metal frame. A test was a success if the burn distance did not exceed three inches from the point of ignition. In order for a carpet sample to pass, seven out of eight tests had to be successful.

3.3.2.2 British Standard Method

Ignition characteristics of carpets were also tested in accordance with British Standard (BS) TM 470 (Hot Metal Nut Test) and required at least three specimens for one carpet sample [52]. Specimens were cut into 300 mm (12 in.) squares and then

preconditioned by the BS method. Carpet samples were tested in the loose lay procedure in which they were placed in the test chamber pile side up and unbounded to a subfloor. A clamp ring was then placed over the sample to hold it down. An iron nut was then heated in a muffle furnace to a temperature of $900^{\circ}\text{C} \pm 20^{\circ}\text{C}$. The nut was then removed from the furnace and placed in the center of the specimen within three seconds, and the test chamber was closed. After 30 seconds, the nut was removed from the specimen and the chamber was closed again until the flame extinguished or reached the clamp ring. Once the flame was extinguished, denoted by no visible flame, smoldering or afterglow, the burn distance on the tuft (front) side and the secondary backing (back) side of the carpet were measured. The burn time for each specimen was recorded along with the maximum of the two burn distances.

3.3.3 Thermal Transmittance

The thermal transmittance for nonwoven glass mat primary backings were preconditioned and tested in accordance with test method ASTM D 1518-85 (Re-approved 2003) [53]. Two specimens from one sample were used and were cut to 510 mm (20 in.) squares, which was large enough to cover the entire surface of the hot plate and the guard plate of the instrument. From the apparatus, the test plate, guard ring, bottom plate and air temperatures were measured along with the wattage used to heat the test plate. Before measuring, the parameters were measured without a specimen present in the apparatus. The specimen was then placed on the hot plate and allowed to reach equilibrium conditions before data was collected.

To calculate the combined transmittance of the specimen plus the air, U_I , Equation 3.1 was used, where P is the power lost from the test plate (W), A is the area of

$$\text{Equation 3.1: } U_I = P / [A \times (T_P - T_A)]$$

the test plate (m^2), T_P is the test plate temperature ($^{\circ}\text{C}$), and T_A is the air temperature ($^{\circ}\text{C}$).

To calculate the intrinsic thermal transmittance of the backing alone, U_2 , Equation 3.2

$$\text{Equation 3.2: } U_2 = (U_{bp} \times U_I) / (U_{bp} - U_I)$$

was used, where U_{bp} is the bare plate transmittance, also calculated using Equation 3.1 with no specimen in the apparatus and thus making U_I in Equation 3.1 now equal to U_{bp} .

3.4 Results and Discussion

3.4.1 Tuft Bind Strengths

The tuft bind strength test was carried out on the initial carpet constructions based on the bare glass mat primary backing (Table 3.2). No trend in whether more or less resin mass improved the carpet could be seen. However, in comparison to a conventional straight loop tufted, broad loom carpet of similar construction with a tuft bind strength of around 7.6 pound-force (lbf.), the results revealed that the best tuft bind strengths achieved with the developed carpets were ~half those exhibited by the traditional carpet. The highest tuft bind strengths occurred in the 6 and 9 oz./yd.² applied resin samples, and

Table 3.2: Tuft Bind Strengths of Loop Pile Carpet Samples. Measurements were in pounds-force.

Backing	Pile	Elvamide® 8063			Elvamide® 8201		
		3 oz./yd. ²	6 oz./yd. ²	9 oz./yd. ²	3 oz./yd. ²	6 oz./yd. ²	9 oz./yd. ²
Glass	Straight Loop	2.24	4.17	3.97	1.68	1.76	4.08
Glass	Cut Loop	0.98	1.06	1.69	1.20	0.98	1.50
PP	Straight Loop	1.40	1.70	1.42	0.50	0.57	4.43
PP	Cut Loop	1.10	0.68	0.98	0.40	0.42	1.98

the tuft bind strengths were much higher in the straight loop than in the cut loop carpet samples. Between the two resins, 66% of the samples produced higher tuft bind strengths with Elvamide® 8063, showing a slight advantage to its use in the final construction.

3.4.2 Delamination of Elvamide® Resin Film from Tufted Backings.

The delamination strengths of the carpets based on bare glass mat and standard PP primary backings are shown in Table 3.3. No definite increase or decrease in delamination strength with mass of resin was apparent. However, the highest delamination strength was obtained with 6 oz./yd.² applied resin carpets, and the weakest delamination strength with the 3 oz./yd.² carpets. Significantly, all of the 3 oz./yd.² applied resin carpets tore during delamination testing.

In comparison, the delamination strength of the PP secondary backing of the conventional broadloom carpet of similar construction was 4.14 lb./in., which was 1.5 times higher than the largest value reported in Table 3.3. Between the PP and the glass mat primary backing carpet samples in Table 3.3, the PP backing resin adhesion was found to be greater than the glass backing resin adhesion, allowing the PP carpet to have a greater delamination strength.

Table 3.3: Delamination Strength of Resin from Carpets. Force measured in pounds/in. The symbol * indicates ripping of the Elvamide® during testing.

Backing	Pile	Elvamide® 8063			Elvamide® 8201		
		3 oz./yd. ²	6 oz./yd. ²	9 oz./yd. ²	3 oz./yd. ²	6 oz./yd. ²	9 oz./yd. ²
Glass	Straight Loop	0.53*	1.06	0.45*	0.78*	0.36*	0.59*
Glass	Cut Loop	0.85*	2.17	0.37	0.56*	1.67	0.42
PP	Straight Loop	1.04*	2.2	1.33	0.73*	1.22	0.74
PP	Cut Loop	0.98*	2.76*	1.42	0.56*	1.9	1.04

The delamination strength of the applied PP secondary backing was not measured because the nylon resin bound the material so poorly that it was easily stripped off the carpet by hand. Viewing Figure 3.3, the extruder slot was apparently too high above the carpet consolidation-merger point, causing the molten resin to cool and harden too soon to allow effective binding of the merged secondary backing. In addition, the merge zone drums were cooled rather than heated, further accelerating the solidification of the resin. Once the binding failure was recognized, the secondary backing was removed by hand from those carpets containing it for future tests of the delamination strength between the resin layer and the tufted primary backing. In addition, with the mass of resin used, the layer could possibly act as the secondary backing to attach the carpet to tack strips after stretching on floor installation, thus eliminating a material layer and application process in the carpet's manufacture.

3.4.3 Carpet Flammability Results

3.4.3.1 Radiant Panel Flammability Test Results

With the inferior tuft bind and delamination strengths exhibited by the carpet samples containing a mass of 3 oz./yd.² of resin (Table 3.3), they were eliminated from the radiant panel flammability testing. With the choices for the samples in the

flammability tests and due to the substantial specimen size required, samples were grouped to their pile, whether they were cut or straight loop, their primary backing nature and the amount of resin applied to the tufts (6 or 9 oz./yd.²), but not on their type of resin since not enough material was available to make another group. However, even with the combination of resins, the set of samples available from the consolidation trials did not allow for the needed three specimens for proper procedures but rather two, so each test sampled one specimen of carpet with Elvamide® 8063 and one with Elvamide® 8201. Even some of those two samples did not meet the total required sample length of 100 cm. The only sample not able to be given a classification was the straight loop, glass primary backing carpet with 9 oz./yd.² resin applied, as the flame did not extinguish within the allotted length of sample. In other words, both tested specimens were shorter than the needed 100 cm length.

The data from the radiant panel flammability tests are shown in Figures 3.4-3.7, and images of the test samples in Figure 3.8. In Figure 3.4, the times in which the samples remained ignited to complete exhaustion of a flame are compared to the amount of Elvamide® resin applied. No significant difference existed in the cut and straight loop samples whether they had 6 or 9 oz./yd.² of resin applied, but significance differences were observed in the burn times between backings. In addition, the PP backing carpets were much quicker to extinguish in the test than were the glass mat backing carpets.

In comparison of burn distances versus time, the performances of carpets with varying amounts of resin applied were also similar. In Figure 3.5, the burn distances were much higher for carpets with the glass mat backings than those with the PP backings. For example, with the straight loop, glass mat backing carpet with 6 oz./yd.² of

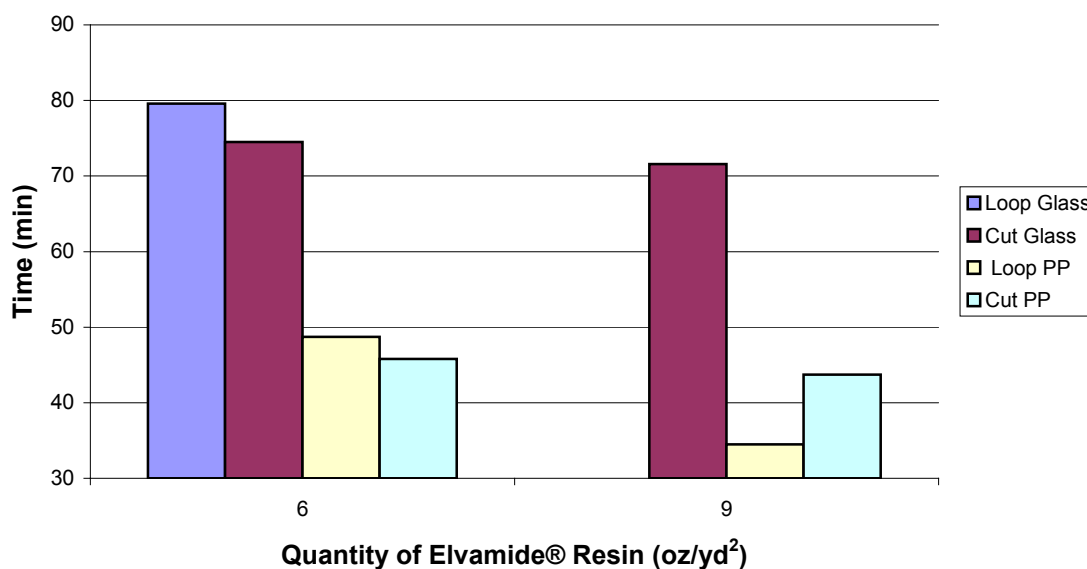


Figure 3.4: Burn Times of Radiant Panel Flammability Samples. Time measured is from start of ignition to the noticed end of any flame, smoldering, or afterglow. Specimens were from glass mat backing samples (Glass) and PP backing samples (PP) of both straight and cut loop pile tufted carpets with varying amounts of Elvamide® resin.

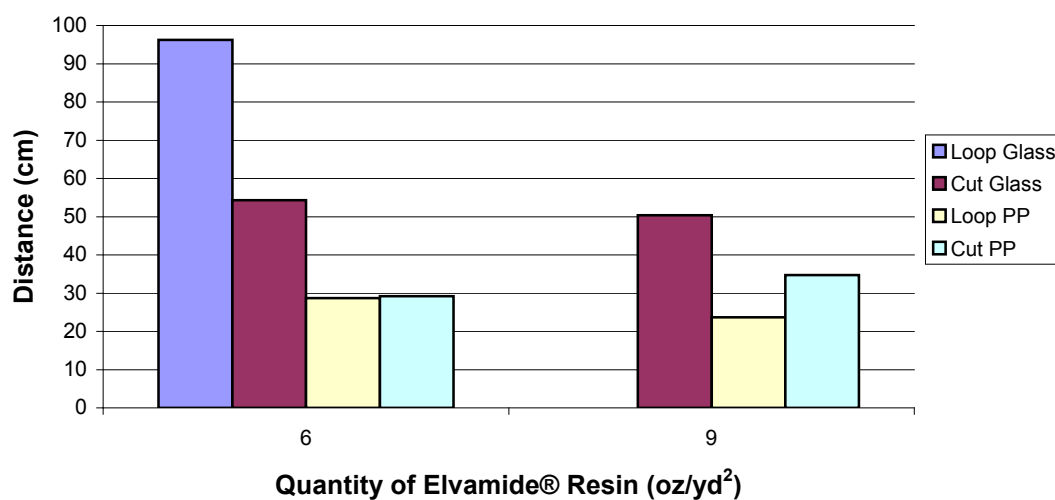


Figure 3.5: Burn Distances of Radiant Panel Flammability Samples. Radius measured from the farthest part of the sample that was burned to the point of ignition. Specimens were from glass mat backing samples (Glass) and PP backing samples (PP) of both straight and cut loop pile tufted carpets with varying amounts of Elvamide® resin.

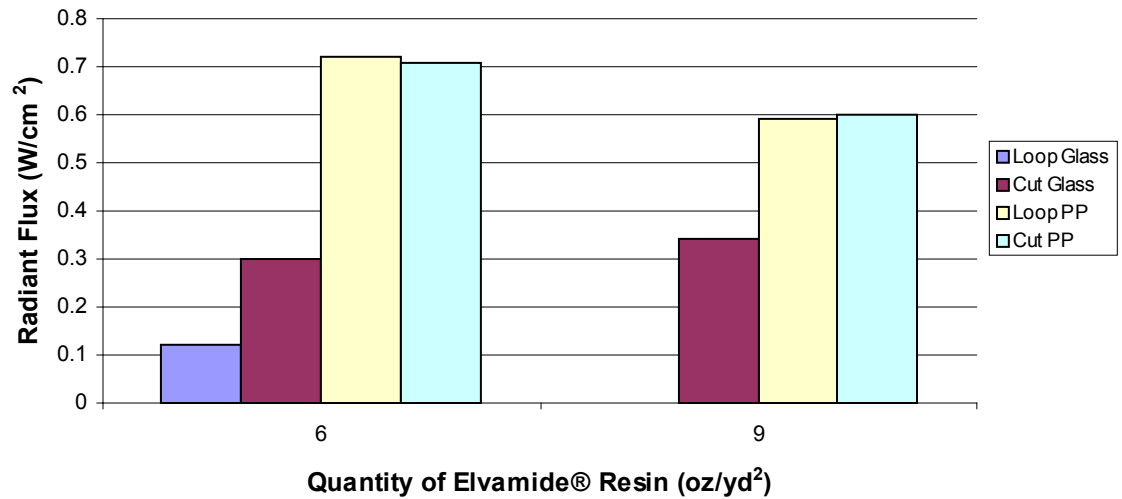


Figure 3.6: Critical Radiant Flux of Radiant Panel Flammability Samples. Specimens were from glass mat backing samples (Glass) and PP backing samples (PP) of both straight and cut loop pile tufted carpets with varying amounts of Elvamide® resin.

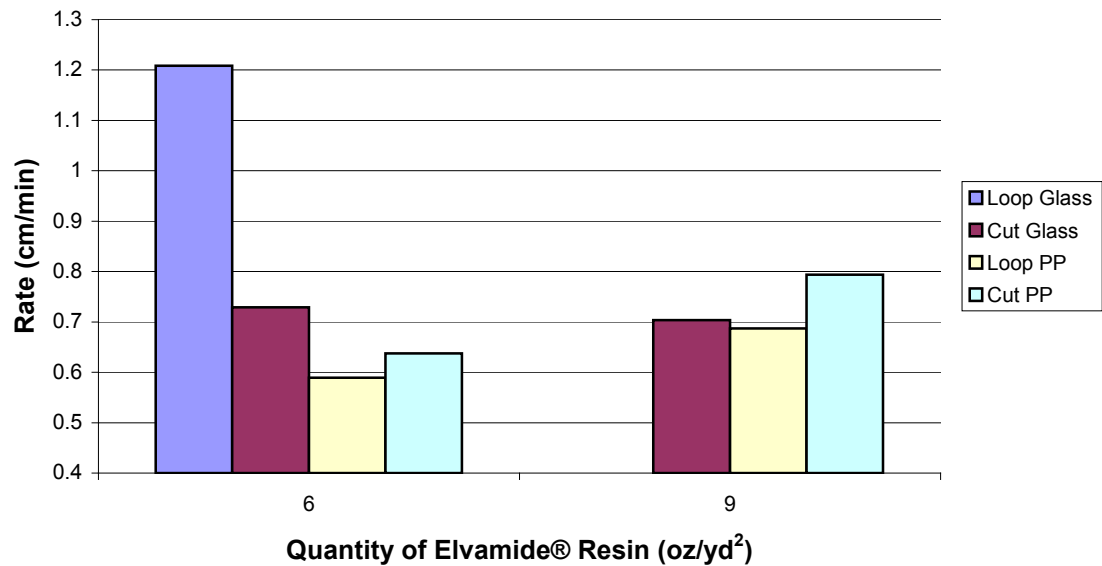


Figure 3.7: Rate of Burn of Radiant Panel Flammability Samples. Data calculated using the radius and time of burn from each corresponding sample. Specimens were from glass mat backing samples (Glass) and PP backing samples (PP) of both straight and cut loop pile carpets with varying amounts of Elvamide® resin.

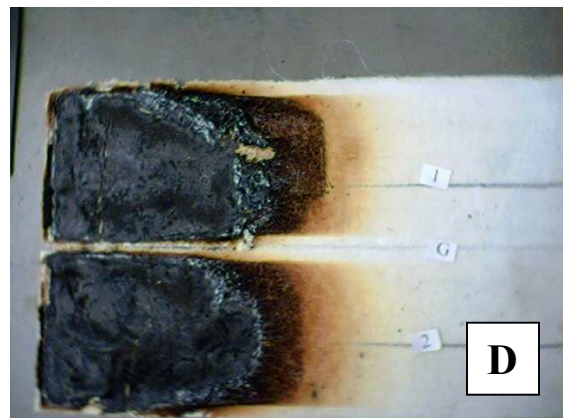
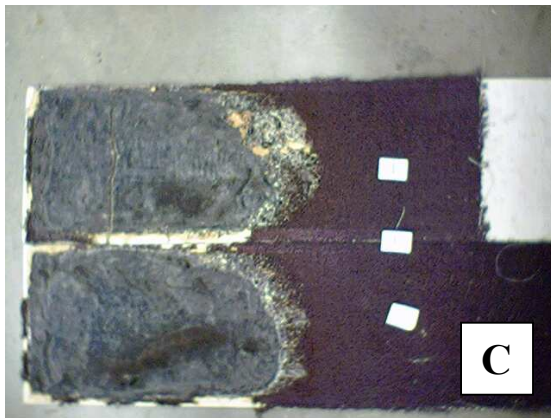
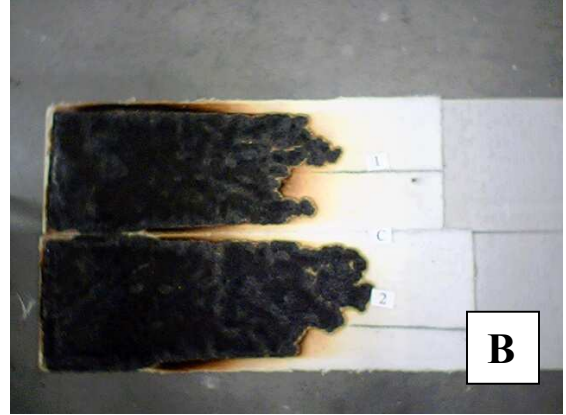
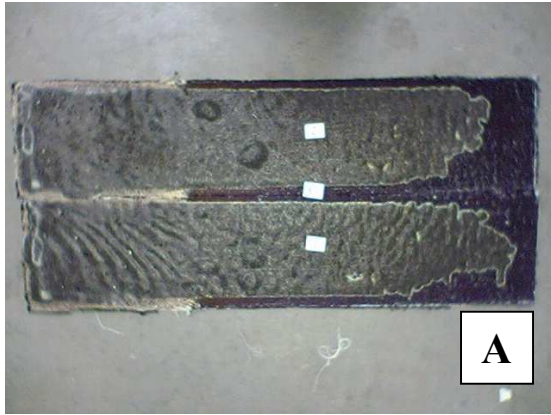


Figure 3.8: Radiant Panel Flammability Carpet Test Samples. **A:** straight loop pile, glass mat backing with 6 oz./yd.² of Elvamide®; **B:** cut loop pile, glass backing with 6 oz./yd.² of Elvamide®; **C:** straight loop pile, PP backing with 6 oz./yd.² of Elvamide®; **D:** cut loop pile, PP backing with 6 oz./yd.² of Elvamide®.

resin applied, the burn distance with almost the entire length of the sample (Figure 5.6.A). Unlike the burn time, the burn distances of the cut pile, glass mat backing carpets were almost half the length of the corresponding straight loop carpets. The burn distance between the PP samples were the same regardless of what type of tuft loop construction was used.

With the measured critical radiant flux, the PP backing carpet samples required more than half the energy per area when they burned than the glass mat backing carpets (Figure 3.6). The radiant heat of energy exposure was noted at the point the carpet “self-extinguished.” The radiant energy measurements were reported as the sample’s critical radiant flux, the minimum energy necessary to sustain flame propagation. Critical radiant flux dictates the industry’s final decision as to what installation areas a carpet can be used where automatic sprinkler protection is not provided [54]. Three class specifications are obtainable for carpet:

Class I – An average minimum radiant flux of 0.45 W/cm^2 was needed for the carpet to be placed within exits, access to exits (corridors) of health care facilities (hospitals, nursing homes, etc.) and new construction detention and correctional facilities [54].

Class II – An average minimum radiant flux of 0.22 W/cm^2 was needed for the carpet to be placed within exits, access to exits (corridors) of day care centers, existing detention and correctional facilities, hotels, dormitories, and apartment buildings [54].

Unclassifiable – An average radiant flux was lower than that of 0.22 W/cm^2 meaning that the carpet cannot be placed in an area where automatic sprinkler protection was not provided [50].

With their measured critical heat flux, the developed carpet systems were assigned the classifications in Table 3.4. The critical radiant flux for the straight loop pile, glass mat backing carpet was low which caused it to be Unclassifiable. The cut pile tuft analog exhibited a higher critical radiant flux, allowing it to receive a Class II rating. The PP samples that exhibited a high critical heat flux received a Class I rating. The energy needed to sustain the flame was so high that it explained the reason why the burn rate was low for this carpet construction. Overall with these flammability tests, no benefit of more or less mass of applied resin could be established.

Figure 3.7 shows the rate of burn of the carpet samples. Between the PP and the glass backings, the straight loop, glass mat carpet had the fastest burn rate of any of the backings. With the use of a cut loop pile instead of a straight loop pile in the glass

Table 3.4: Carpet Classification Based on Critical Radiant Flux. N stands for not enough length material for testing procedures and X stands for the classification given to the carpet sample.

Carpet Description			Classification		
Backing	Amount of Resin	Pile Loop	Class I	Class II	Unclassifiable
Glass	6 oz./yd. ²	Straight			X
Glass	9 oz./yd. ²	Straight			N
Glass	6 oz./yd. ²	Cut		X	
Glass	9 oz./yd. ²	Cut		X	
PP	6 oz./yd. ²	Straight	X		
PP	9 oz./yd. ²	Straight	X		
PP	6 oz./yd. ²	Cut	X		
PP	9 oz./yd. ²	Cut	X		

backing carpet, the burn rate was reduced because the straight loop tuft carpet was a 1/8th gauge product with 8 stitches per inch and the straight cut loop carpet was a 1/10th gauge product with 10 stitches per inch. While both carpet samples used 2-ply yarns with a denier of 2567, the straight loop pile carpet had a less dense pile that allowed for a high air-to-fiber ratio. Since the availability of air has an effect on the burning rate, flame propagation is less in high-density pile carpets, resulting in a reduced burn rate [55, 56].

3.4.3.2 Hot Metal Nut Test Results

Due to the large quantity of samples needed to conduct the ASTM 2859-04 test, the British Standard TM 470, known as the Hot Metal Nut Test, was instead conducted. In addition, since there was not enough of each Elvamide® resin carpet samples to complete each test, samples were grouped as to their pile, whether they were cut or straight loop, their backing nature, and the amount of resin applied to the tufts. From the radiant panel flammability tests, since both resins produced the same thermal results, no benefit was evident between the resin types.

From the burn distance in Figure 3.9, the straight loop tuft, glass mat carpet was the only one that failed the test. As the amount of resin in the backing increased, a slight improvement in reduction of the burn distance resulted. With the cut loop tuft, glass mat carpet, as the amount of resin increased the burn distance decreased, indicating that the amount of resin applied does impart serious flammability deficiencies to this backing system. With the PP backing carpet samples, only a slight increase in the burn distance was observed with more resin applied to the back.

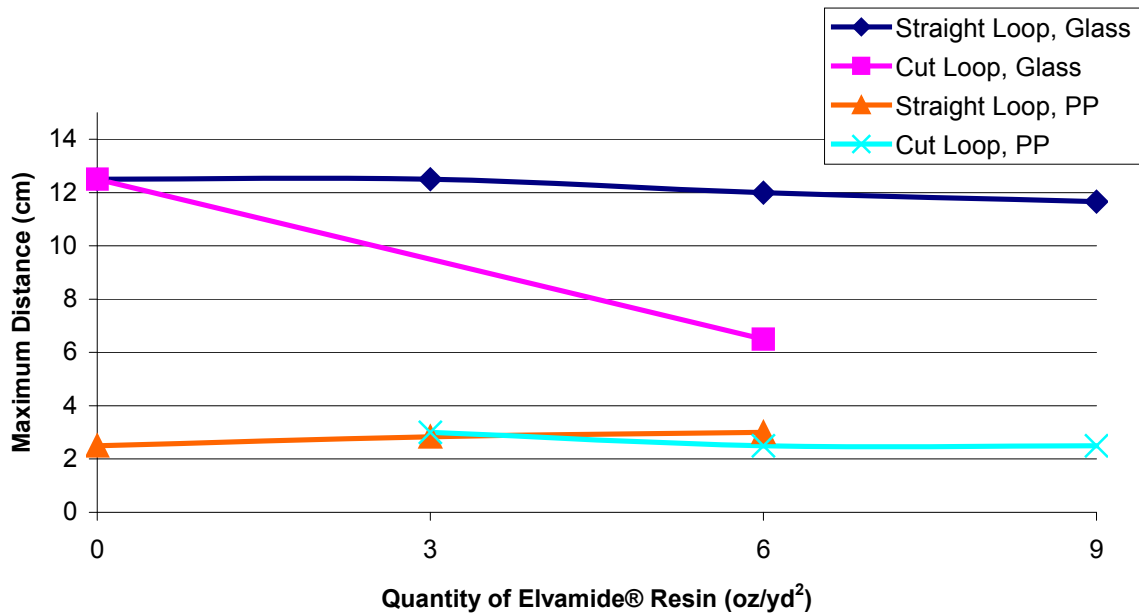


Figure 3.9: Burn Radiuses of Samples Using the Hot Metal Nut Method. Radius measured from the farthest part of the sample that was burned to the point of ignition. Specimens were from glass backing carpet samples (Glass) and PP backing carpet samples (PP) of both straight and cut loop tufts with varying amounts of Elvamide® resin.

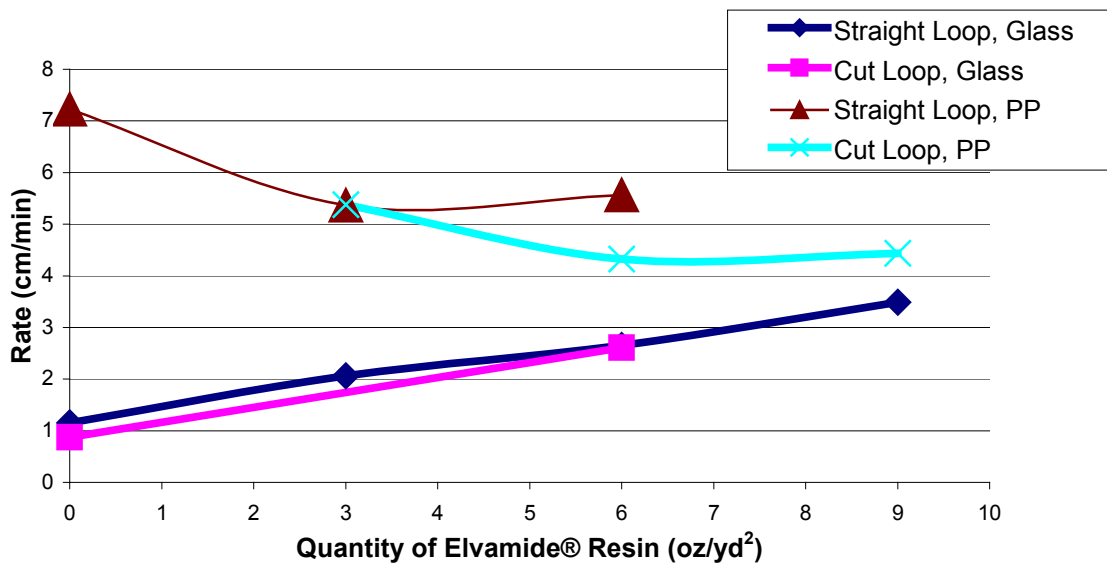


Figure 3.10: Burn Rate of Samples using Hot Metal Nut Method. Data calculated using the radius and time of burn from each corresponding sample.

By reviewing the burn rate of the carpet samples in Figure 3.10, as the amount of resin applied increased to 6 oz./yd.² of Elvamide® with the glass mat backing carpets, the slower the burn rate of both cut and straight loop samples. Above 6 oz./yd.² of Elvamide® resin, the burn rate plateaued. Increasing the amount of resin applied in the PP backing carpet samples increased the rate of which the samples burned. In the images seen in Figure 3.11.A and 3.11.B, the flame spread and burned slowly in the glass mat backing carpets, but ignited and burned quickly with little dispersal in the PP backing carpets.

As seen in Figure 3.11D, the PP backing carpet samples burned completely through, which revealed the sub-floor plate. The glass mat backing carpets did not burn completely through, which left the glass backing intact and simply charred/melted the Elvamide® resin. In Figure 3.12, the microscopy images of a cut loop pile, glass mat backing carpet with 3 oz./yd.² of Elvamide® 8201 resin carried through the Hot Metal Nut Test can be seen.

In Figure 3.12.A, the glass mat backing carpet was not melted or distorted from its original shape as was the PP backing carpet. The visual black specks attached to the glass mat fibers were composed of the melted tuft yarn that had flowed into the backing, and the darkened glass fibers were due to the build up of ash. Figure 3.12.B shows the unburned backside of the tuft from a straight loop, glass backing carpet sample with 3 oz./yd.² of applied Elvamide® 8201 resin. Although unburned, the tuft displayed some melt behavior, but still retained its yarn form.

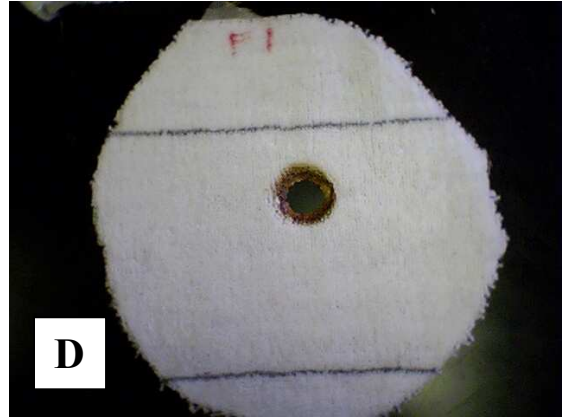
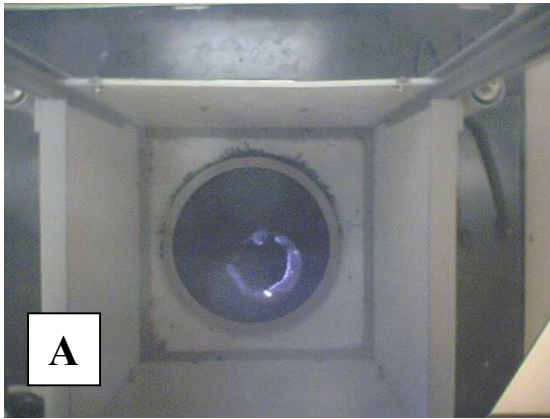


Figure 3.11: The Hot Metal Nut Test Samples. **A:** straight loop pile, glass mat backing carpet with 3 oz./yd.² of applied Elvamide® 8063 being tested; **B:** cut loop pile, PP backing carpet with 3 oz./yd.² of applied Elvamide® 8063 being tested; **C:** straight loop pile, glass mat backing carpet with 3 oz./yd.² of applied Elvamide® 8063; and **D:** cut loop pile, PP backing carpet with 3 oz./yd.² of applied Elvamide® 8063.

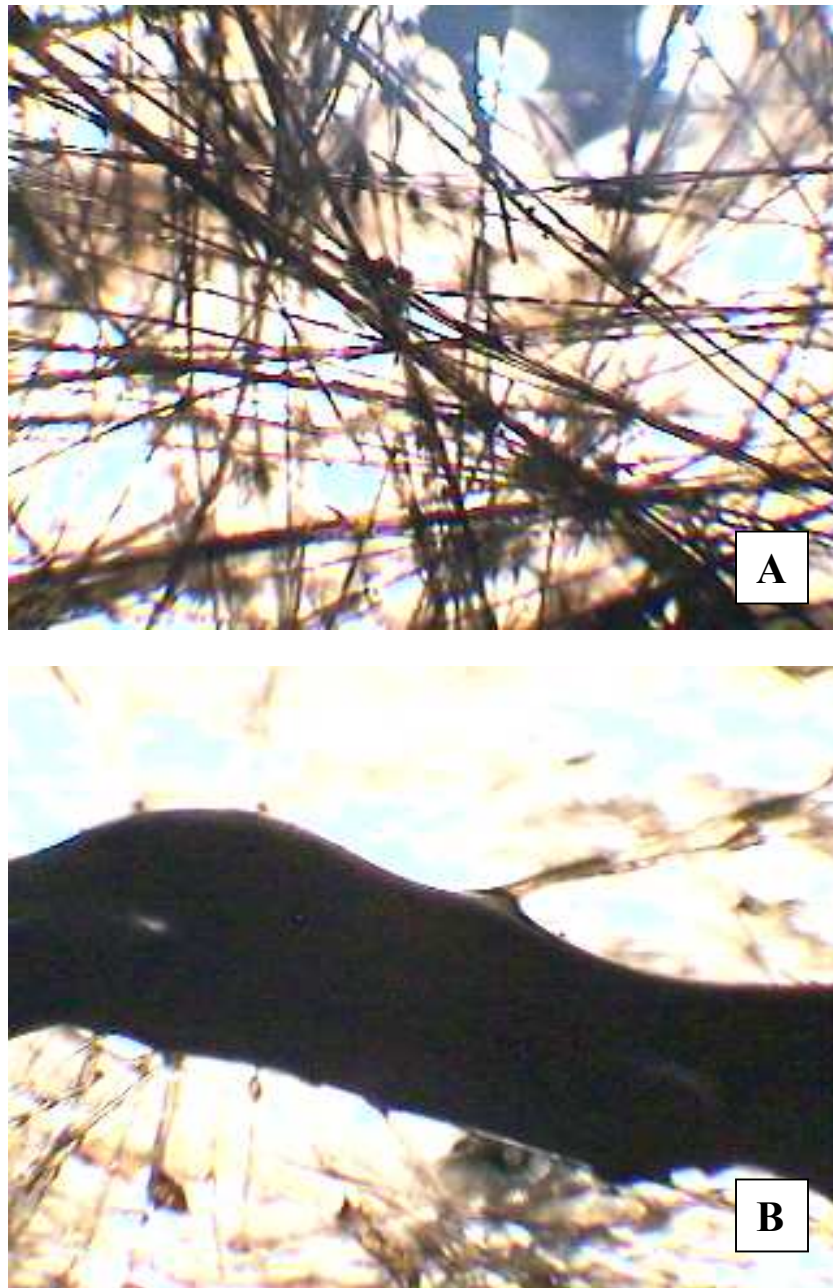


Figure 3.12: Microscopy Images at 4x Magnification of Hot Metal Nut Method Samples. **A:** an image of the glass mat backing, viewed from the back of a straight loop pile, glass mat backing carpet with 3 oz./yd.² of applied Elvamide® 8201 resin; **B:** an image of the post-test tuft, viewed from the back of a straight loop pile, glass mat backing carpet with 3 oz./yd.² of applied Elvamide® 8201 resin.

3.4.3.3 Discussion of Carpet Flammability Results

Without the data, the glass mat backing carpets were projected to exhibit better overall flammability results than the PP backing carpets due to the lack of combustibility of the non-carbon glass (E-glass is mainly silica) [42, 57]. Three postulates were developed to explain why the glass mat backing carpets actually gave poorer performances in the flammability tests than the PP backings.

The first postulate dealt with the binder used to consolidate the glass mat primary backing. The binder was an acrylic polymer of proprietary composition, applied to the nonwoven glass mat at ~20% by weight solids add-on. Acrylic polymer, unlike glass, is composed mainly of the elements carbon-hydrogen, and is thus highly combustible in the presence of fire, i.e., it provided hydrogen radicals on thermal degradation to fuel and sustain the fire in the carpet flammability tests. With the Hot Metal Nut Test on just the untufted glass mat backing, the structure ignited and supported a flame for about 20 seconds. If nylon yarn had been present as the tufted material, the binder in the backing would have ignited the yarn, thus propagating the fire.

A second reason for the test outcomes was that the glass mat backing, unlike the PP backing, was a highly “open” nonwoven structure that gave easy access to air flows feeding the fire from the sides, and thus supplying oxygen to sustain it. Air permeability tests conducted on the glass mat backings proved impossible, since the test apparatus could not build up enough pressure with the open mat for the apparatus to operate. In Figure 3.9, the results show that with the addition of more resin, the burn distance is decreased due to a blockage of air supply from underneath the flames provided by the Elvamide® resin.

Finally, the third reason for the outcome was due to the thermal resistance of the glass backing. In Figure 3.13, several nonwoven glass mats were ordered and provided by Owens Corning Co. to measure the thermal transmittance of the glass backings. The glass mats were made in the same way as the nonwoven glass mat from which the carpet samples were created. The impregnation factors for these 10 mats can be seen in Table 3.5. The data showed that as the mat's density increased, the thermal transmittance decreased. The lower the thermal transmittance of the backing, the lower the amount of heat/energy will be transferred to the back of the carpet. The thermal transmittance of the bare glass backing that was used in the tufted carpet was $9.7 \text{ W/m}^2 \text{ K}$, and because E-glass could withstand the thermal heat of the flammability test methods without melting, most of the thermal energy was kept at the surface of the carpet (side facing towards the environment), in turn keeping the critical radiant flux low.

3.4.4 Tensile Properties of Carpets

The breaking load of both the glass mat and PP backing carpet samples made with Elvamide® 8063 resin were measured in both the machine direction (tufting direction) and cross machine direction. The breaking load of the carpets in the machine direction can be seen in Figure 3.14. As the mass of applied resin was increased, the carpets' resilience to break increased. Samples of untufted glass backings with applied Elvamide® 8063 resin were also tested and compared to the tufted carpet. The data showed that the untufted backings were more resilient to breakage than the tufted carpets, which inferred that the tufting process induced damage in the glass backing, weakening the overall structure.

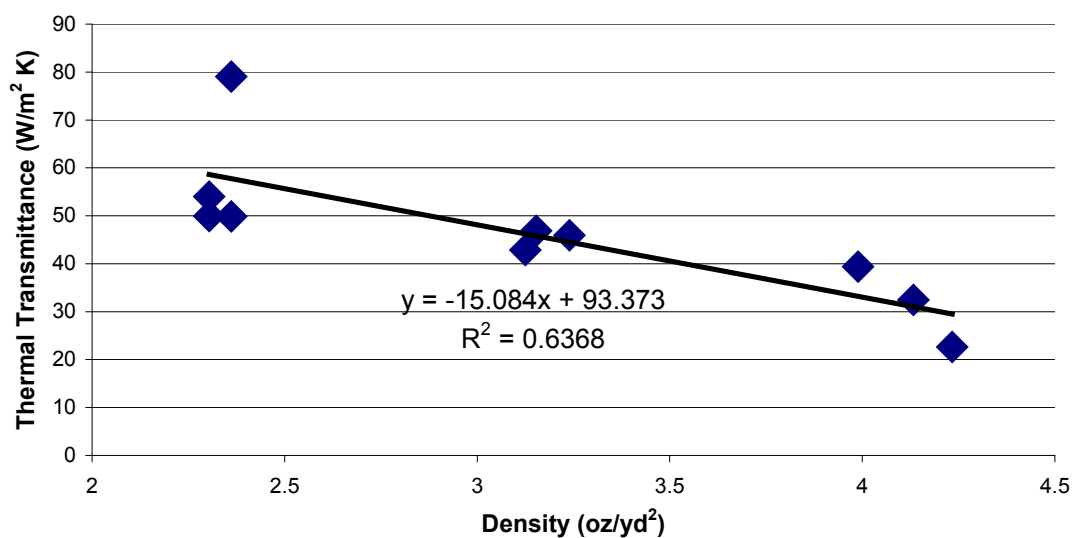


Figure 3.13: Intrinsic Thermal Transmittance of Varying Glass Mats.

Table 3.5: Impregnation Factors for Glass Mats.

Sample	Staple Length	Fiber Diameter	Mat's Minimum Weight (oz./yd. ²)	Mat's Maximum Weight (oz./yd. ²)	Percent Acrylic Binder
4	0.5 in.	11µm	2.30	2.32	20.1
5	0.5 in.	11µm	3.15	3.23	19.9
6	0.5 in.	11µm	4.23	4.39	19.6
7	0.5 in.	16µm	2.30	2.49	17.7
9	0.5 in.	11µm	2.36	2.39	10.7
10	0.5 in.	11µm	3.12	3.17	10.2
11	0.5 in.	11µm	4.13	4.44	10.6
12	1 in.	16µm	2.36	2.52	9.0
13	1 in.	16µm	3.24	3.44	8.2
14	1 in.	16µm	3.99	4.12	8.3

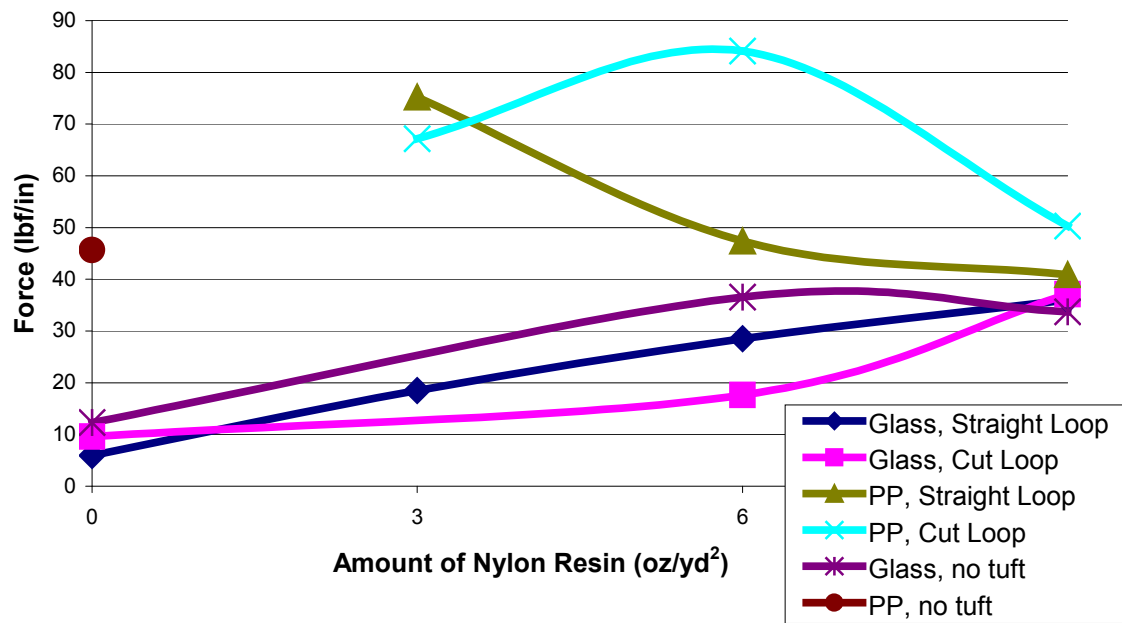


Figure 3.14: Breaking Force of Carpet Made from the Glass Backing with Elvamide® 8063 Resin, Machine Direction.

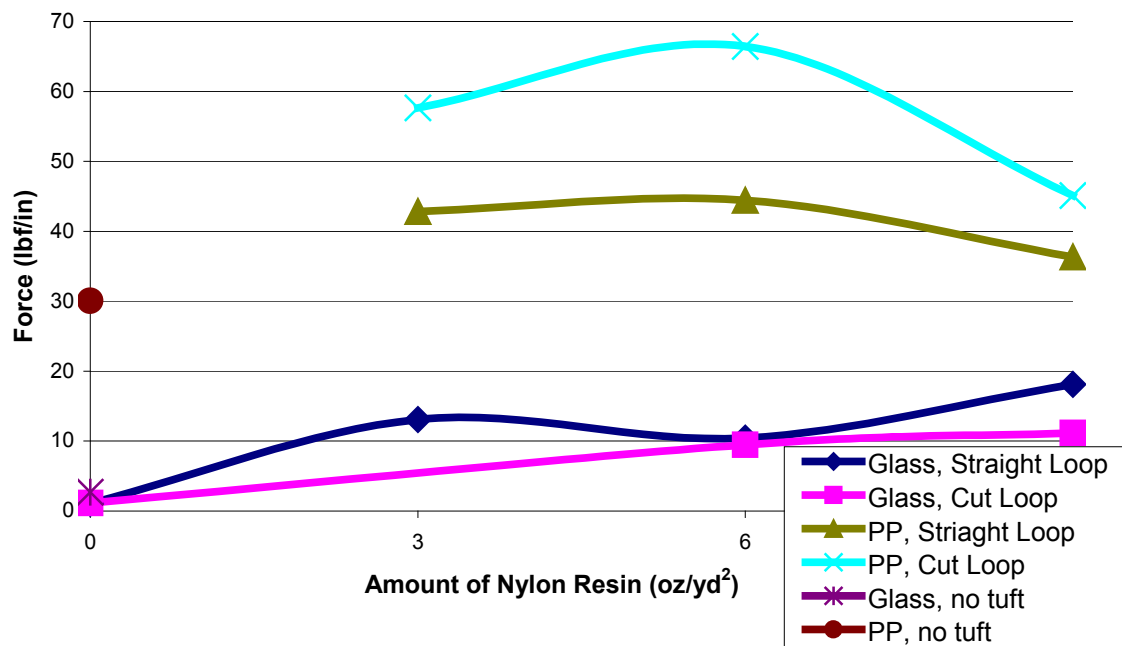


Figure 3.15: Breaking Force of Carpet Made from the Glass Backing with Elvamide® 8063 Resin, Cross Machine Direction.

The breakage strengths of the PP backing carpets were different than those of the glass mat backing carpets. As the amount of resin applied to the tufted PP backing increased from 3 to 6 oz./yd.², the breaking strength increased, but with 9 oz./yd.² resin application, it actually decreased. In comparison, the delamination strength (Table 3.3) of the resin was much higher with the 6 oz./yd.² carpets than with the 3 or 9 oz./yd.² carpets. As the structures were pulled apart, the resin layer separated from the tufted backing, reducing the overall breaking strength. With a 9 oz./yd.² resin application, the resin application became too thick that it hindered itself from penetrating/binding to the tufts, thus lowering the mechanical binding to the tufts and the breakage strength of the carpet from the 6 oz./yd.² resin application samples [58-60].

In Figure 3.15, the PP backing carpet samples showed higher load to break performances with 6 oz./yd.² of applied resin (Figure 3.15), while with the glass mat backing carpet samples, no clear advantage existed for any mass of applied resin. The breakage force showed that for best results, 6 oz./yd.² of resin should be applied to the carpet (glass mat or PP backings).

3.4.5 Tensile Properties of Glass Mats

Tensile tests on the various nonwoven glass mats supplied for the thermal transmittance measurements (see Section 3.4.3.3) showed how varying the density of the glass and weight percentage of utilized acrylic binder affected the breaking load. In Figures 3.16 and 3.17, as the density of the glass mat increased, so did the load to break. The same trend was observed with increasing weight percent acrylic binder. The increase in the tensile properties was due to the nature of the wet laid process. As the density of

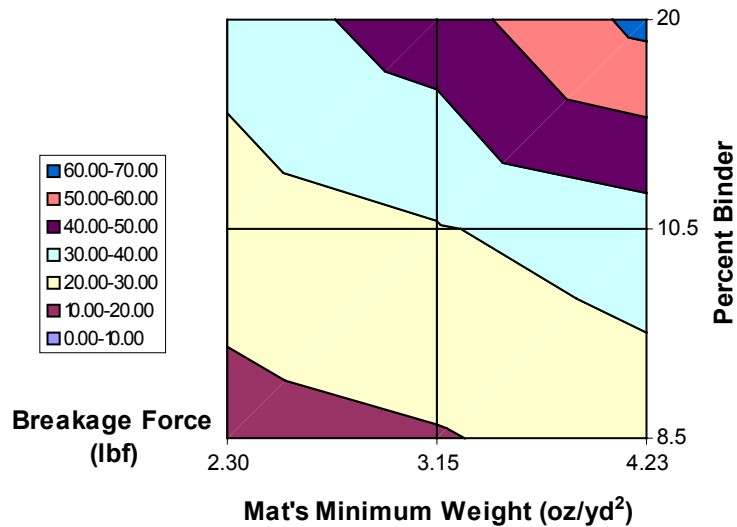


Figure 3.16: Breakage Force in Machine Direction of Glass Mats Varying in Percent Binder, Weight, and Staple Length. The colored areas in the figure represent different breakage forces achieved by the mats. The breakage force of the glass mats increased diagonally from left to right. The figure shows that increasing the glass mat's minimum weight and percent binder increased the breakage force.

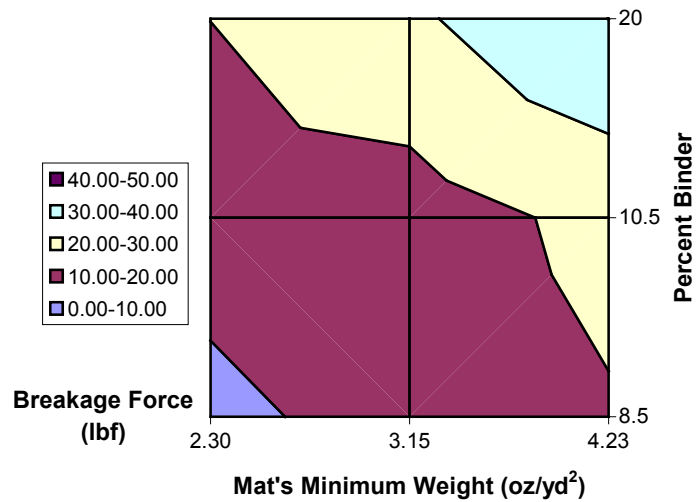


Figure 3.17: Breakage Force in Cross Machine Direction of Glass Mats varying with Percent Binder, Weight, and Staple Length. The colored areas in the figure represent different breakage forces achieved by the mats. The breakage force of the glass mats increased diagonally from left to right. The figure shows that increasing the glass mat's minimum weight and percent binder increased the breakage force.

the glass mats increased, so did the probability of more glass fibers directed into the cross machine direction. Higher tensile properties of the glass mat and also improved multilateral tensile strengths of the backing resulted.

Overall, the percent binder imparted more strength to the mats than was attributable to simply an increase in their weight. With 20% by weight binder present in the glass mats, breakage forces equal to those of the woven PP tape backing were achieved with a minimum mat density of only 3.15 oz./yd.². With less percent binder in the glass mats, comparable strengths to that of the PP backing were not achieved, even with maximum glass mat weights of 4.23 oz./yd.².

CHAPTER 4

ANALYZING THE TUFTING PROPERTIES OF PRIMARY CARPET BACKING SYSTEMS

The desire to create new tufted carpet backing systems, with the intent to approximate the mechanical properties of the traditional polypropylene (PP) woven tape backing system, led to the development of a novel test method to analyze primary carpet backings as to tuft ability. This test method enabled primary backings to be analytically characterized based on tufting factors. The intent in developing the test method was to gather preliminary data on candidate backings that would aid in identifying those most capable of surviving the rigorous needle tufting process, thus minimizing large-scale machine tufting trials [39-41, 61, 62]. The developed test procedure determined: the penetration force of the tufting needle on the backing; the withdrawal force of the needle from the backing; and the degree of damage the backings underwent during the needle tufting cycle.

4.1 Introduction

4.1.1 Composite Primary Backings

To address problems with the initial primary backing construction described in Chapter 3 such as the escape of glass from the backings on tufting and the easily removed secondary backing from the formed carpet, several composite backings were constructed to not only improve the mechanical properties, but to also use less glass. To meet this goal, several two-component primary carpet backings were made with the use of varying weights of nonwoven glass mat and nylon 6 planar structures. Elvamide® planar structures were not used since they are not commercially produced today in film or nonwoven forms. Another change in the composite backings involved a lower-diameter glass fiber. The original backing consisted of 16 μm diameter glass fibers and this version was continued in the **3892**, **3893**, and **3894** backings. However, in the **A**, **B**, and **C** backings, the diameter of the glass fibers was reduced to the more-flexible 12 μm version to reduce brittle breakage behavior, and thus lower or eliminate “fly” generation in tufting.

4.1.2 Composite Backing Break Down

Eight primary carpet backing candidates were tested, coded: **3892**, **3893**, **3894**, **A**, **B**, **C**, and the glass backing from Chapter 3 which will be further noted as the *original glass mat backing* (see Table 4.1 for descriptions). A standard 15 pick, woven tape PP primary backing was used for base property comparisons. The “face” of the primary backings in Table 4.1 dictated the surface from which the tufts projected, i.e., the surface of the installed carpet that would be toward the room environment. The “back” referred

Table 4.1: Glass Composite Backing Descriptions. All backings contained 8-10 percent by core weight of acrylic binder except the original glass mat backing, which contained 20 percent by weight of binder.

Backing	Description			
	Back	Core	Face	Stitching/Other
3892	None	Nonwoven Glass Veil: 3.40oz./yd. ²	Nonwoven Nylon: 0.85oz./yd. ²	Chain Stitch and 0/90 Tricot Knit, 275 Tex Yarn
3893	None	Nonwoven Glass Veil: 3.40oz./yd. ²	Nylon Film: 1.79oz./yd. ²	Chain Stitch and 0/90 Tricot Knit, 275 Tex Yarn
3894	Nonwoven Nylon: 0.30oz./yd. ²	Nonwoven Glass Veil: 3.40oz./yd. ²	Nonwoven Nylon: 0.85oz./yd. ²	Chain Stitch and 0/90 Tricot Knit, 275 Tex Yarn
A	Nonwoven Nylon: 0.53oz./yd. ²	Nonwoven Glass Veil: 2.40oz./yd. ²	Nonwoven Nylon: 0.82oz./yd. ²	Chain Stitch
B	Nonwoven Nylon: 0.58oz./yd. ²	Nonwoven Glass Veil: 3.04oz./yd. ²	Nonwoven Nylon: 0.79oz./yd. ²	Chain Stitch
C	Nonwoven Nylon: 0.58oz./yd. ²	Nonwoven Glass Veil: 4.22oz./yd. ²	Nonwoven Nylon: 0.86oz./yd. ²	Chain Stitch
original glass mat	None	Nonwoven Glass Mat: 8.92oz./yd. ²	None	None

to the surface that contained the tight “back loop” of the tufted yarn, is adhered to the secondary backing and is against the floor of the installed room environment. With the glass veils, chain stitching with a 120 denier, 0.012 cm diameter monofilament polyethylene terephthalate (PET) polyester fiber was necessary to hold the nylon 6 structures (either a nonwoven veil or an extruded film) to the glass core of the composite primary backings. The term “veil” designated an individual component of the backing and the term “mat” designated the backing as a whole, or with the case of the composite backings, the nonwoven core glass component surrounded on either side with nylon veil or film layers.

In the creation of the composite primary glass backings, the first step was the extrusion of E-glass filaments with diameters of 12 or 16 μm , which were then chopped into the desired staple length of either 1 or 0.5 inches. The backings **3892**, **3893**, and **3894** contained glass filaments of 16 μm in diameter, as did the *original glass mat* backing. The backings **A**, **B**, and **C** contained glass filaments of 12 μm in diameter, which is a more flexible, more expensive Advantex© E-glass fiber which reduced the brittle fiber fracture problems experienced on tufting with the original glass mat.

In the formation of the nonwoven glass mats, a wet-laid formation process was utilized [42]. The wet-laid process began by suspending the glass fibers in water. Specialized paper machines were then used to separate the water from the fibers to form a uniform sheet of material, which was then bonded by use of an acrylic binder and dried [42, 63]. The percent acrylic binder in the original glass mat was 20% by backing weight, which was shown to be a source of ignition in the carpet flammability tests (Section 3.4.3). To reduce the flammability, all of the glass mats in the composite

backings contained no more than 10% acrylic polymeric binder. To assess impact on flammability, three percent by weight of a proprietary brominated flame retardant was applied to one of the developed primary backings, **B** (Table 4.1). The pre-made nylon 6 veils were then applied to the face and/or back of the formed glass mats, and the composite structures were then chain stitched together with the polyester monofilament fiber. The chain stitching consisted of 12 stitches per 5 cm at a stitch length of 0.5 cm.

The driver for using nylon 6 layers in composite backing constructions was to reduce or eliminate the escape of small E-glass fibers, or fly ash, resulting from brittle fracture of the fibers during the needle tufting process. Such emissions were visually observed in minimal quantities during the first tufting trials of the *original glass mat* (a single-component, acrylic-bound nonwoven glass mat). The nylon 6 veils were also projected to increase the tuft bind strength of the tufted carpets.

The “0/90” designation found in the construction descriptions of Backings **3892**, **3893**, and **3894** in Table 4.1 refers to a tricot knit construction of flat glass filament yarns of 275 Tex that was applied to the back of the central glass veil and held with the chain stitch, thus serving as the secondary backing of the final composite carpet construction. In these “layered” constructions, the nylon resin was no longer solely responsible for locking the secondary backing into the consolidated carpet, thus increasing the force necessary for delamination of the final product [42].

By grouping the primary glass-based backings, two classes were identified. In Class I (Backings **3892**, **3893**, **3894**), each of the constructions contained identical glass veil cores but differed in the weight of nylon layers applied to the front or back of the sample. In Class II (Backings **A**, **B** and **C**), each backing contained matching weights of

nylon but differed in core glass veil properties. The *original glass mat* was a plain, nonwoven glass mat with no nylon added, so it stood alone as a primary backing construction.

4.2 Backing Modifications

4.2.1 Thermal Consolidation

The prepared backings *A*, *B*, and *C* were thermally consolidated in a post-formation process using a Teflon coated transport belt which supported the sample through a series of heating and cooling zones. A total of seven heating zones gradually brought the backings to the designated consolidation temperature (the point at which the nylon 6 fibers in the nonwoven layers first began to undergo softening and minimal flow) and then back to room temperature. A Teflon coated belt was necessary to prevent the adhesion of the softened nylon 6 to the machine, which had previously occurred in attempting to thermally consolidate the Class II backings with a metal contact calendar roller at Shaw Industries' Cartersville, GA facility. Attempted thermal consolidation of the *A*, *B* and *C* backings by this latter method resulted in the nylon 6 veils separating from the backing and remaining attached to the calendar roller [13, 38].

4.2.2 Tufting of Backings

Candidate backings *A* and *C* were tufted on a pilot tufter at a rate of 400-500 rpm to give a straight loop pile carpet with a width of 0.762 meter (30 inch). For reference, full-scale tufting machines run around 1200 rpm. The tufting needles were 1/8 gauge, being spaced to provide 40 stitches per 15 cm. The needle gauge was recommended to

help lower the propensity of the primary backing to “scissor” (ripping of the backing along the tufts) [13]. The employed tufting yarn was a three-ply twisted yarn of 4,050 denier (grams mass per 9,000 yards length).

4.3 Qualitative and Quantitative Analyses of Composite Backing Carpets

4.3.1 Microscopy

A Motic B3 Professional Series optical microscope with 4, 10, 40, and 100 magnification capabilities was used to study the morphology of the nylon 6 nonwoven layers on the composite backings and the holes formed from the tufting needle during the formation process. The backing specimens were cut to accommodate the microscope’s stage. The microscope images were captured and measured using the Motic Images 2000 software and a notebook computer with USB 2.0 connectivity.

4.3.2 Thermal Analysis

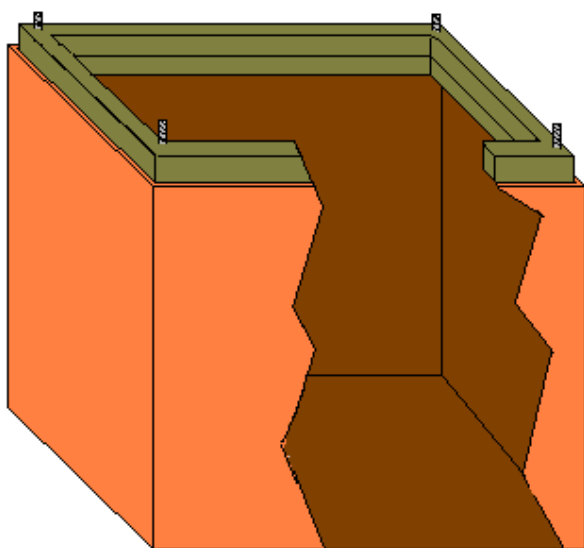
Differential Scanning Calorimetry (DSC) was used to study the melt and crystallization behaviors of the nylon 6 veils in the composite backings. DSC scans were performed with a TA Instruments DSC 2920 unit. The samples were first run through a full heating and cooling cycle followed by a second heating. The temperature was raised and lowered at a rate of 10°C/min. from a range of –100 to 300°C. The melt, glass transition and crystallization temperatures were taken at the corresponding transition peaks.

4.3.3 Developed Needle Force Test Apparatus

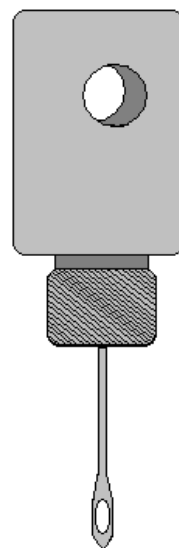
Due to the unconventional construction of the glass-based primary backings, tuft bind strength was a concern. Since it would be timely and expensive to convert all of the developed backing candidates into actual carpet on a pilot tufting machine, the properties of tufting into the glass-based primary backings were measured and compared to those of a standard 15 pick, woven PP tape backing. The measured parameters were the penetration force of the tufting needle entering the backing construction, and the corresponding force of withdrawal of the tufting needle exiting the backing.

The developed apparatus for measuring the forces acting on the tufting needle is shown in Figure 4.1. The apparatus was comprised of three components: a stage, two frames and the tufting needle mount. The stage consisted of a rectangular 1 ft. cubic hollow box made of half inch thick plywood, which held the two wooden square frames and also insured that the tufting needle only impacted the backing. The two frames served as a clamp that when bolted together held the backing taut, just enough to resist sagging of the backing during tufting. Each frame's dimensions were 1 ft. by 1 ft. square by one inch thick. The needle assembly consisted of a standard, eight-gage carpet tufting needle attached to a custom-made, cylindrical steel holder, and mountable to an Instron 5567 Tensile Testing Machine's 10kN load cell (Figure 4.1.B).

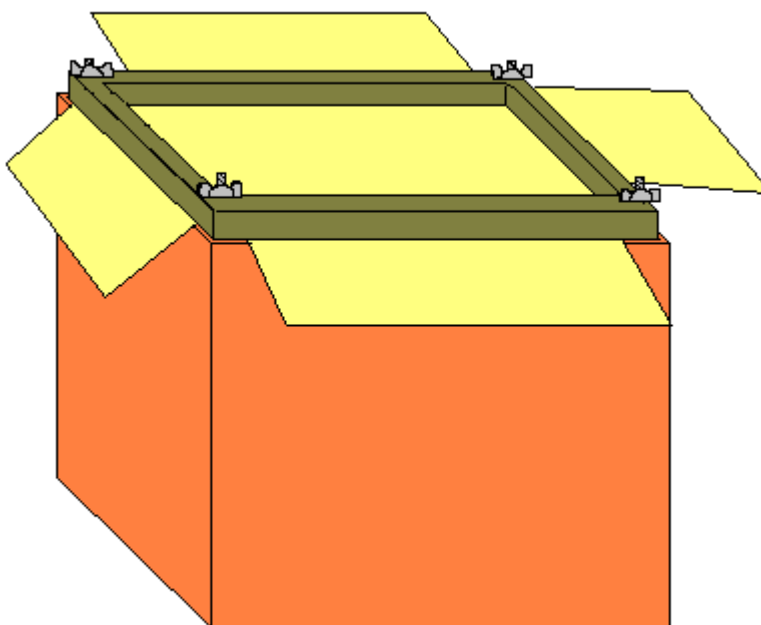
To measure the tufting properties of a primary backing construction, the specimens were first brought to moisture equilibrium in the standard atmosphere for testing textiles, as directed in ASTM D 1776 [45]. To mount the conditioned primary backing into the frame, it was first cut into a 20 inch square. Four inch squares were then cut out of the corners of the sample to create a cross formation that allowed for the



4.1.A Stage with Half Frame



4.1.B Tufting Needle and mount



4.1.C Sample Backing in Frame on Stage

Figure 4.1: Apparatus to Measure and Hold the Primary Carpet Backing along with the Tufting Needle (Not to Size). 4.1.A: Inside look of stage with half of frame with bolt holes; 4.1.B: Schematic of tufting needle attachment for Instron; 4.1.C: Representation of primary backing being held in the frame on the stage.

sample to be drawn taut. The cut specimen fit around the bolts that compressed the two frames together, thus rigidly holding the backing in place (Figure 4.1.A). After the sample was mounted, the second frame was bolted to the first frame, and the full assembly was set into the stage (Figure 4.1.C).

The backing in the described assembly was then placed under the tufting needle assembly mounted in the Instron load cell. A total of 15 testing sites were marked for testing of each backing sample: six random sites and six in a linear line to determine the forces acting on the tufting needle, and three more random sites so that the tuft reparability of the backing could be assessed [15]. In tufting operations, defects occasionally occur in which the yarn does not tuft correctly into the primary backing, and the situation must be rectified. To determine the tuft reparability, at each site the needle was penetrated and withdrawn four times in the same position. In this manner, the needle multi-insertion/withdrawal step in a single hole in the primary backing measured how damage imparted by the initial needle cycle affected the ability to repair the backing. The closer the next consecutive force measurement was to the initial force measurement, the more likely that a repaired tuft in that area would visually appear and perform like the “regular” tufts.

To calculate the damage inflicted, the cyclic penetration or withdrawal force was used. In Equation 4.1, D is the percent difference between the forces; F_0 is the first recorded cyclic force; and F_n is the next recorded cyclic force.

$$\text{Equation 4.1:} \quad D = 100 \times [(F_0 - F_n) / F_0]$$

The six randomly chosen-sites were at least 4 cm apart and not in a straight horizontal or vertical direction from other sites in the set. The other six needle penetrations were made by moving in a straight line in the cross machine ~ 0.5 cm away from each other to simulate the multiple tufting needles of a machine's tufting bar. The machine direction (MD) was not measured because in the tufting process the backing is constantly moving in the MD, and in the reported test procedure this action could not be replicated.

The test was conducted so that the needle carrying no yarn penetrated through the backing at a controlled run speed of 20 mm/min. (8 in./min.) to at least a three cm depth, and was then withdrawn at the same speed. The three cm. penetration length took into account the shape of the tufting needle. At that length, the widest part of the tufting needle passed completely through the backing, thus giving the maximum penetration force.

For each up/down cycle of the needle through the backing, the forces of penetration and withdrawal on the needle were measured (Figure 4.2). The first six measurements were taken at the random sites to obtain an average of tufting forces to compare them to the forces measured at the six linear sites. If a significant difference existed between the linear measurements and those of the random measurements, the specimen would more likely undergo "scissoring" (ripping of the backing along the tufts), or a significant weakening of the cross-machine tensile strength of the construction upon tufting [15, 16].

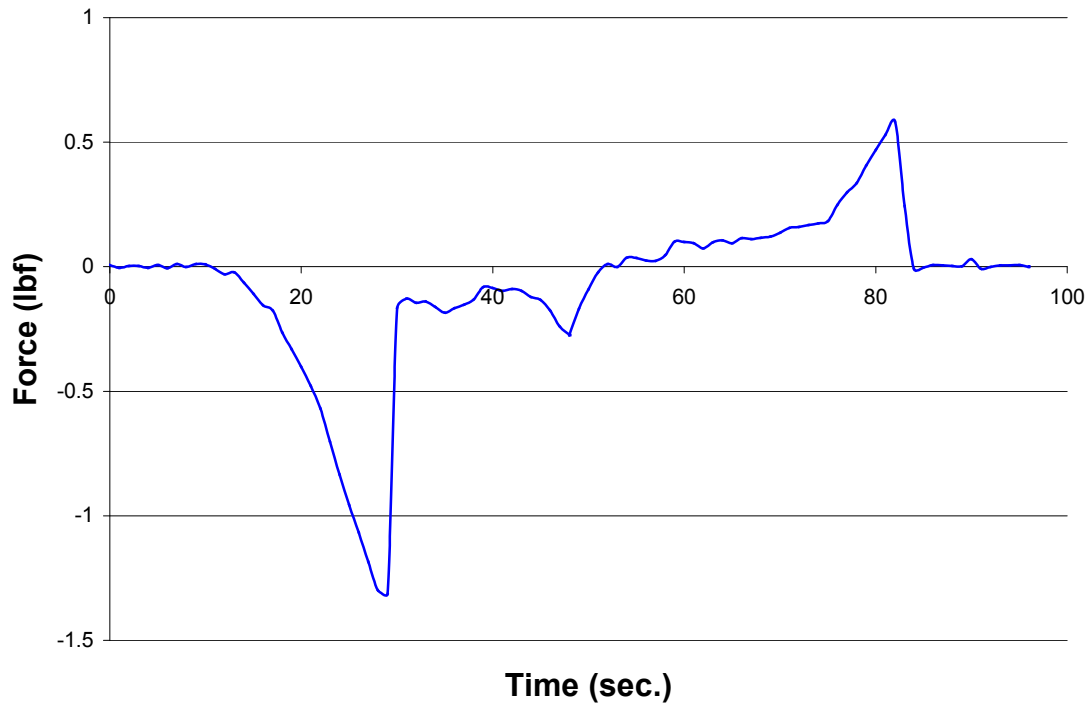


Figure 4.2: Measurements of the Tufting Forces Acting on the Tufting Needle. The figure depicts the force acting on the tufting needle as it penetrated and withdrew from the 15 pick PP backing. The first negative peak is the penetration force and the last positive peak is the withdrawal force. The negative peak around 50 seconds is the penetration force due to an increase in the width of the tufting needle's shaft.

4.4 Results and Discussion

4.4.1 Tuft Measurements

4.4.1.1 Penetration Force Analyses

Due to the differences in the mass of nylon that was applied to the face and the back (Table 4.1), testing of the penetration and withdrawal forces was conducted on each side to determine if either side exhibited any advantages to being the “back” of the carpet, i.e., the side of the backing presented to the tufting bar needles. The results of the penetration and withdrawal forces on the tufting needle with the various primary backings are contained in Figures 4.3 and 4.4. All of the glass-based composite backings exhibited higher penetration forces than the 15 pick woven tape PP backing and the original glass mat backing. Comparing the penetration forces from the designated “back” and “face” directions of the composite backings in Class I and II showed that needle penetration of the face required more force than did the back in each case. From examining the constructions in Table 4.1, all of the Class I/II carpet backings had a higher mass of nylon 6 layer applied to the face of the construction than the back.

As the tufting needle began to enter the backing, the nylon layer’s elastic properties allowed it to be stretched into the glass core until a point of nylon penetration occurred. The glass core acted as a barrier that increased the nylon’s resistance from being easily penetrated. Once through the face layer of nylon, the nonwoven glass core was much easier for the needle to traverse until the needle reached the nylon layer on the back of the construction. Unlike the face nylon, needle penetration through the back nylon was much easier, as nothing backed the layer to prevent/postpone breakthrough and subsequent full needle penetration of the structure.

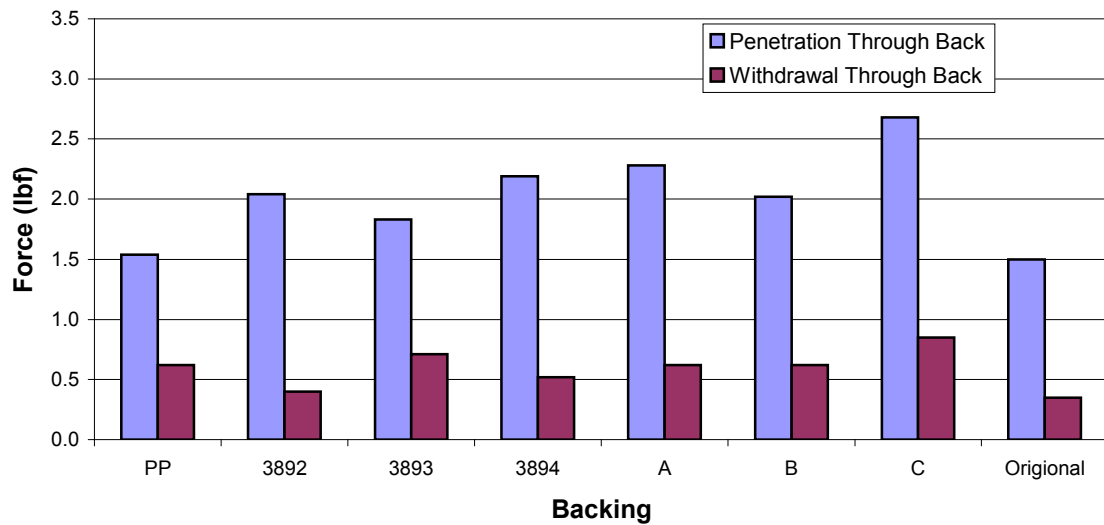


Figure 4.3: Bare Needle Tufting Forces of Carpet Backings: Back Tuft. Tufting needle penetration and withdrawal forces as it entered and left the backing constructions through the designated back (normal direction of tufting).

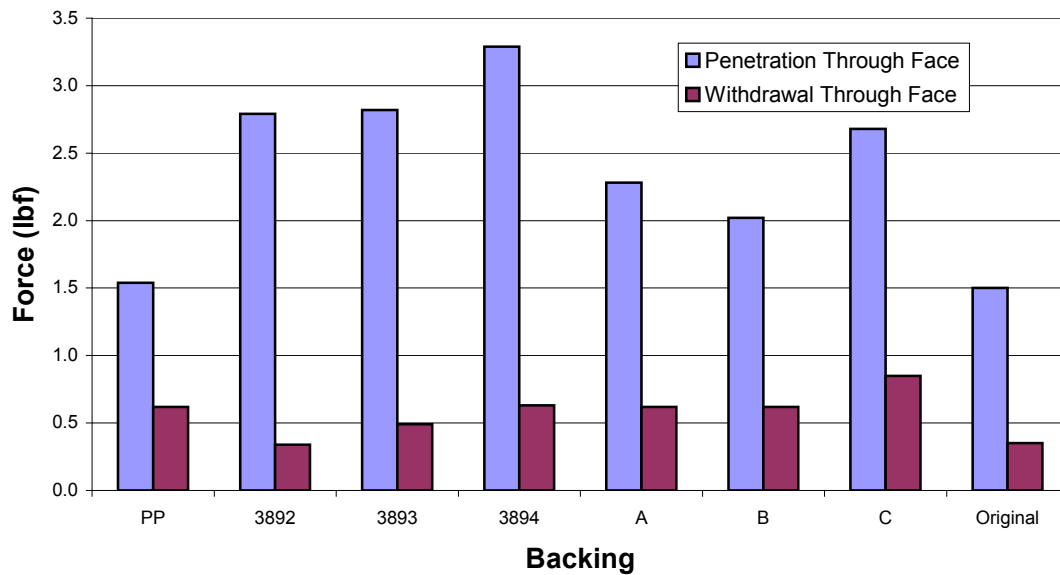


Figure 4.4: Bare Needle Tufting Forces of Carpet Backings: Face Tuft. Tufting needle penetration and withdrawal forces as it entered and left the backing constructions through the designated face (reverse direction from normal tufting).

Backings **3892** and **3893** each had a nylon layer on the face but no subsequent layer on the back. By comparing the two backings in Figures 4.3 and 4.4, when the needle penetrated through the nylon layer first, it produced a larger penetration force than when penetrating the nylon layer last. The data supports the theory that applying nylon layers to the surface or the back of the glass-based primary backings imparts significant tufting property changes.

As the similarities between the designated “face” and “back” of the constructions approached equality, so did the tufting force values in the two directions. The best example of this convergence was observed by the behavior of the woven PP backing, which was identical on both sides and thus supplied the same resistance to tufting forces regardless of the direction. The glass backings **A**, **B**, and **C** in Class II each had similar amounts of nylon on the face and back compared to that of the backings in Class I, which caused each particular backing to exhibit approximately the same penetration and withdrawal force whether the needle traversed from the face or the back direction. The other observation from Class II backings was that even with similar amounts of nylon applied to the face and the back, they differed in tufting values.

The Class II composite backings differed in their core glass mat densities, which demonstrated that changing the core density could also change the tufting forces. The actual core glass mat properties will be discussed later in this chapter. With the Class I backings, the data demonstrated that by keeping the core densities the same and increasing the mass of nylon applied, the amount of force needed to tuft the backing increased. The tufting needle penetration results can thus be used to design carpet backings with the desired level of resistance to tufting.

Finally, an assessment regarding all the primary backings was made. By comparing the tuft penetration force values of the six randomly chosen sites as an average/baseline for the other six, with the composite glass backings described in Table 4.1 no decrease was discovered and the resulting averages were equal, i.e., no problems could be identified at this point.

4.4.1.2 Withdrawal Force Analysis

The tufting needle withdrawal forces indicated the ability of the backings to hold the tufting needle, and thus served as a tool to identify backings that would exhibit superior tuft bind strengths [15]. Two tendencies of the withdrawal forces are exhibited in Figures 4.3 and 4.4. The first trend: as the combined total weight of nylon present increased on the designated “face” and “back”, the withdrawal force also increased. With more nylon capable of surrounding and holding the tufting needle, the resistance to withdraw the tufting needle was much higher the heavier the nylon layer.

The second trend was that the side of the backing that gave the highest tuft penetration force also gave the lowest tuft withdrawal force, and vice versa. For example, Backing **3893** had a nylon film (as opposed to a veil) on its face, and required more force to penetrate through the face than the back. The penetration of the needle through the film caused the nylon to stretch and then break, and when the needle was removed, less nylon remained in and around the needle hole to surround and hold it. When penetrating through the backside of the construction, little force was needed to pierce through the face nylon, resulting in minimal stretching of the film. When pulling

the needle out, there was more nylon available to exert force on the needle, resulting in a higher tuft withdrawal force.

4.4.1.3 Damage Determination

Figure 4.5 shows the results of two penetration cycles. After the initial penetration of the standard PP primary backing, any further penetration cycles caused ~32% of the initial penetration force to be lost, and the withdrawal force decreased by ~14%. Further penetration and withdrawal of the tufting needle caused little additional damage. In comparison to the other backings, the PP backing exhibited the greatest resistance to damage. With the PP backing woven from slit film tapes, as the needle penetrated, the flexible and semi-elastic woven tape first separated and then “sprang back” onto the entering needle, causing little to no damage. When the needle was removed, the backing recovered in a similar manner and a minimal, permanent hole remained.

Unlike the PP backing, the glass-based primary backings were much more rigid, and the glass fiber itself was more brittle than PP fiber. As the needle penetrated the glass composite backings, more damage was caused to the backing than was observed with the PP standard, and larger holes resulted on initial tufting needle penetration/withdrawal. When the needle penetrated a single hole a second time, the relatively large diameter of the initial hole dictated less contact between the fabric and the needle, resulting in a much lower force needed to penetrate the backing through it. This fact indicated that in mending defects in the developed tufted backings, the higher the percent difference between the first and second needle penetration forces utilizing a

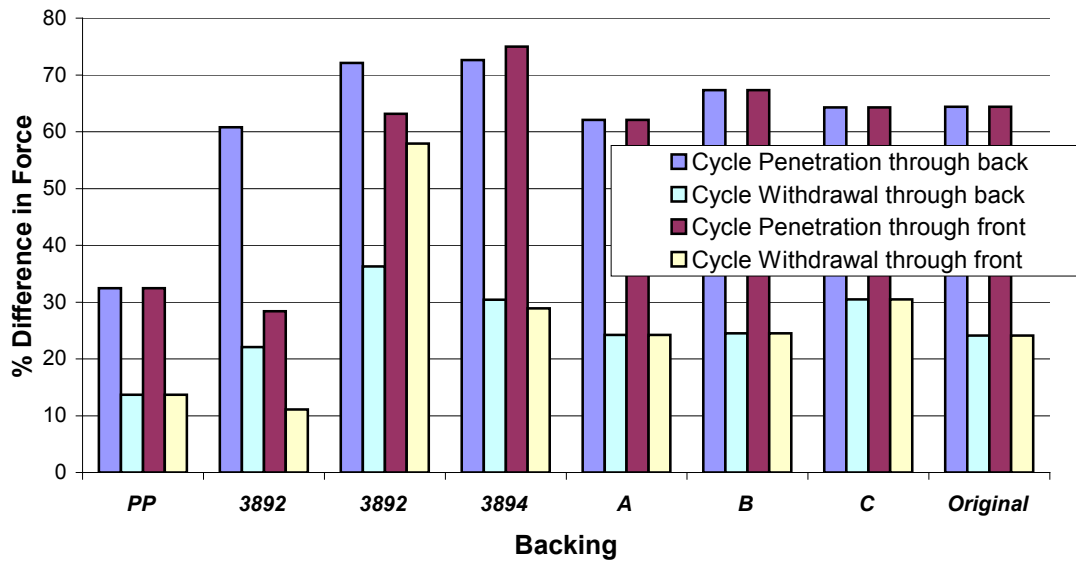


Figure 4.5: Reductions in Tufting Forces From Initial Penetration and Second Penetration Cycles. The percent difference between the initial penetration force and the subsequent penetration force, with the tufting needle entering the same location (hole) (see Equation 4.1).

single hole, the more likely the pull strength of the mended tuft would be significantly lower than other “regular” tufts in the backing.

The only apparent trend with the glass-based primary backings was the difference in the needle penetration or withdrawal forces through the designated “face” and “back”. As the second penetration or withdrawal occurred, the forces were greatly reduced. On further needle penetration cycles beyond the initial one, the percentage of damage suffered by the backing was minimal compared to the initial cycle damage.

4.4.2 Glass Mat Analysis

To characterize the degree in which the nylon veils affected the tufting forces with the composite glass backings, the glass mats created for the thermal transmittance in Chapter 3 were used. The penetration forces are in Figure 4.6, the withdrawal forces are in Figure 4.7, and the impregnation factors for the glass mats can be found in Table 3.5.

The glass mat penetration data in Figure 4.6 shows a linear response between the mat’s weight and the corresponding penetration force. The linear relationship is understandable when considering the quantity of glass fibers the tufting needle physically contacts as it traverses through the mat structure. As the glass fiber density increases, the number of fibers that actually contact the tufting needle increases, thus increasing the needle/fiber frictional force and the tufting force deriving from it.

No relationship was evident between fiber staple length in the mats and needle penetration force. Fiber length did not affect the number of fibers contacting the single tufting needle on mat transversal, but rather the probability that the same fiber would come into contact with a different needle during actual needle bar tufting. Likewise, no

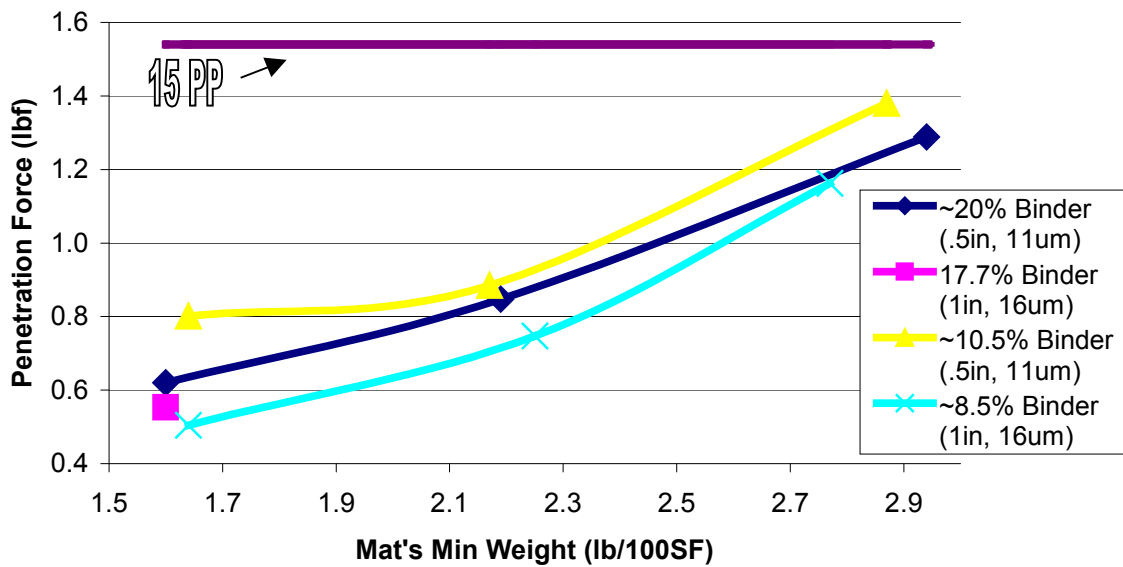


Figure 4.6: Needle Penetration Forces of Bare Glass Mats. The data is grouped by percent binder, staple length, and diameter of the glass fibers.

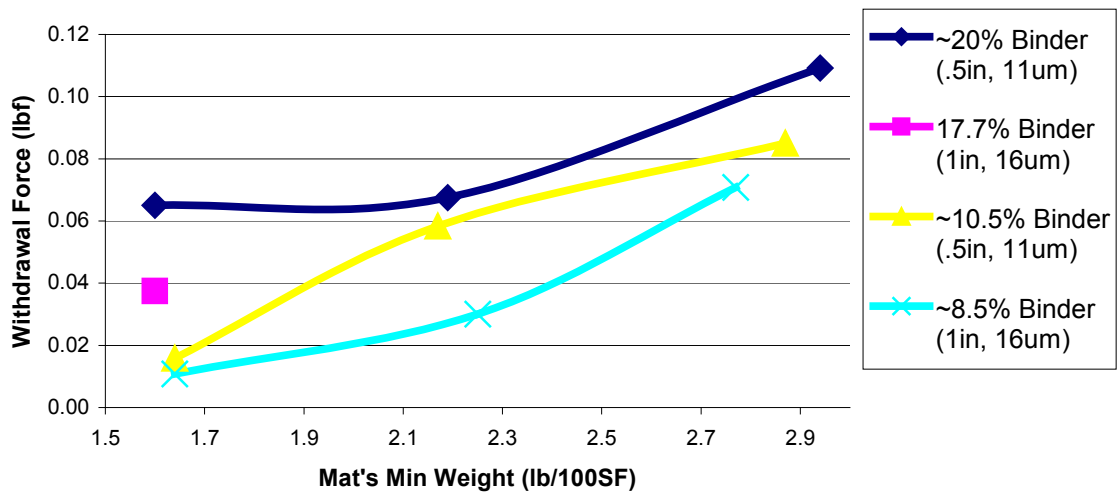


Figure 4.7: Needle Withdrawal Forces of Bare Glass Mats. The data is grouped by percent binder, staple length, and diameter of the fibers. No nylon involved.

apparent relationship existed between the needle penetration force and the percent acrylic binder used in the mats. In Figure 4.6, the glass mat that displayed the highest penetration force contained ~10.5% binder by weight, versus the maximum mat acrylic binder level of 20%. In summary, the factor most responsible for generating a desired tufting needle penetration force in glass composite backings core glass mat's fiber density.

If the final backing consisted of a bare glass mat, to achieve the same penetration force as the 15 pick, woven PP backing, the amount of glass needed would be ~4.5 oz./yd.². The density of the original glass mat backing that was successfully machine tufted (see Chapter 3) was 8.92oz./yd.². The amount of glass in the Class I backings was ~3.4 oz./yd.², which indicates that with the addition of nylon veils to the backing, the tufting forces are increased while maintaining a minimal amount of glass.

Concerning the withdrawal forces of the glass veils, the same trends observed for the penetration force can be identified with the withdrawal force (Figure 4.7). The needle withdrawal force increased with mat density. In Figure 4.7, the glass mats containing 20% binder exhibited the highest needle withdrawal forces. With mats of the same weight, as the percent binder decreased, the withdrawal force also decreased. However, the differences were within experimental error, and thus no definite benefit of having more or less binder present in the backing could be concluded.

When comparing the withdrawal forces of the PP backing to the glass mats as a group, the latter's needle withdrawal forces were significantly lower than that of the former (PP backing = 0.62 lbs. force), which could be seen in the holes formed by the tufting needle. The penetration of the tufting needle in the glass backings produced

bigger, permanent holes in the glass backings than the PP backing which was associated with the decrease in the withdrawal force between the two types of backings, see Section 4.4.6.1. The lower needle withdrawal forces for the glass mats dictate that an addition of one or more nylon layers is needed for the final glass composite backing to achieve similar tufting results to the PP backing standard.

4.4.3 Determination of Consolidation Parameters

4.4.3.1 Determination of Consolidation Time

Thermal consolidation of the composite primary backings, accomplished by heating the structures to the softening/minimal flow temperature of nylon 6, allowed better adhesion of the nylon layers to the core glass mats while further decreasing the propensity of glass “fly” to escape the structures during the machine tufting process. Of the six new composite primary backings, only one, **3893**, had a nylon 6 film applied to the glass mat, while the others had nylon 6 nonwoven veils applied to the glass mats’ surfaces. The film was less likely to tear during the delamination process, allowing for adequate testing.

In determination of the thermal consolidation temperature, a DSC scan of the undried nylon 6 film was conducted (Figure 4.8). From the DSC, the melt temperature of the nylon 6 film was ~218°C. The endotherm peak appearing in the DSC plot at ~70°C in the initial heat cycle, but not in the second heat cycle, was attributed to the vaporization of residual regain moisture present in the nylon film.

A temperature of 230°C was selected to run trial consolidation samples of the **3893** backing. From the DSC analysis, the 230°C temperature would allow slight melt

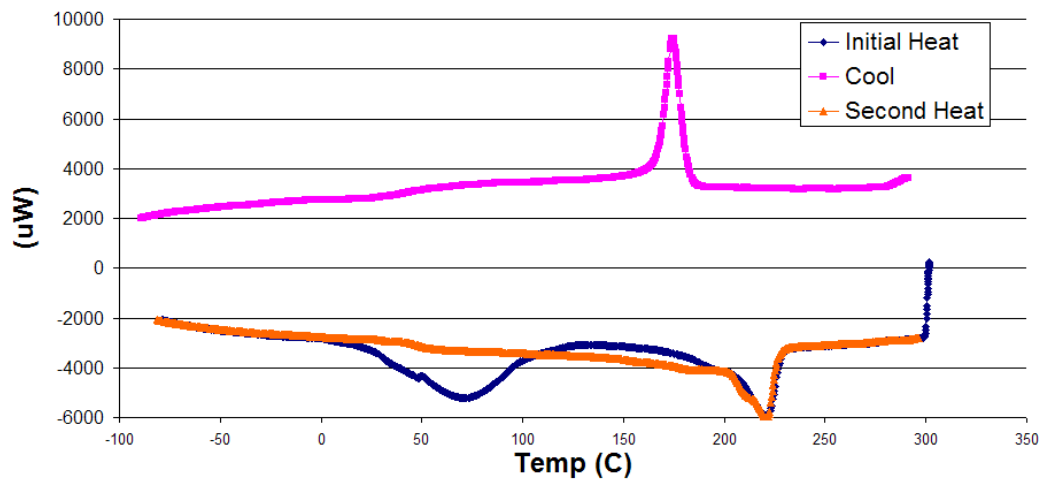


Figure 4.8: DSC of Nylon 6 Film Removed from Backing 3893

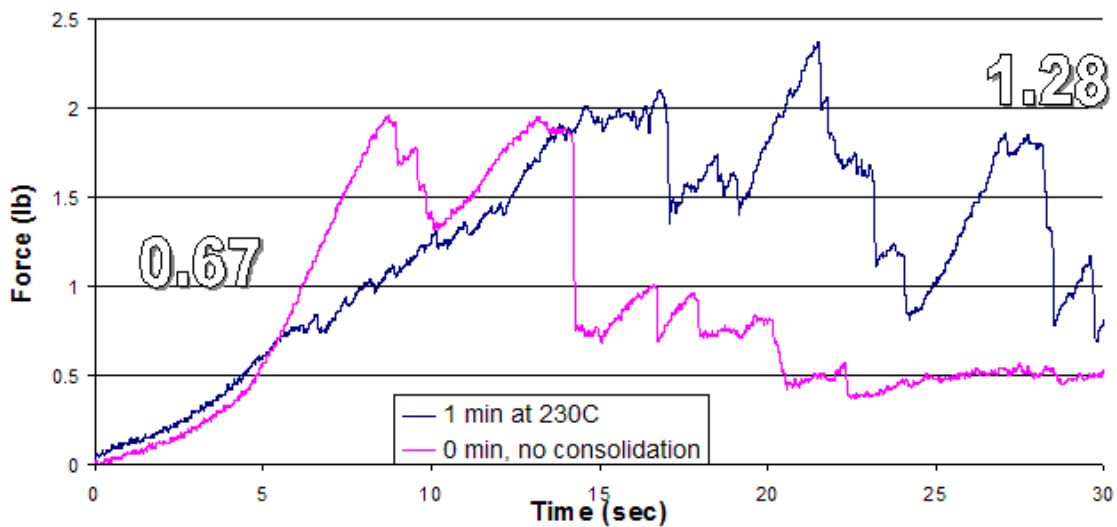


Figure 4.9: Delamination Force of Nylon 6 Film from Glass Veil in Backing 3893. The figure shows the force acting on the load cell as film separated from the glass mat backing. The delamination strength of the nylon 6 film in the unconsolidated composite backing was 0.67 lb./in. The delamination strength after 1 min./230 $^{\circ}\text{C}$ consolidation rose to 1.28 lb./in.

flow to occur in the nylon 6 films while a consolidation time frame could be established. Six samples of construction **3893** composite backing were heated for 1, 2, 4, 6, 8 and 10 minutes in a batch 230°C oven, with a seventh sample retained as the unconsolidated standard. After heating, the delamination forces of the samples were measured for the unheated backing sample and the sample heated for one minute at 230°C (Figure 4.9).

The delamination force analysis procedure stated in Section 3.2.2 was followed, but instead of separating the nylon resin layer from the carpet backing, the nylon film was separated from the glass mat core of the composite backing. After heating for one minute at 230°C, the delamination strength ~doubled, from 0.67 to 1.28 lb./in. The rest of the samples heated at varying times were not tested due to the inability to achieve the minimal manual separation of the nylon film from the glass veil needed to produce the end lengths to run the delamination test according to TM ASTM D 3936-97. The nylon films when heated for longer than 1 minute were too well-adhered to the glass mat or ripped on attempted manual separation at the sample ends, not allowing generation of enough lengths of material at the ends to mount the samples in the Instron Tester's grips.

To insure that the nylon 6 film was intact after thermal consolidation, micrographs of the samples were taken. In Figure 4.10, as the consolidation time increased, the holes in the nylon film caused by the penetrating polyester monofilament yarn composing the chain stitch constantly increased, i.e., at longer periods of thermal time exposure, more of the glass mat was exposed. To achieve effective consolidation of the nylon film to the glass mat without excessive film structure loss, a rapid consolidation time at 230°C was dictated by the data.

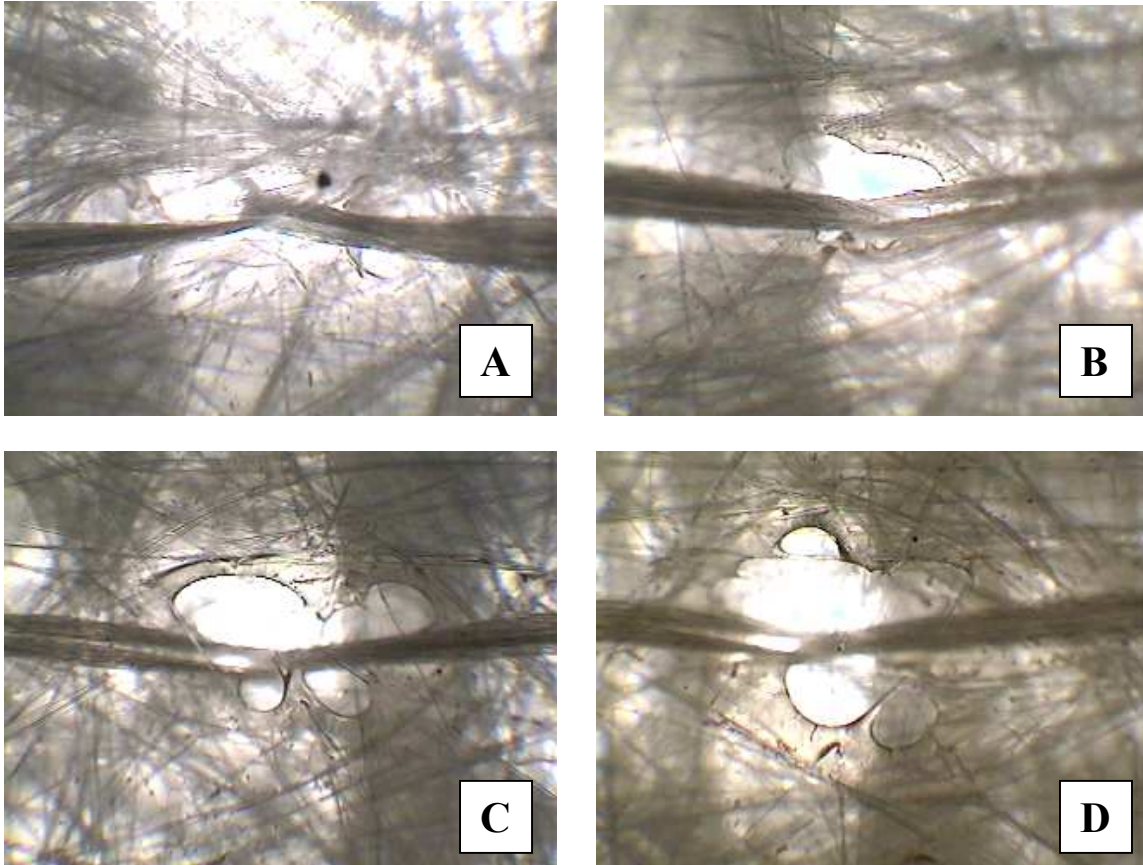


Figure 4.10: Microscopy Images of Backing 3893 at 4x Magnification After Several Consolidation Temperatures. A: Backing **3893** with no consolidation; **B:** Backing **3893** consolidated for 1 minute at 230°C; **C:** Backing **3893** consolidated for 6 minutes at 230°C; **D:** Backing **3893** consolidated for 10 minutes at 230°C.

4.4.3.2 Determination of Consolidation Temperature

To find the ideal consolidation temperature and to determine if the thermal consolidation of the composite backings would be better done before or after tufting, composite backing *C* containing nonwoven nylon veils on both sides of a glass mat core was consolidated at several temperatures in the batch oven. The time that each of the specimens was heated was kept below one minute in accordance to the findings with the delamination of consolidated backing **3893**. The needle penetration and withdrawal forces on the consolidated *C* samples are shown in Figure 4.11. The unconsolidated sample was noted at the 21°C mark, or room temperature.

As the temperature of consolidation increased to 218°C, the force to penetrate the needle decreased, but the withdrawal force increased. As to the needle penetration force, since as the nylon flows and encapsulates the glass, the veil ultimately thins, presenting less thickness for the needle to penetrate. The increase in withdrawal force of backing *C* at this consolidation temperature is most likely due to an increase in the frictional force of the needle against the backing. In the unconsolidated samples, the withdrawal force/frictional force acting upon the needle was due to more of individual components of the backing, where in the consolidated sample the backing was no longer a “sandwich” of components but rather a unified backing and the frictional forces are thus united.

As the consolidation temperature increased, the nylon continually thinned and ultimately pooled, forming droplets at the intersections of the glass fibers and adding to the binding force of the glass nonwoven structure (Figure 4.12). The excessive flow of the nylon veil at the higher consolidation temperatures eventually created a rigid backing with no elastic properties to aid in developing the desired needle penetration forces.

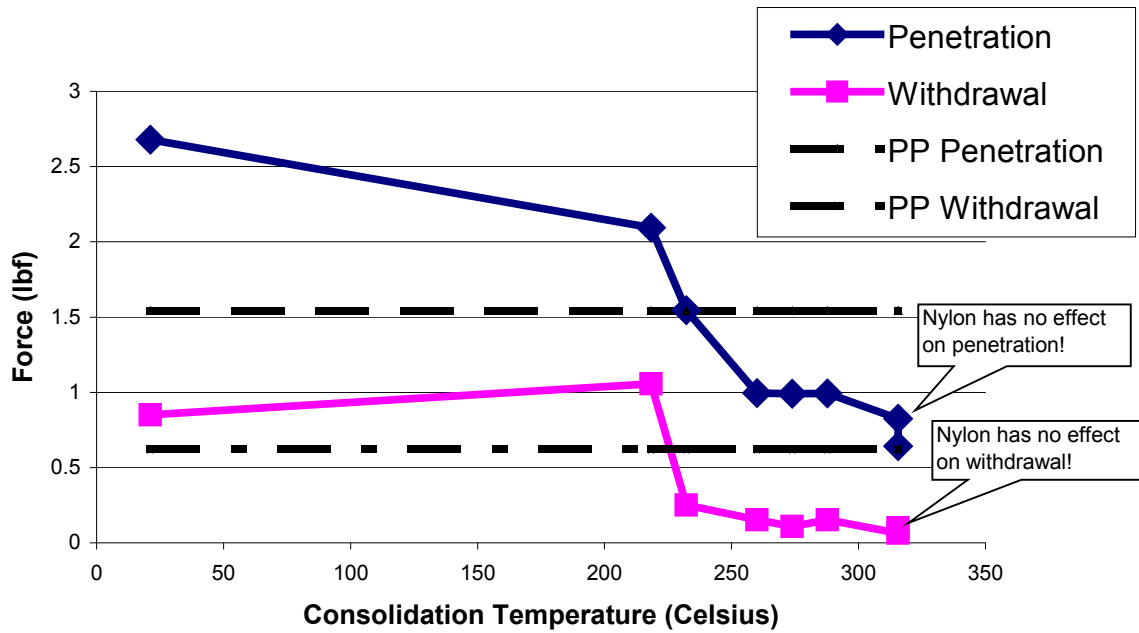


Figure 4.11: Needle Penetration and Withdrawal Forces of Thermally Consolidated Backing C. Each point on the plot represents a temperature at which a sample of backing C was consolidated. For comparison, the needle forces for the PP backing are represented by the solid and dashed lines. The callouts mark the points where the backing behaves like a glass veil and not a composite backing.

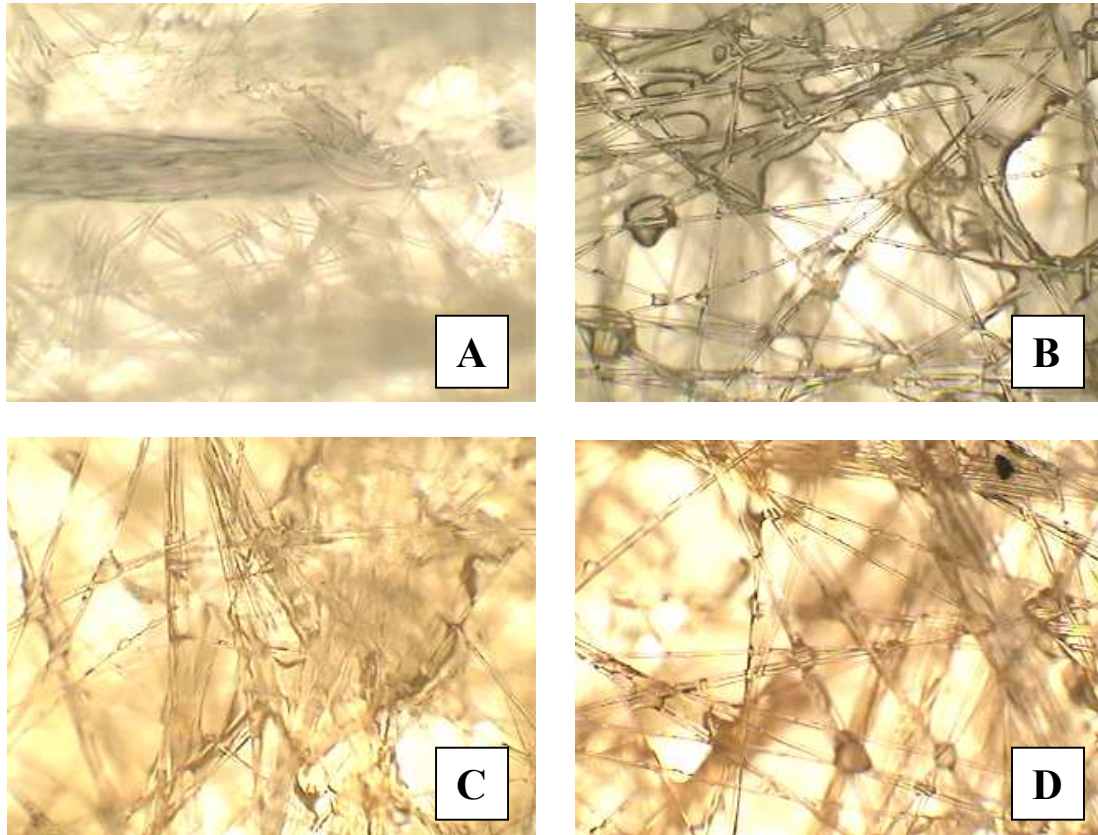


Figure 4.12: Microscopy Images of Thermally Consolidated Backing C. All Figures are at 10x magnification of the backings surface: **A:** Sample consolidated at 218°C for 40sec.; **B:** Sample consolidated at 260°C for 30sec.; **C:** Sample consolidated at 288°C for 20sec.; **D:** Sample consolidated at 315°C for 10sec.

Table 4.2: Standard Deviation of Needle Forces Versus Consolidation Temperature.
Data comes from Figure 4.11.

Consolidation Temperature (Celsius)	21	218	232	260	274	288	316	316
Penetration STDEV (lbf.)	0.37	0.31	0.23	0.13	0.14	0.12	0.13	0.09
Withdrawal STDEV (lbf.)	0.18	0.19	0.11	0.04	0.04	0.03	0.04	0.05

When the temperatures reached 288°C, the needle forces were equivalent to those of the initial bare glass mat backing (estimated from the data in Figures 4.6 and 4.7), and the nylon no longer played a contributing role in the forces. Table 4.2 data supports the plot in Figure 4.12. As the consolidation temperature increased, the nylon droplets in the glass mat became more uniform. The thinning and pooling of nylon on the surfaces as viewed in the micrographs (Figure 4.12) became more symmetrical and uniform throughout the backing cross section. The melted nylon's melt drop uniformity is thus reflected in the standard deviation of the data from testing the samples. The increased uniformity of the composite backing with temperature of consolidation was accompanied by a decrease in the tufting needle forces, and raised the possibility of increased release of glass "fly" during tufting due to the exposure of the glass core upon nylon veil disintegration.

Of the tested composite glass backings, the Class II backings were thermally consolidated because the backings were fully encased in nylon preventing any glass fibers from escaping. The Class I backings all contained exposed glass surfaces composed of the 16 micron (brittle) E-glass fiber that could potentially contribute to fine particle "fly" generation during the machine tufting process. As a result, only the thermally-consolidated Class II backings **A, B and C**, in which the probability of fractured glass fibers escaping during tufting was minimal due to the nylon veils encasing the core glass melt and the flexible 12 micron glass fiber used to form the latter, were carried forward to machine tufting on a pilot unit at Shaw Industries' Research & Development Laboratories in Dalton, GA.

As indicated in Figures 4.11 and 4.12, the most effective consolidation temperature was 218°C for 45 seconds, which resulted in the highest obtainable tuft withdrawal without exposing the glass core. Figure 4.12, Image A, confirmed that the developed consolidation process did not expose the glass core.

4.4.4 Consolidation of Composite Backings *A*, *B* and *C*

After consolidation of the composite backings under the optimized conditions, consolidated at 218°C for 40 seconds, the tufting needle penetration and withdrawal forces were measured (Table 4.3). The continuous consolidation process with backings *A* and *B* did not produce the desired results in comparison to those of the ideal consolidated sample *C*. The resulting needle forces for backings *A* and *B* from this process either remained the same or decreased significantly. The reason for the failure to generate the expected needle forces was unexpected heating problems encountered during consolidation. In the industrial trial, several heat zones failed to maintain the set temperature, forcing adjustment of other heating zones to compensate. If the continuous consolidation process had exactly duplicated the trial run conditions, the needle force results should have been approximated, i.e., they should have increased under the thermal consolidation conditions. However, microscopy showed that the consolidation did not expose the glass cores, and the main purpose for consolidating the composite backings to better encapsulate the glass core was achieved.

Table 4.3: Needle Force Measurements of Consolidated Composite Backings *A*, *B*, and *C*. The forces are of the unconsolidated analogs and the standard 15 pick woven PP primary backing to the consolidated backings at 218°C for 40 seconds.

	Penetration (lbf.)		Withdrawal (lbf.)	
Backings	Unconsolidated	Consolidated	Unconsolidated	Consolidated
Tape	1.54	Not Applicable	0.62	Not Applicable
<i>A</i>	2.28	0.63	0.62	0.12
<i>B</i>	2.02	1.94	0.62	0.30
<i>C</i>	2.68	2.71	0.85	0.45

4.4.5 Tuft Bind Strength Versus Yarn Denier of Mended Primary Backings

To project how the developed backings will behave in the machine tufting process, the PP and Class I and II glass backings were tufted using a pneumatic hand tufter, or mending tool, which is used to repair defects in carpet in manufacturing plants, and the tuft bind strengths of the various backings were compared (see instrument and process descriptors below). The procedure detailed in Section 3.2.4 was followed to measure the tuft bind strength of the hand-tufted backings. The tuft bind strengths of the composite glass backing carpets were ~half those for the PP backing carpet (Figure 4.13). As shown in Table 4.3, the hand tufted, thermally-consolidated backings *A*, *B*, and *C* produced lower tuft bind strengths than the unconsolidated backings (Figure 4.13).

The tuft bind strengths of the hand-tufted backings cannot be directly linked to the backings' measured needle penetration-withdrawal forces, Figures 4.3, 4.4, and 4.3, as the industrial mending tool uses a metal tube instead of a tufting needle to insert the yarn into the backing. A metal cylinder penetrates the backing and a compressed air stream forces the yarn through the backing to form the tuft. With this method, more damage is

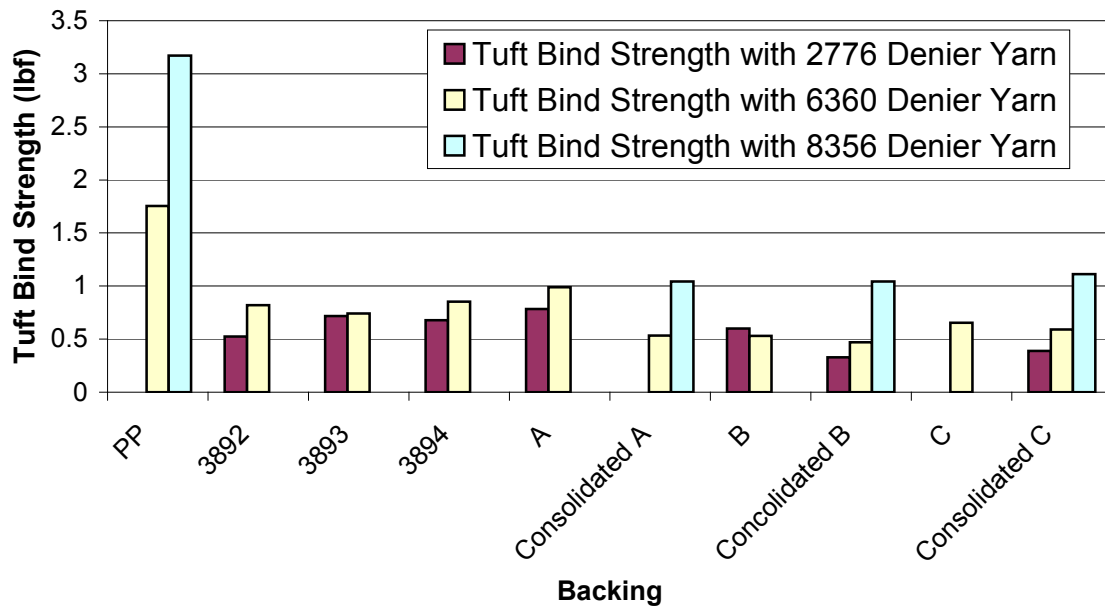


Figure 4.13: Tuft Bind Strengths of Hand-Tufted Composite Glass Backings. The hand-tufted yarns were: a two-ply, 2776 denier; a three-ply, 6360 denier; and a four-ply, 8356 denier construction.

created in the backing than with the empty tufting needle, resulting in a “looser” tuft in the backing than would have been obtained with needle insertion.

4.4.6 Validation of Test Method

4.4.6.1 Tuft Needle Penetration Force Correlated with Damaged Area

The tufting needle penetration method exhibited a relationship between the reduction in penetration force of the needle for multiple cycles and the size holes left in the backings from the first needle penetration. The holes left in the backings from the needle on first cycle penetration can be seen in Figure 4.14. As anticipated, the holes created in the standard woven PP backing were much smaller than those in the developed glass backings, attributed to the elastic nature of the PP that allowed it to contract after the needle was removed from the hole. In plotting hole sizes versus reduction in needle penetration force for the first cycle in Figure 4.15, a linear relationship resulted.

4.4.6.2 Tuft Bind Strength Versus Needle Withdrawal Force

To verify whether the needle forces could be correlated to the tuft bind strength, backings thermally-consolidated *A*, *C*, and the *original glass mat* were machine tufted along with the woven 15 pick PP backing. *A* and *C* were tufted and not *B* because during the tufting process, backing *A* scissored repeatedly, which caused the omission of sister backing *B* (the only difference in the two construction was that *B* contained a brominated flame retardant in its acrylic binder) and direct transition to the tufting of the heavier glass mat core construction, *C* (Table 4.1). When consolidated backing *C* was tufted,

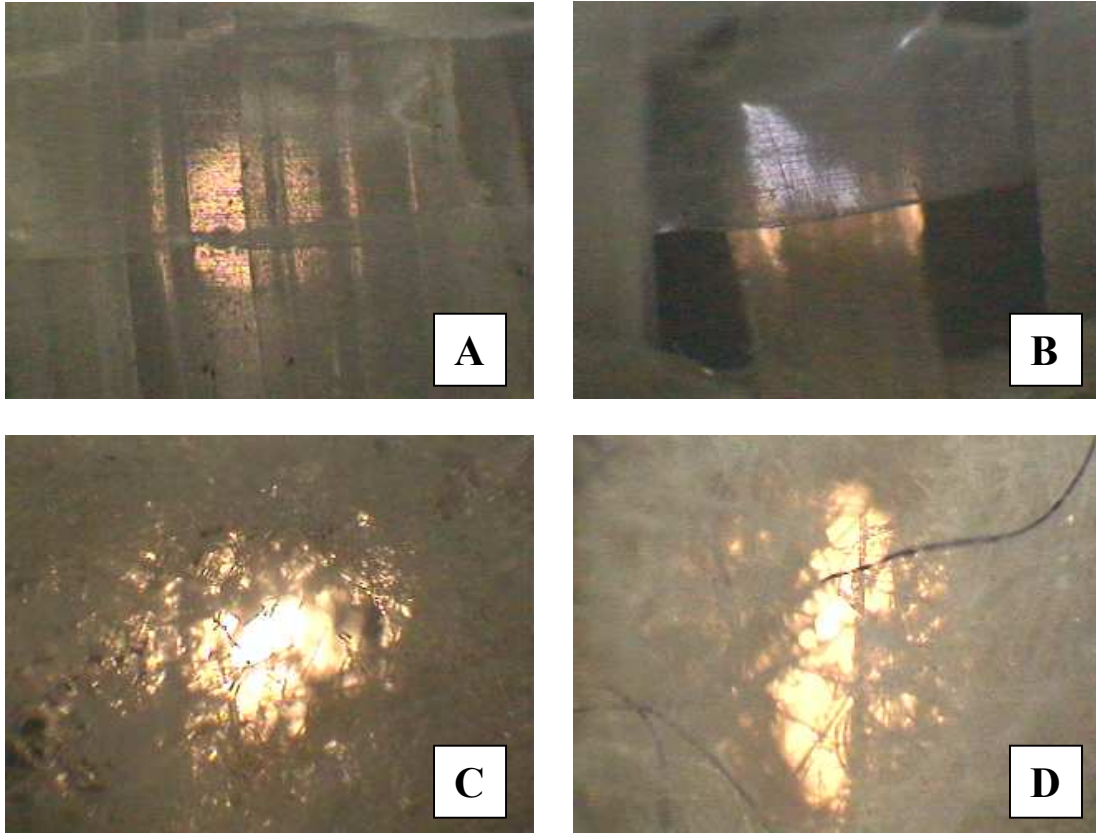


Figure 4.14: Microscopy Images of Backings After Tufting Needle Penetration. All Figures are at 4x magnification of the backing's surface: **A:** Untufted woven, 15 pick PP backing; **B:** Tufted woven, 15 pick PP backing; **C:** Tufted consolidated *A* glass backing; **D:** Tufted consolidated *C* glass backing.

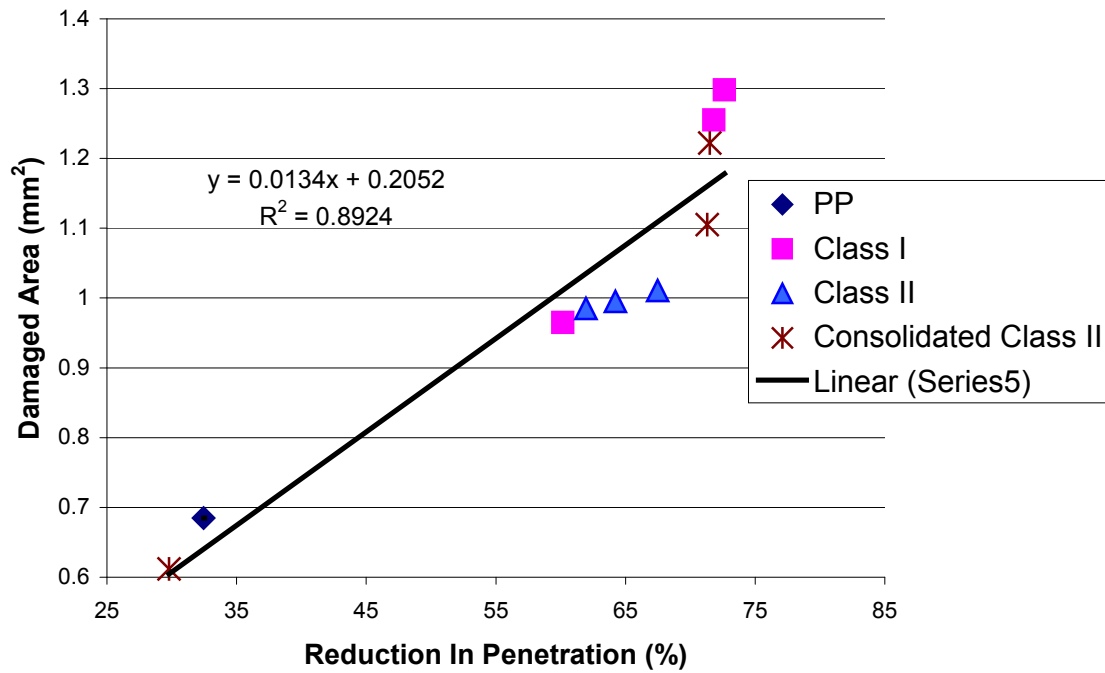


Figure 4.15: Damaged Area on Backing Versus Reduction in Tuft Penetration.
 Damaged area was calculated from 12 images and averaged.

scissoring was not evident, but the backing was weakened on tufting in the cross machine direction, as tufted material could be easily pulled apart by hand force.

From examining the data in Figure 4.16, a linear relationship existed between the tuft bind strengths of machine tufted, glass-based backings and needle withdrawal forces (R^2 value of 0.99). When the PP backing was included in the data to determine the trend line, the R^2 value decreased to 0.88, indicating that backings made from different materials into different base constructions by different formation processes cannot be directly compared in this type analysis. From the trend line in Figure 4.16, the equation that relates the tuft bind strength to the tuft withdrawal force is Equation 4.2 (the equation of a straight line):

Equation 4.2: Tuft Bind Strength = (Needle Withdrawal Force x 0.94) + 0.39 lbf.

Equation 4.2, with the gradient being close to 1.0, quantified a direct link between the two forces. The real difference between the two measurements was the plot's ordinate intercept value 0.39 lbf. Since the needle withdrawal force measurements were made without yarn in the tufting needle, this added value is apparently the frictional force against the backing that the yarn adds to the tuft bind strength [15, 16].

Similarly, a correlation between the tuft bind strengths and the needle penetration forces of the backings was evident (Figure 4.17). The glass-based backings again produced a close fit trend line (R^2 value of 0.92), but the relationship was not as linear as that shown in Figure 4.16.

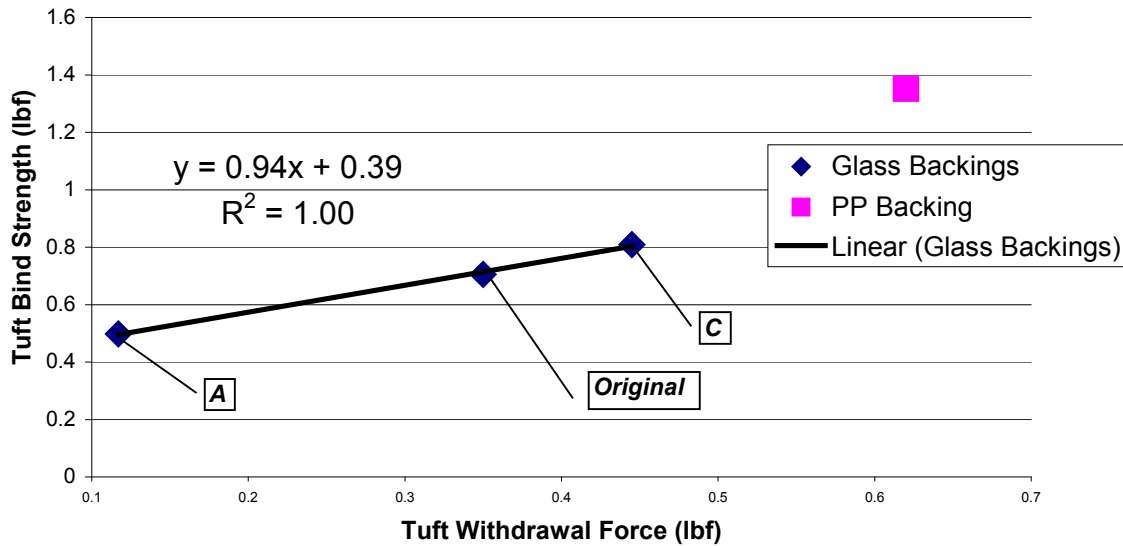


Figure 4.16: Tuft Bind Strength Versus Needle Withdrawal Force. The glass backings are separated from the PP backing in the determination of the trend line. “Original” refers to the initial bare glass mat backing that was the first machine tufted material.

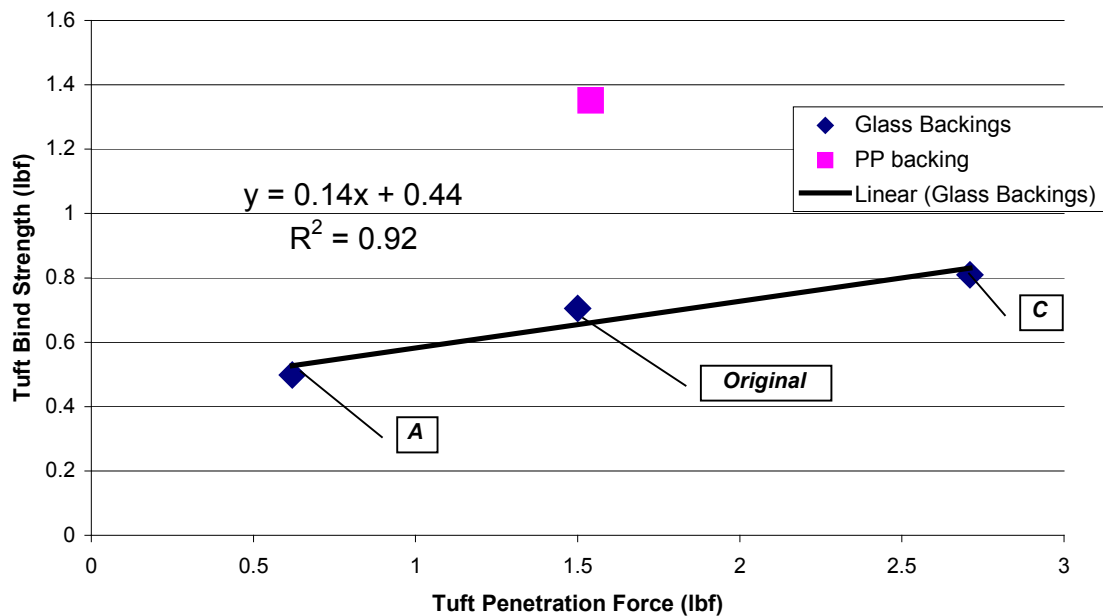


Figure 4.17: Tuft Bind Strength Versus Needle Penetration Force. The glass backings are separated from the PP backing in the determination of the trend line. “Original” refers to the initial bare glass mat backing that was the first machine tufted material.

CHAPTER 5

DYEING OF TUFTED CARPET AND COMPOSITE BACKINGS

After the tufting process, the carpets and composite backings without tufted piles were dyed to assess their stability to commercial wet processing conditions. After tufted carpets are dyed in industry, the latex (conventional process) or the Elvamide® resin (developed process) would be applied in the final carpet consolidation step to complete the manufacturing process. However, with a layer of Elvamide® resin already applied to the initial bare glass mat backing in the in pre-dyeing extrusion step, most of the experiments in this chapter will simulate industrial coloration of the tufted carpet (only cut pile, un-dyed yarn constructions) after the extruded resin application. The composite glass backings were dyed without going through the tufting process to characterize their dyeability without the interference of the tufts since the backings contained nylon 6 veils that were dyeable.

Two methods of dyeing were explored with the developed carpet constructions, simulating both continuous and batch processes. The continuous process, although hard to truly replicate in a laboratory setting, simulated such variables as padding procedures, liquor concentrations and the effects of steam on the carpet. The batch process, simulating atmospheric exhaust beck dyeing of carpet, was the easiest to replicate by

simple beaker dyeings. The aspects of dyeing such as time and temperature on exhaustion were quantified.

5.1 Introduction to Dyeing

Dyeing methods vary with dye class, the substrate to color and the form of the material. Two laboratory methods were used to dye the developed carpet substrates, simulating conditions employed in commercial batch exhaust (beck) or continuous dyeing.

5.1.1 Atmospheric Batch Dyeing of Carpet

Commercial carpet beck dyeing is a batch exhaust process in which the carpet, in rope loop form, is rotated via a winch or reel through the stationary dye bath. In some beck operations, pumps are also used to circulate the dye bath through the carpet as the latter is simultaneously rotated through the bath by the winch [14, 18]. With either process, the beck is first filled with water to the specified liquor ratio, the carpet is loaded and rotated to wet it out, the dye formulation concentrate is dropped into the machine, and the temperature is then raised to the maximum hold point at a heating rate of 3-5F/min. with direct saturated steam injection. After holding at the maximum temperature for a specified period of time (often 30 min.), the container is then drained of its dye liquor and filled with water to rinse the carpet of unexhausted dye. Overall, the batch beck dyeing process produces excellent color uniformity throughout the carpet sample, but is obviously limited to the amount of carpet that can be loaded into the beck per cycle.

5.1.2 Continuous Dyeing of Carpet

In a commercial continuous dyeing process, the open-width carpet first traverses a padding operation to apply the dye solution concentrate, and then passes through a steam chamber to fix the dye to the substrate. The padding operation may be by a simple “saturated pad- pressure nip” process, or more often today, by a Kuester’s Fluidyer Applicator® fitted with a air inflatable rubber bladder that presses the face of the carpet against the slot from which the dye liquor exits [64]. After steam fixation of the dye, the carpet then traverses through several washers to insure the removal of any unfixed dye, and finally it is passed through a drying oven to remove the water.

5.1.3 Nylon and Acid Dyes

In the developed constructions, both the face yarn and parts of the composite primary backings consisted of nylon components (either veils or films). For dyeing, nylon is characterized by its polymer chain end groups. The end groups consist of a weakly basic amine, -NH_2 , and a weakly acidic carboxylic acid, -COOH , both of which can be ionized in water at an appropriate pH range [65]. Ionic attractions occur between the fiber charges and oppositely charged colorants present in the corresponding dye baths. For the vast bulk of commercial nylon carpet containing regular-dyeable nylon 6 or 66 yarn tufts, the amine group is converted in the dyeing process to the corresponding ammonium cation, -NH_3^+ , by reducing the pH of the dye bath to less than 7 with addition of an acid (normally acetic, although phosphoric is also being used) after dye leveling has been achieved. Acid dyes, which contain negatively charged sodium sulfonate functional groups, $\text{-SO}_3^- \text{Na}^+$, are in the class of choice for coloration of nylon carpets [18, 65].

5.2 Tufted Carpet Dyeing Procedures

5.2.1 Beaker Dyeing of Developed Carpet Constructions

To replicate exhaust batch dyeing of carpets in becks, samples were first cut into 3 by 3 inch squares. The samples were then placed into 1 L glass beakers that contained an appropriate acid dye liquor formulation, and the baths were heated by hot plates. The dye formulation consisted of 2.5% o.w.f of C. I. Acid Red 361 dye (Tectilon Red 2 B from Sigma-Aldrich), 1.0% o.w.f. Irgalev PBF (an anionic alkyl diphenyl-ether derivative used as a leveling agent for nylon coloration manufactured by Ciba Specialty Chemicals), 2.0% o.w.f. ammonium sulfate, and 0.3% o.w.f. sodium thiosulfate [66]. Percent o.w.f., *On Weight of Fabric*, is an industry term used to express concentration of colorants and auxiliary chemicals in dye formulations based on the weight of substrate employed.

With the % o.w.f. and mass of the sample, the weight of every chemical was measured and placed in the corresponding beaker where it was then diluted with distilled water. The amount of added distilled water gave a liquor ratio, L.R., of 30:1, i.e., for every one gram of carpet, 30 mL of distilled water was used in the dyeing process. For samples that were dyed at the atmospheric boiling point of water, the dye liquor was either heated to the boil before the carpet entered the bath (henceforth termed *instantaneous boil* exposure) or after it entered the bath (termed *rise to boil* exposure).

5.2.2 Pressure Dyeing of Developed Carpet Constructions

To simulate commercial jet dyeing of carpets, a process occasionally used to color nylon-containing constructions such as 90% nylon-10% polyester yarn blends, dye the

samples under slight pressure, a Roaches Colortec® Small Package, Beam and Loose Fiber Dyeing Machine was used [67]. Carpet samples of 2 in. by 10 in. were used. To simulate commercial jet dyeing of carpets, pressure dyeing was utilized in the Colortec® machine to reach temperatures above the boiling point of water. The machine was set to dye the carpet samples at 115°C while it pumped the dye liquor through the samples at a rate of 5 L./min. The dye recipe consisted of 2.5% o.w.f. of C. I. Acid Red 361 dye, 1.0% o.w.f. Irgalev PBF leveling agent, 2.0% o.w.f. ammonium sulfate and 0.3% o.w.f. sodium thiosulfate. With no samples present in the machine, the volume of liquid needed for operation was 2.5 L. The L.R. for this dyeing process is dictated by the minimum volume requirement coupled with the sample's weight. The L.R. used in the dyeing process was ~120:1.

The bath temperature was raised at a rate of 5°C/min., and was left steady for 30 min. at 115°C. Since the machine utilized pressure to achieve the 115°C temperature with the water medium, it dictated that all the samples be heated from ambient to the hold temperature, so only a *rise to boil* method could be utilized. After the 30 min. hold cycle at 115°C, the hot liquor was drained out of the machine, thus allowing the pressure to equalize for the removal of the samples. Once removed, the hot carpet samples were then thoroughly rinsed in room temperature water to remove any unfixed dye.

5.2.3 Pad-Steam Dyeing of Developed Carpet Constructions

In the continuous dyeing simulation procedure, the pad bath consisted of 4 g. of C. I. Acid Red 361 dye, 0.7 g. of ammonium sulfate, 0.1 g. of sodium thiosulfate and 1 mL of Iragalev PBF leveling agent dissolved in 1 L. of distilled water. The dyed carpet

samples were 2 in. wide by 8 in. in length. The pad bath temperature was either at room temperature or heated to induce higher exhaustion. Samples were placed in the pad bath for two minutes to saturate them with dye liquor. After two minutes, the sample was removed from the bath and squeezed dry by hand, giving a wet pick-up of pad bath of ~40% by weight of carpet.

To fix the dye to the substrate, the carpet samples were mounted on a metal frame, not under tension, and placed over a steam bath with the tufts of the carpet (the face) directed toward the surface of the steam bath. The frame was designed to hold the mounted sample over the water bath under slight tension to prevent it from sagging falling into the water steam bath [68]. The frame consisted of two aluminum plates that were 1/8th inches thick by 5 inches wide by 18 inches long. In the center of each plate, two rectangles were cut out that were 1.5 inches wide by 6 inches in length so that the carpet sample was exposed to the steam without falling through the frame. The frame was drilled and tapped to accept bolts so that the two metal plates could be bolted together and “frame” the sample.

The steam was produced using a Precision* General-Purpose Water Bath that was filled with enough water so that the sample was ~two inches from the water surface. The reason for the close proximity to the water was to condense the steam in the tufts, not in the atmosphere [17, 19, 68]. The close proximity also excluded as much air as possible, otherwise the presence of air would lower the rate of heat transfer from the steam to the carpet [17]. The bath was then brought to a vigorous boil to produce enough steam to ensure dye fixation.

After the sample was mounted in the frame, the assembly was placed over the steam bath for one minute to allow the sample to reach steam temperature, and then held for another four or six minutes for dye fixation. Based on commercial festoon steamers, the steam exposure time was judged long enough to effect substantial penetration of the dye into the mass and individual fibers of the substrate [17]. The samples were then removed from the steam bath and the frame, washed and allowed to air dry before additional tests were conducted.

5.3 Determination Of Dye Exhaustion

5.3.1 Lambert-Beer Law

The selective absorption of electromagnetic radiation is one of the most widely used techniques for both qualitative and quantitative analyses of materials. With the Lambert-Beer Law, a relationship between the absorption of light in the visible spectrum and that of the concentration of the absorbing dye molecules can be established [66]. Equation 5.1 depicts the Law where A is the absorbance, a is the absorptivity constant of the dye molecule, b is the path length of the sample, and c is the concentration of the

$$\text{Equation 5.1: } A = abc$$

sample in distilled water (ppm units). Equation 5.1 along with a spectrophotometer was used to calculate dye exhaustion in the sample carpet dyeings.

5.3.2 Spectrophotometer

From the electromagnetic spectrum of sunlight, the visible component (400-700 nm.) was used in the analyses of dye solutions. With the use of a Spectronic GENESYS* 6 UV-Vis Scanning Spectrophotometer and the principles of the Lambert-Beer Law, the exhaustion (transport) of the dye from the solution into the substrate was monitored by measuring the absorbance of the dye liquor at various times of the dye cycle. The spectrophotometer measured the drop in power of monochromatic radiation as it passed through the dye bath sample and relayed that information as either the transmittance or the absorbance of the sample.

The spectrophotometer had four basic components: the lamp, the wavelength selector, a detector and a sample holder with sample (Figure 5.1). The purpose of the lamp was to provide a spectrum of electromagnetic radiation to pass through the dye bath sample. The radiation was then passed from the lamp through a wavelength selector, which was set to allow a particular desired wavelength of the spectrum to pass through the sample, where absorbance took place. The radiation then was analyzed by the detector. The power level of the radiation passing through a standard, distilled water containing no light-absorbing chemical, to that of the initial power level was related to the transmittance of the dye bath sample as seen in Equation 5.2, where T is the transmittance, P_o is the power of the radiation before entering the sample, and P is the power after leaving the sample. The relationship

$$\text{Equation 5.2:} \quad T = [P / P_o]$$

between absorbance and transmittance is shown in Equation 5.3 where the absorbance of the sample is the negative logarithm of the transmittance. With the absorbance

$$\text{Equation 5.3: } A = -\log_{10} [T] = -\log_{10} [P / P_0]$$

measurement from Equation 5.3, Equation 5.1 was used to calculate the concentration of dye in the solution. In Equation 5.1, the path length (the inside width of the cuvet) was one cm., and the absorptivity constant a was calculated from the measured absorbance of several known concentrations of dye liquor. The individual, real-time sample dye concentration values were then extrapolated from that relationship.

5.4 Evaluation of Carpet Coloration by C. I. Acid Red 361 Dye

For dyeing purposes, an acid dye was chosen to dye the nylon in the backings and the nylon yarn. C. I. Acid Red 361 dye was chosen for its bright red shade so that once the sample was colored, varying depths of shade and any unevenness could be easily visually ascertained.

5.4.1 Determination of Absorptivity Constant, a

The first step in finding the absorptivity constant of the Lambert-Beer Law of the utilized dye molecule was to determine what wavelength to set the spectrophotometer so that maximum wavelength of absorption of the dye could be obtained. If the machine was not set to this wavelength in further work, e.g., establishing A vs. C plots, accuracy would be compromised. A sample of the dye liquor at a concentration of 50 ppm was

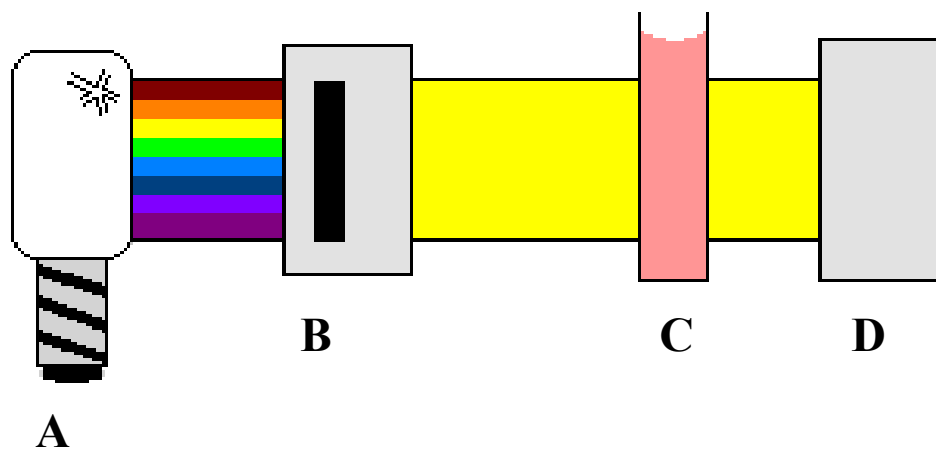


Figure 5.1: Simplified Schematic of the Spectrophotometer. **A** was the light source, **B** was the wavelength selector, **C** was the sample in a square cross-section cuvet, and **D** was the detector.

placed in a cuvet. The dye liquor was a solution of commercial C. I. Acid Red 361 colorant and distilled water. The cuvet was cleared of any air bubbles or fingerprints that would alter the absorption. The cuvet filled with dye solution was then placed in one of the sample holders of the Spectronic GENESYS* 6 UV-Vis Scanning Spectrophotometer, and another cuvet filled with distilled water was placed in the standard holder. The cuvet filled with distilled water acted as a calibration for the sample (zero absorbance) so that in the 50 ppm dye sample, only the absorption of the dye was taken into account.

The instrument was set to scan the visible spectrum (400-700 nm.), and the absorbance of the sample was measured every 3 nm across the range. The absorbance of C. I. Acid Red 361 dye versus wavelength can be seen in Figure 5.2. From the data, the wavelength of maximum absorbance was determined to be 506 nm. The instrument was set to this wavelength for all future measurements involved with this dye.

To determine the absorptivity constant, a , the absorbencies of various known concentrations of C. I. Acid Red 361 dye in distilled water were needed. Six dye concentrations were prepared: 50, 20, 10, 5, 2, and 1 ppm. By rearranging Equation 5.1, dropping out $b = 1$ cm and assuming an intercept of zero (no absorbance at zero dye concentration) Equation 5.4 results:

$$\text{Equation 5.4: } a = A / c$$

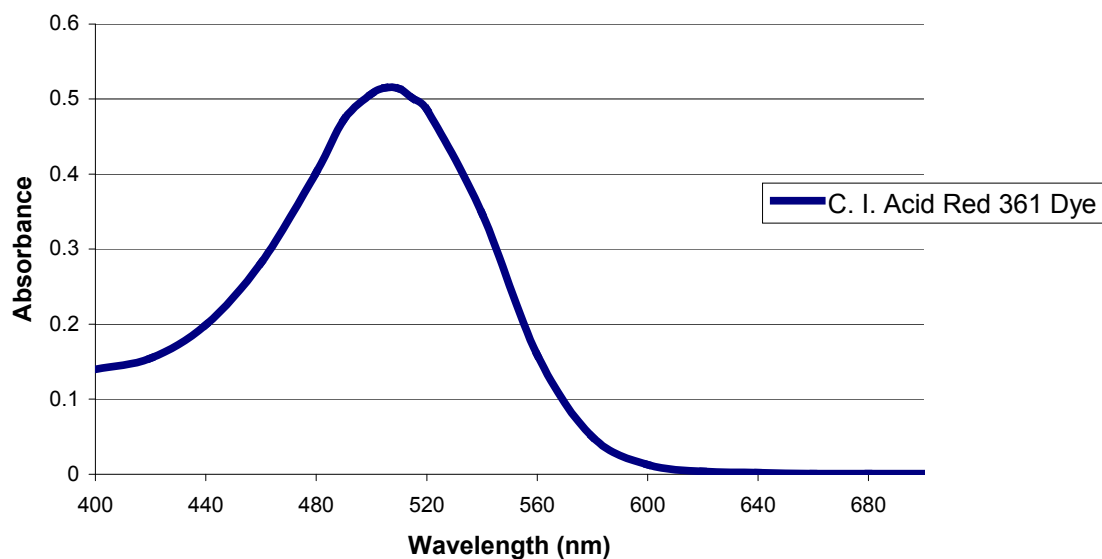


Figure 5.2: Absorbance Versus Wavelength for C. I. Acid Red 361 Dye. Yields the maximum wavelength of absorbance at the peak of 506 nm.

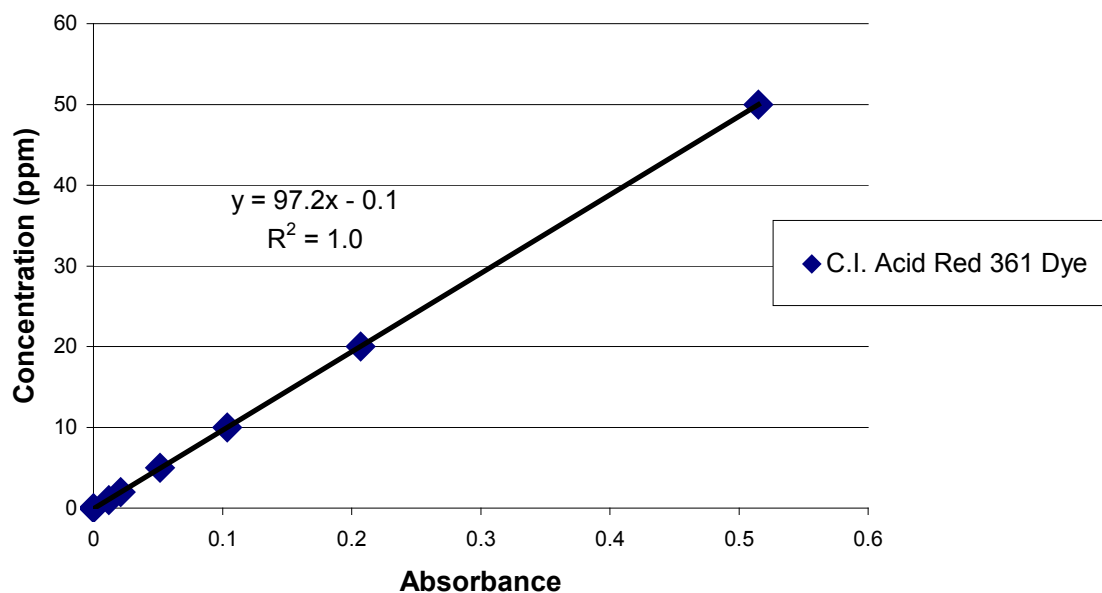


Figure 5.3: Dye Concentration Versus Absorbance for C. I. Acid Red 361 Dye. Slope of the straight line yielded the adsorptivity constant for a maximum wavelength of 506 nm.

By thus plotting absorbance vs. concentration of the dye with a (0,0) intercept, the slope of the resulting straight line was the absorptivity constant (Figure 5.3), which for C. I. Acid Red 361 dye gave a value of $97.2 \text{ cm}^{-1} \text{ ppm}^{-1}$.

5.4.2 Exhaustion

Calculating the dye exhaustion required two readings: a. The absorbance of the dyebath before the addition of samples ($t = 0$); and b. The absorbance of the dyebath at a certain time, t . The measurements were then applied to Equation 5.1 where the concentrations were equated. Equation 5.5 was then used to solve for the percent exhaustion (% E), where Co was the initial concentration of the bath and C was the

$$\text{Equation 5.5: } \% E = [(Co - C) / Co] * 100$$

concentration of the bath at a designated time t . To calculate the final exhaustion of the bath, the sample was removed and the entrained liquid dye bath was squeezed out and back into the container so that all unfixed dyes were left in the bath to contribute to the final concentration.

5.5 Dyeing Results and Discussions

5.5.1 Batch Dyeing of Glass-Based Primary Carpet Backings

Each of the next generation carpet backings was cut into three by three inch squares and weighed to determine the mass. Each beaker was filled to the appropriate volume of distilled water and was stirred to ensure dissolving of the chemicals. The

backings were then placed in a beaker with the dissolved dye, auxiliary chemicals and distilled water, and the beaker was placed on a hot plate. Once heated to the boil at a rate of 5°C/min., the samples were left to dye for 30 minutes. During this time, each sample was frequently stirred, and if needed, distilled water was added to maintain the liquor ratio. After 30 minutes, the samples were removed from the bath and the exhaustion was calculated. The dyed samples are shown in Figure 5.4.

5.5.2 Exhaustion Behavior of Glass-Based Composite Primary Backings

In Figure 5.5, the final percent exhaustion of the dye into the nylon veil fibers of the backings was measured and plotted. As the exhaustion plot shows, the **3893** backing exhibited the highest dye exhaustion of any of the backings. As seen in Figure 5.5, the two parameters run side by side. Of the developed backings, **3893** contained the highest weight of nylon per total backing mass, thus allowing for a greater percentage of dye exhaustion into the backing. The more nylon present in the backing, the more dye-sites for C. I. Acid Red 361 dye molecules to couple, which in turn provided for a darker shade and explained the visual variation of shade depth among the samples (Figure 5.4).

5.5.3 Batch Dyeing Of Tufted Carpets

With the analysis of how the backing constructions reacted to the dyeing process, the next logical step was to characterize how developed carpets would perform in the dyeing process. Since the first stage of prototype backings (*original glass mat* and PP) were machine tufted, they were used in this phase of testing along with the second stage composite backing **C**, which was also successfully tufted (see Section 4.4.6.2). Backing

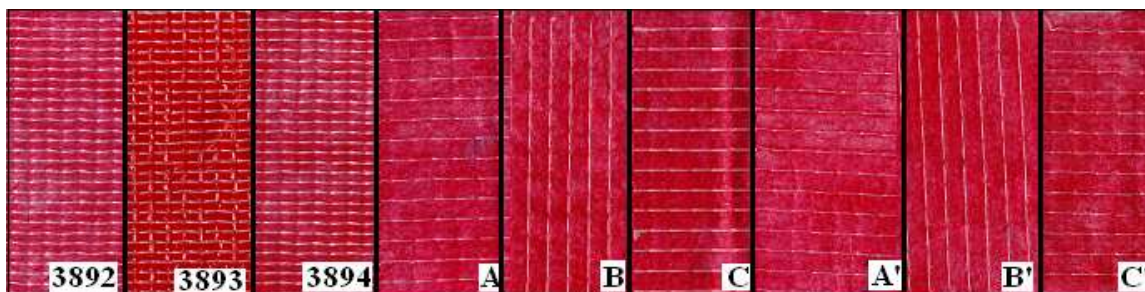


Figure 5.4: Images of Glass-Based Primary Carpet Backings. “3892” stands for backing 3892, “3893” stands for backing 3893, “3894” stands for backing 3894, “A” stands for backing A, “B” stands for backing B, “C” stands for backing C, “A” stands for consolidated backing A, “B” stands for consolidated backing B, and “C” stands for consolidated backing C.

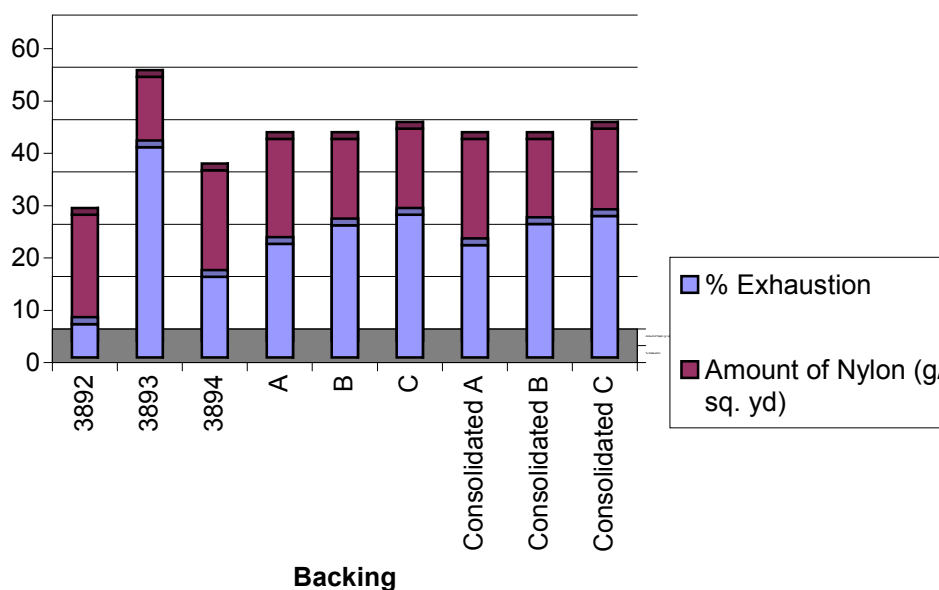


Figure 5.5: Dye Exhaustion Analyses of the Various Composite Glass Backings. The percent dye exhaustion is compared to the amount of nylon (g/yd.^2) present in the backings.

C was tufted with a predyed yarn, so the main focus of dyeing the carpet will be on dyeing the nylon 6 veils of the backing. In these initial dyeings of the first stage carpets, the applied PP secondary backing was removed by hand before dyeing due to its weak delamination strength.

The carpet dyed first was the cut pile (un-dyed) PP and bare glass mat backing carpets with 6 oz./yd.² of applied Elvamide® 8063 resin. The 3 and 9 oz./yd.² samples were not included in the dyeing studies since the tuft bind strengths and delamination strengths of the constructions were found to be the highest with the 6 oz./yd.² samples (see Chapter 3). The carpets made with Elvamide® 8201 was saved to be dyed later due to its lack of abundance needed for these initial dyeing trials. Only the cut pile carpet samples were used because the nylon 6,6 yarn tufted into the construction was undyed, while the yarn in the straight loop carpet was pre-dyed.

5.5.3.1 Dye Exhaustion Versus Temperature

The first carpet used in the batch dyeing analysis was the woven 15 pick PP primary backing with cut loop, un-dyed pile tufted yarn containing 6 oz./yd.² of applied Elvamide® 8063 resin. To determine the effects of exhaustion versus time, a sample of the carpet was dyed at the appropriate temperature while absorbance measurements of the bath were taken at selected time intervals. The carpets under went exhaust batch dyeing as detailed in Section 5.2.1. The solution's absorbance was measured and the bath was then raised to the appropriate temperature (either 50, 60, 70, 80, 90 or 100°C) via hot plate heating. Once the hold temperature was reached, a carpet sample was placed in the bath. At the following times: 5, 10, 15, 30, 45, 60, 75, and 90 minutes, the absorbance of

the dyebaths was measured and the exhaustion data was calculated. The exhaustion data in Figure 5.6 shows that as the temperature of the bath and the dyeing duration increased, so did the level of exhaustion. The data in Figure 5.6 began to plateau at around 30 minutes at the higher temperatures (80°C and higher). To achieve maximum dye adsorption, all samples were dyed at the boil for a period of 30 minutes.

5.5.3.2 Plasticized Flow Of Elvamide® 8063 Resin Film

After dyeing the carpet samples, a noticeable difference was observed in the appearance of the Elvamide® 8063 film, which appeared to have undergone water-induced plasticized flow [3, 69]. Since the melt temperature of the resin was 176 °C, the hot aqueous dyebath did not induce a true thermal polymer melt flow. From microscopy images of the backings (following procedures detailed in Section 3.2.5), Figure 5.7, the resin appeared to have instead undergone a plasticized flow, and moved into the back-tufts of the yarn [3, 69]. As the bath temperature increased, so did the movement of the Elvamide® film into the yarn back-tuft bundles. At the boil, the plasticized flow left irregular gaps in the resin film.

Plasticized flow is the induction/onset of segmental mobility for polymer chains in the amorphous (unordered) regions of the solid-state structure, and many commercial fibers are plasticized by small amounts of water or poor organic solvents (the latter called “plasticizers”) [3]. In these aqueous dyeing experiments, the water at the higher hold temperatures entered the nylon resin film in the amorphous regions, breaking the hydrogen bonds between nylon polymer chains. The breakage of these hydrogen bonds caused the free volume of the polymer network to increase and the resulting wet glass

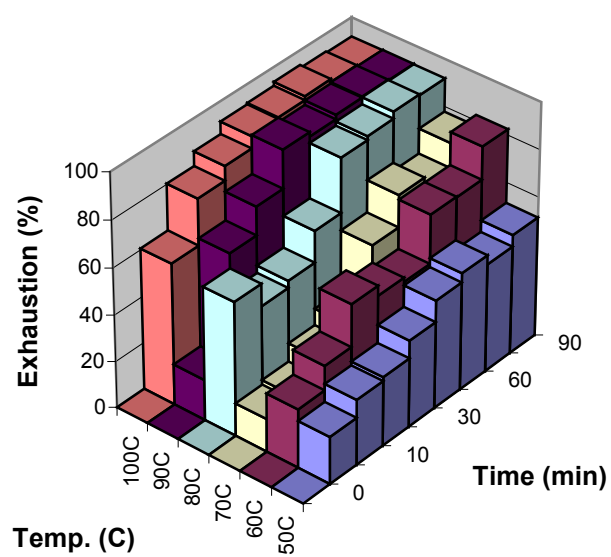


Figure 5.6: Dyeing Analyses of C. I. Acid Red 361 Dye Applied to Cut Loop, PP Backing Carpet with 6 oz./yd.² of Applied Elvamide® 8063 Resin. Samples were dyed in an instant boil mode.

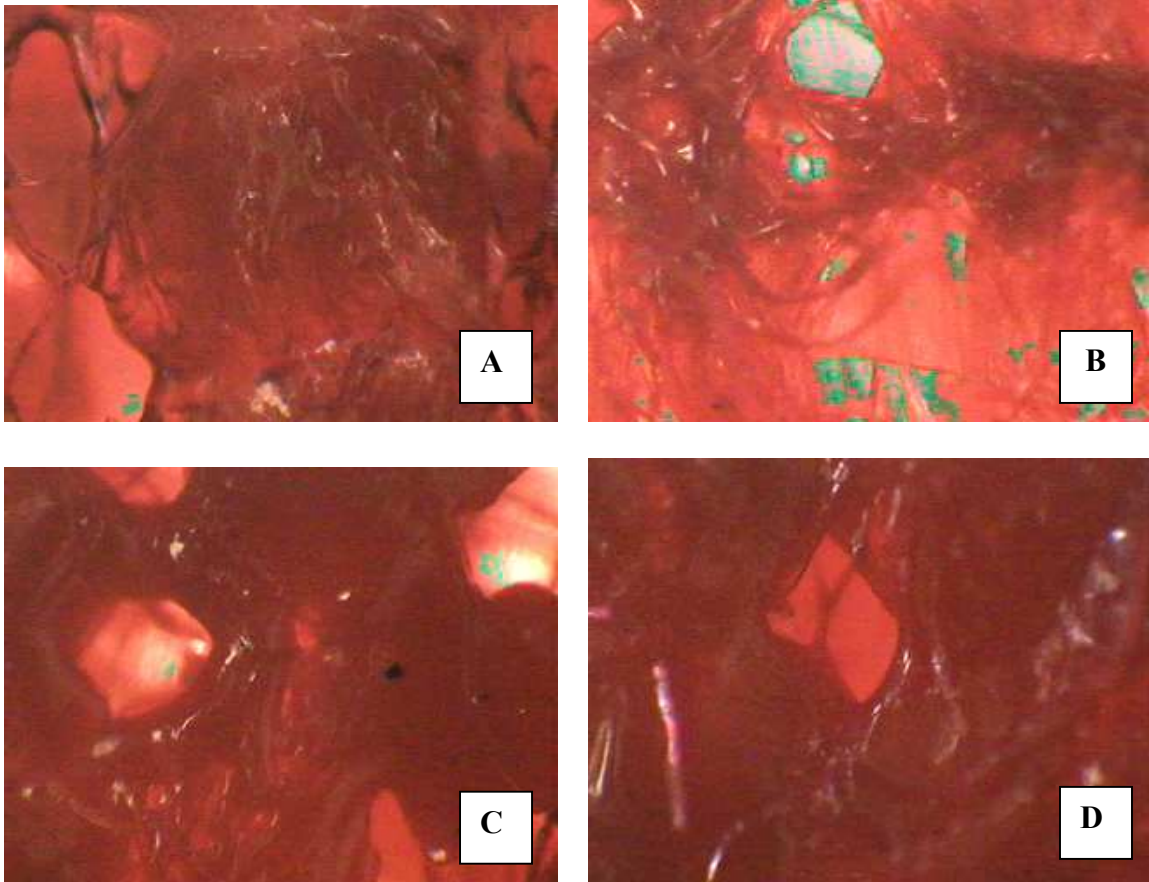


Figure 5.7: Microscopy Images of Dyed, Cut Pile, PP Carpet with 6 oz./yd.² of Applied Elvamide® Resin at 4x Magnification. Figures **A** and **B** was instant boil samples. **A** was dyed for 30 min. and **B** was dyed for 90 min. Figures **C** and **D** were rise to boil samples. **C** was dyed for 30min. and **D** was dyed for 90 min. The green tint/spots in the micrographs are due to the light passing through the samples from the microscope.

transition temperature to lower. To summarize, the water at the higher dyeing hold temperatures promoted chain mobility and movement of the Elvamide® resin into the tufts of the carpet via induced plasticized flow.

To determine if the irregular gaps caused by plasticized flow in the resin would be as severe if the sample were not boiled for 90 minutes, the experiment was repeated with a hold time of 30 minutes at temperatures of 90 and 100°C. Upon removal, the same irregular gaps were present in the Elvamide® resin except that they were not as large, see Figure 5.7. The extent of plasticized flow of the resin was thus proportional to the hold time spent in the dyebath at the fixed hold temperature (in this case, just below or at atmospheric boil).

The carpet samples were being placed in the dye bath at the boil, thermally “shocking” the construction. To identify if this “shocking” factor was the cause for the resin film’s plasticized flow, samples of the carpet were dyed by the rise to boil technique at a heating rate of 5°C/min., incorporating hold times of 30 and 90 minutes. Reviewing the post-dyed carpets showed similar gaps in the resin film to their instantaneous boil technique counterparts, but with larger, more uniform gaps that contoured the backs of the tufts, see Figure 5.7. The plasticized flow increased with hold time and temperature by the rate of rise technique, and thermally “shocking” the backing induced even more film flow.

Another critical observation made in these dyeing studies was that as the nylon resin film plasticized flow increased, the carpet samples began to deform or curl, i.e., dimensional stability was impaired. To see if these resin flows damaged the backing, the tuft bind strength of each of the dyed carpets were determined.

5.5.3.3 Tuft Bind Strengths of Dyed, Developed Carpets

The tuft bind strengths of the dyed carpets are shown in Figure 5.8. The procedure for determining the tuft bind strength is in Section 3.2.4. The instantaneous dyed samples that were dyed below 80°C all showed weaker tuft bind strength than that of the undyed sample. As the hold temperature progressed to 90 and 100°C, the tuft bind strengths increased, correlating with the visual micrographs that the resin had more effectively penetrated the back-tufts of the yarn. From handling the hot carpet backings at the higher dyeing temperatures, if the resin layer contacted either itself or the nylon yarn above 80°C, it became strongly adhered. Below this temperature, any adhesion properties of the resin were unnoticeable, which explains why the tuft bind strength did not increase at the lower hold temperatures. The reduction in tuft bind strength at the lower hold temperatures (<80°C) was due to swelling of the nylon yarn causing some physical separation of the resin layer from the yarn surfaces, coupled with a lack of water-induced plasticized flow below the critical 80°C temperature [11].

A time of hold at temperature investigation revealed that the longer the carpet sample was exposed to the hold temperature, the greater the increased tuft bind strength of the yarn (Figure 5.8). Although achieving an increase in the tuft bind strength that was more than three times that of the un-dyed carpet, the tendency of the carpet samples to curl and permanently distort introduced a practical physical problem to the concept of applying the initial Elvamide® resin layer before the carpet was dyed. The curling of the backing was due to the induced plasticized flow in the carpet samples. When the resin began to flow, it moved into the tufts/backing, causing the resin to shrink and the backing begins to curl due to the build-up of tension forces in the carpet structure. To avoid

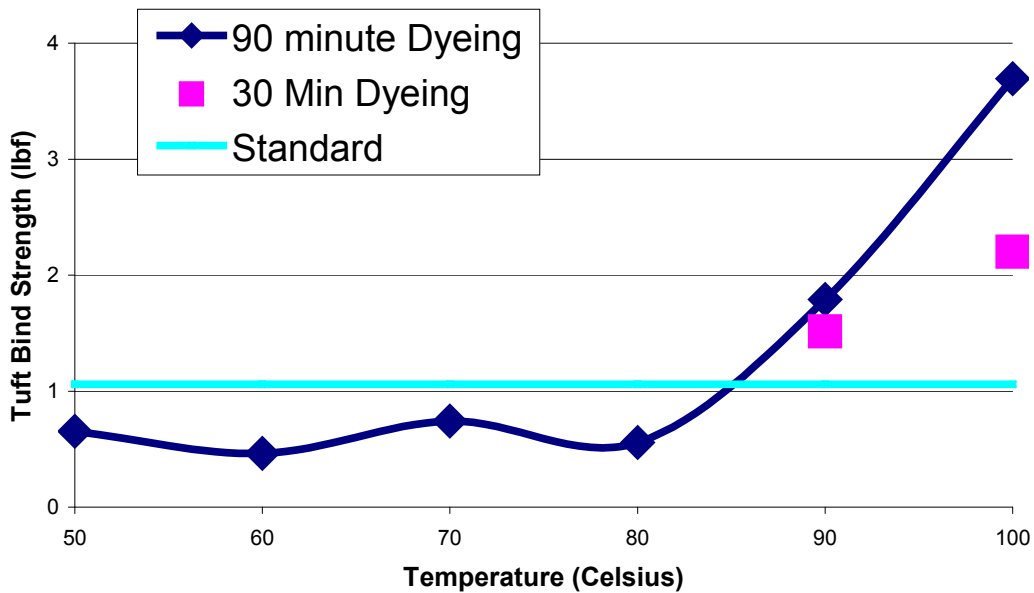


Figure 5.8: Tuft Bind Strengths of Dyed, Cut Pile, PP Carpet with 6 oz./yd.² of Applied Elvamide® 8063 Resin Colored in an Instantaneous Exposure Mode. Samples were dyed for 30 and 90 min. The standard refers to the tuft bind strength of an undyed carpet sample.

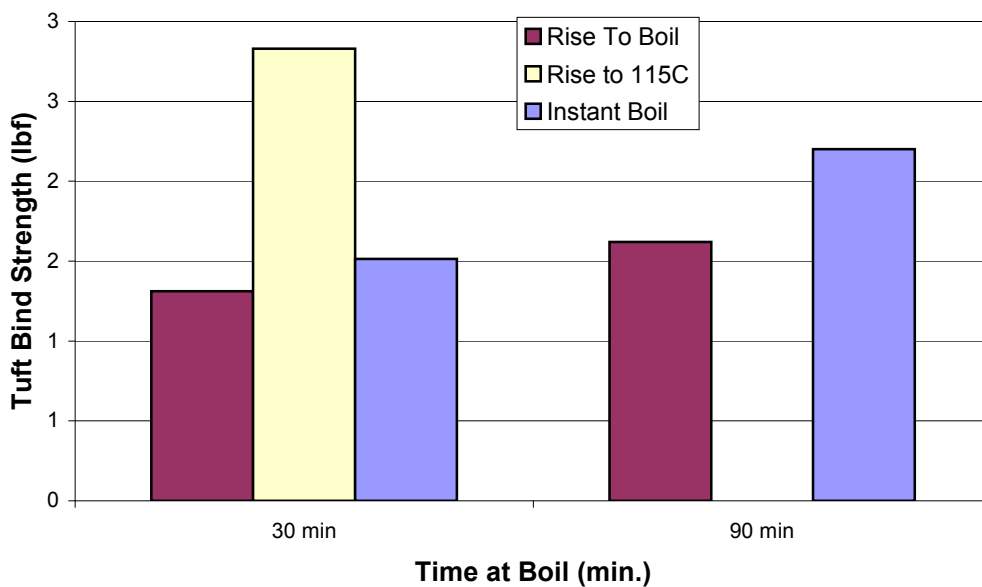


Figure 5.9: Tuft Bind Strengths of Dyed, Cut Pile, PP Carpet with 6 oz./yd.² of Applied Elvamide® 8063 Resin Colored by Several Techniques. The sample dyed for 30 min. at 115°C was under adequate pressure to reach the hold temperature.

plasticized flow of the resin film, the dye bath temperature would have to be held to $<80^{\circ}\text{C}$, an impractical limitation on commercial operations from dye exhaustion, levelness and productivity considerations at the low temperature.

5.5.3.4 Instantaneous Versus Rise To Boil Carpet Dyeing Techniques

With the carpet dyed by the instantaneous boil technique, the construction underwent a thermal “shock” that is not employed in industrial exhaust batch dyeing processes. Instead, the carpet is normally placed in a dyebath and the temperature is gradually raised to the boil (usually at a rate of 3-5F/min.). The rise to boil procedure was also employed to dye the carpet samples, and results compared to those obtained with the instantaneous boil procedure (Figure 5.9). Although not producing the same tuft bind results as the instantaneous boiled samples, the rise to boil samples did show improvement in the tuft bind strengths after dyeing for 30 minutes and even more improvement in the 90 minute dyed sample. With the curling of the carpet samples between these two techniques, the rise to boil method carpet samples displayed less curling than the instantaneous boil method. However in both dyeing techniques, the curling of the carpet specimens increased with the duration of the dyeing.

An advantage of commercial exhaust batch dyeing versus continuous dyeing processes for carpet dyeing is that in former, the carpet can be dyed above 100°C via modern pressure jet dyeing machines. A carpet sample was dyed at 115°C for 30 minutes and the tuft bind strengths were calculated. Paralleling the atmospheric boil studies, as the dyeing hold temperature increased, the tuft bind strength also increased (Figure 5.9), but unfortunately the curling of the backing was also present.

The Elvamide® 8201 resin versions of the cut loop pile, PP backing carpet were also batch dyed by the procedures detailed in Section 5.6.2.1, and these samples showed the same plasticized flow and the relative tuft bind strength increases found with the 8063 version. The plasticized flow was expected since both Elvamide® versions were nylon 6/6,6 copolymers that differed only in their backbone monomer constituencies and resulting physical properties [43]. With these Elvamide ® 8201 samples, the secondary PP backing was included in the dyeing process. After dyeing, an increase in the hand delamination force was noticeable where the secondary backing was more difficult to separate from the carpet than before the carpet entered the dyebath (see Section 3.4.2), which showed that not only the tuft bind strength but also the apparent delamination force could be increased through dyeing the carpet. A problem with the Elvamide® 8201 resin was that the curling and loss of dimensional stability of the backing increased with dyeing temperature to approximately the same degree as the 8063 version. The thermal instability of the 8201 carpet samples were attributed to the same reasons as the 8063 carpet samples. The only difference noted between the two Elvamide® resins was that the curling/plasticized flow in the 8201 resin occurred at 60°C instead of 80°C. The plasticized flow occurred at a lower temperature because the 8201 resin had a 14°C lower melt temperature than the 8063 resin which was attributed to the termonomer present (Table 3.1). So presumably the 8201 resin also had a lower wet glass transition temperature implying that water induced plasticized flow occurs at a lower hold temperature than the 8063 resin.

Due to the lack of carpet samples with Elvamide® 8201 resin still containing the secondary backing, the experiment could not be reproduced with a large enough sample

to meet the delamination sample length required for testing (see Section 3.2.2). The sample size used in the dyeing of the carpet samples was also too small for testing purposes.

5.5.3.5 Exhaust Batch Dyeing of Cut Pile, Glass Mat Backing Carpet

The analogous bare glass mat backing carpet with 6 oz./yd.² of applied Elvamide 8063 resin was dyed at a 30 minute hold time by both rise to boil and instantaneous boil procedures (see Section 5.2.1). The effects of the applied nylon resin film, both beneficial (improved tuft bind strength) and detrimental (curled/deformed carpet samples) were approximately the same as with the PP backing (Figure 5.10). As the dyeing hold temperature increased, so did the tuft penetration. The thermal shock behavior was also observed with this carpet construction. The plasticized flow of the resin layer can be seen in Figure 5.11, which like in the PP sample, also produced gaps in the film after exposure to the dye bath conditions at the higher hold temperatures.

5.5.4 Continuous Dyeing of PP Backing Carpets

With the quantity of material needed for testing, the cut pile, PP backing carpet with 6 oz./yd.² of applied Elvamide® 8063 resin was the only one that could be dyed via a simulated continuous dyeing procedure (Section 5.2.3). The dye pad bath used in this trial was first kept at room temperature and then increased in further runs. The logic behind using progressively hotter pad bath temperatures was to identify if there was any benefit to its use on the tuft bind strength of the carpet samples. After the samples were

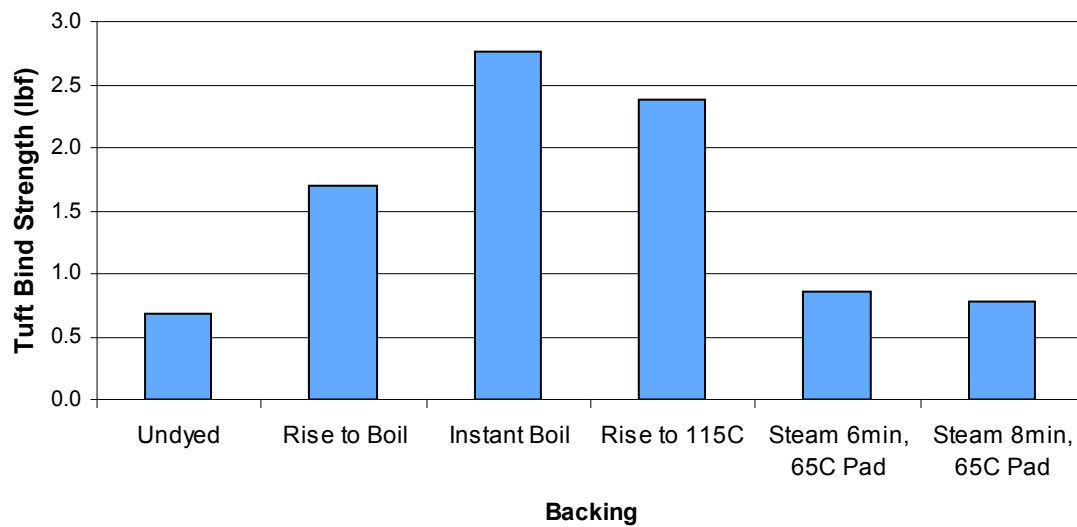


Figure 5.10: Tuft Bind Strengths of Dyed, Cut Pile, Bare Glass Mat Backing Carpets with 6 oz./yd.² of Applied Elvamide® 8063 Resin Colored by Several Procedures.

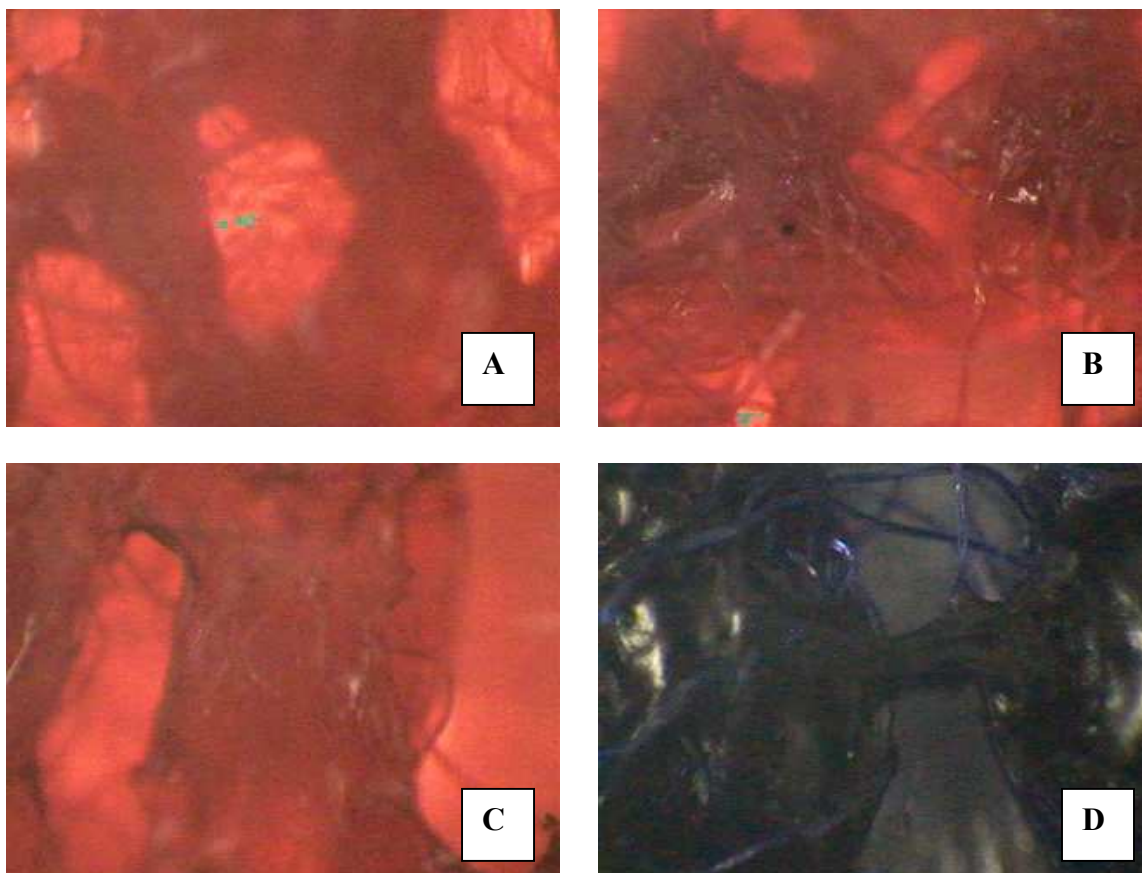


Figure 5.11: Microscopy Images of Dyed, Cut Pile, Bare Glass Mat Backing Carpets with 6 oz./yd.² of Applied Elvamide® 8063 Resin at 4x Magnification. Figures A and B were instant boil samples. A was dyed for 30 min. and B for 90 min. Figures C and D were both dyed for 30 min. C was a rise to boil atmospheric dyeing and D was a rise to 115°C pressure dyeing.

allowed to soak in the pad bath for two minutes, half of the six prepared carpet samples were steamed for four minutes and the other half were steamed for six minutes.

Washing the dyed carpet showed that the fixation of the colorant was accomplished in both the four and six minute steam exposure times. The tuft bind strength data for the steam-exposed carpets showed that increasing the time in the steam environment actually caused a decrease in the tuft bind strength, i.e., that the tuft bind strengths of the four- and six-minute steamed carpets were less than that of the un-dyed carpet (Figure 5.12).

Viewing the resin applied to the back of the carpet samples during steaming explained why the tuft bind strength decreased as the samples dwelled longer in the steam environment. As steam rose through the tufts, the resin layer trapped it. As time increased, the steam pressure built under the resin layer and eventually lifted it away from the tufts, resulting in the lowering of tuft bind strength. The lifting or “ballooning” of the resin occurs in a matter of minutes. The carpets that were dipped in a room temperature dye pad bath and then exposed to two additional minutes of steam time resulted in a loss of 17% in the tuft bind strength, which was most noticeable in the two samples that were wetted out in the 65°C bath and steamed for two different times. By steaming the sample for 30 minutes, any increase in the tuft bind strength, as seen in the six minute, steam exposed sample, was lost.

To determine if increasing dye pad bath temperatures could increase the tuft bind strength, several samples were padded out in heated dyebaths for two minutes and then steamed for six minutes. The dyebath temperatures were kept below 80°C to insure that any increase in tuft bind strength due to “shocking” was prevented, see Section 5.5.3.3.

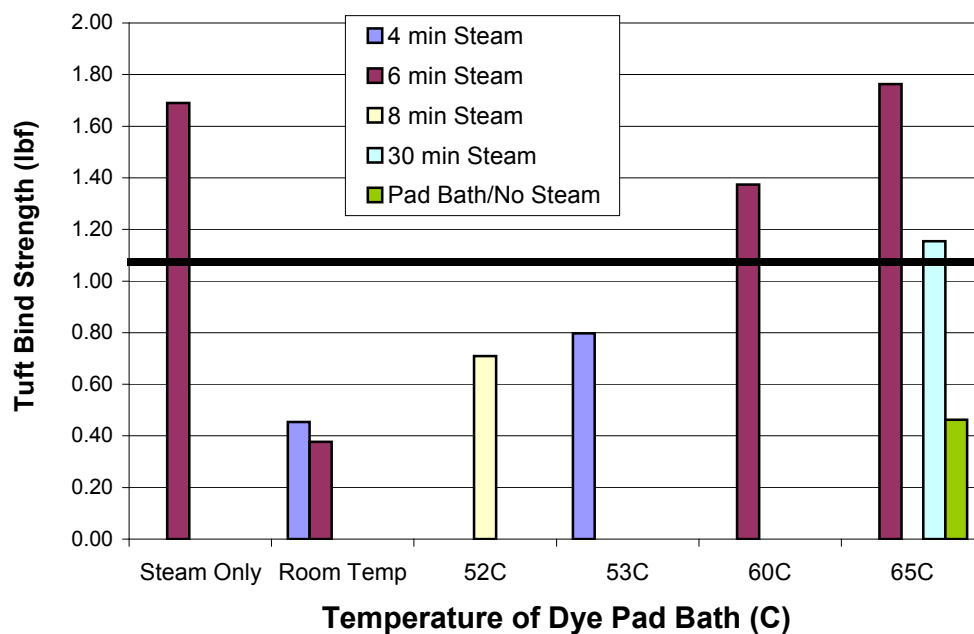


Figure 5.12: Tuft Bind Strengths of Cut Pile, PP Backing Carpet with 6 oz./yd.² of Applied Elvamide® 8063 Resin Colored by Pad-Steam Process. The bold black line represents the tuft bind strength of an undyed sample.

The data revealed that increasing the dyebath temperature provided an increase in the tuft bind strength (Figure 5.12). The carpet exposed to a 60°C dye pad bath and steamed for 6 minutes exhibited an increase in the tuft bind strength greater than the undyed carpet, which defined a threshold temperature of thermal pre-treatment before steaming.

The reason for the increase in the steam dyed carpet tuft bind strengths from the that of the undyed sample was due to the thermal properties of heating the construction. The carpet saturated with the dyebath solution required more energy to heat the sample to induce plasticized flow of the resin film. Correspondingly, a carpet sample that was placed dry in the steam environment without going through the room temperature dye pad bath saturation step exhibited a tuft bind strength more than four times greater than the samples that did. Without the need to heat the dye liquor in the tufts of the saturated carpets, all of the thermal energy transferred from the steam to the carpet went efficiently toward heating up the structure to the maximum temperature in a short time period, inducing the water-induced (from steam condensation) plasticized flow of the resin and the corresponding tuft bind strength. Again curling of the carpet samples were seen where the greater the level of plasticized flow, the greater the degree of curling in the carpet samples.

Thermal conductivity of nonmetallic liquids generally decreases with increasing temperature, the exception being water, which is insensitive to pressure except near the critical point. For water, the thermal conductivity increases from the freezing point to around 150°C and then decreases [70]. The increase in the thermal conductivity explained why the tuft bind strength increased in samples exposed to increasing dye pad bath temperatures before steaming. More energy was transferred from the steam to the

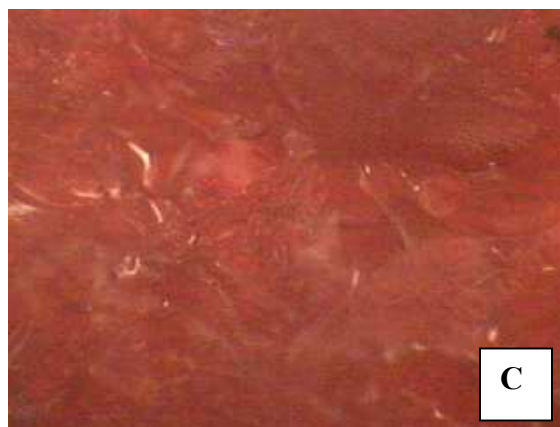
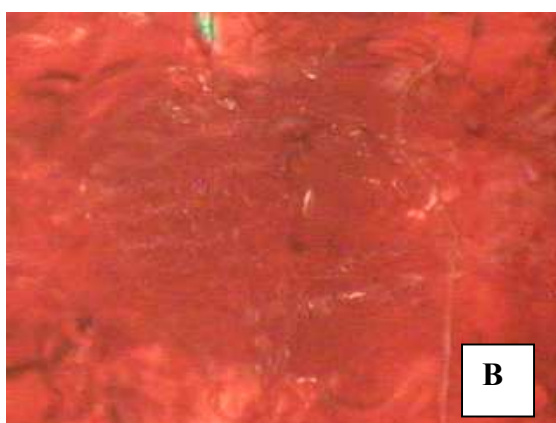
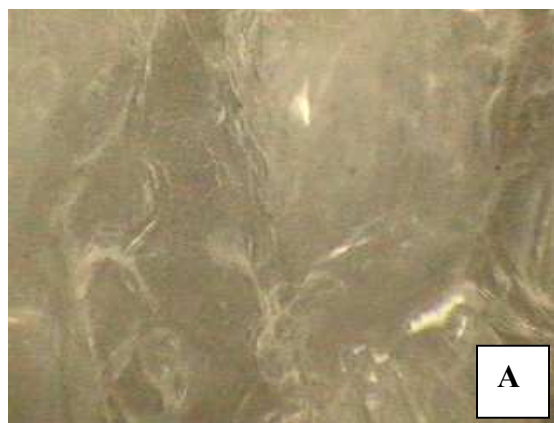


Figure 5.13: Microscopy Images of Dyed, Cut Pile, PP Carpet with 6 oz./yd.² of Applied Elvamide 8063 Resin at 4x Magnification. A was a carpet sample that was not pad-dipped and steamed for 6 min. B was a carpet sample pad-dipped in a 53°C bath and steamed for 4 min. C was a carpet sample pad-dipped in a 60°C bath and steamed for 6 min.

low heat capacity resin when the dye liquor in the solution was preheated, thus allowing for more plasticized flows of the resin into the fiber and subsequent higher tuft bind strengths (resin images in Figure 5.13). At the 60°C pad bath temperature, the thermal conductivity of the dyebath was high enough so that adequate energy was available at the steam temperature/time exposure profile to induce flow in the resin layer. However, below this pad bath temperature, too much of the steam energy went toward heating up the dye bath in the short exposure time frames, resulting in less plasticized flow of the resin film while the structure was at maximum temperature, thus leading to weaker tuft bind strengths.

The swelling of the nylon resin layer also played a part in the reduction of tuft bind strength. In Figure 5.12, a carpet is shown that was placed in a 65°C pad bath for two minutes exactly like the other samples, except the sample did not undergo steaming. The tuft bind strength was much lower than that of the undyed sample, evidence that the water-induced swelling of the nylon yarns and resin played a role in the final tuft bind strengths of the continuous dyed carpet. If steam is not applied to the carpet after dye bath padding to fixate the colorant, then the tuft bind strength cannot recuperate from the loss due to the differential swelling of the carpets nylon components.

The thermal dimensional instability of the resin layer resulting in curling was also found to occur in the pad-steam dyeing process, but the degree of curling and deformation was visually less than that observed for carpets colored by the two exhaust batch dyeing methods, regardless of which Elvamide® resin was used.

5.5.5 Dyeing of Carpet Made From Composite Backing C

Thermally-consolidated backing **C** (Table 4.1) was successfully tufted into carpet on a pilot scale machine, but it presented several problems during the formation process, including “fly” of a powdered glass/nylon mixture and loss of tensile strength in the cross machine direction (see Section 4.4.6.2). Due to these problems, application of an Elvamide® resin layer to tufted **C** was not conducted, but the dyeing behavior of the nylon 6 veils applied to the face and back of the glass mat core in the construction were studied. The consolidated **C** backing carpet samples were carried through both instantaneous and rise to boil batch dyeing procedures, along with continuous dyeing using a room temperature dyebath for initial testing. The tufted consolidated backing **C** was dyed to see if the nylon 6 veils applied to the back and front of the glass veil will cause the same thermal dimensional instability behavior as did the Elvamide® resin layers.

The tuft bind strength measurements for the dyed **C** carpets are seen in Figure 5.14. Dyeing by either rise to boil or instantaneous boil procedures produced increases in the tuft bind strength, but not to the same degree as the samples containing Elvamide® resins (Figure 5.10). Exhaust batch dyeing caused a smaller degree of water-induced plasticized flow of nylon 6 into the tufted yarn, which produced a correspondingly small increase in tuft bind strength. The same trend in continuous dyeing was found, where increasing the steam time decreased the tuft bind strength, which was due to the swelling of the nylon 6,6 yarn and nylon 6 veils. The swelling loosened the tufted yarn within the backing, making it easier to remove. Upon weighing the samples after leaving the steam chamber, the six minute sample gained more weight than the four minute sample. The

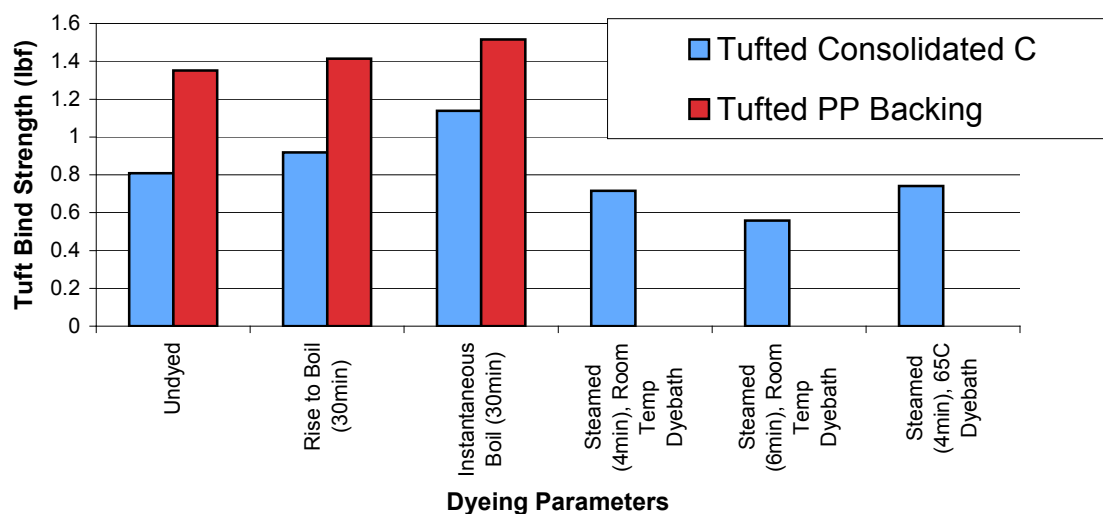


Figure 5.14: Tuft Bind Strengths of Dyed Consolidated Backing C and PP Backing Carpets. Consolidated backing C and the standard PP backing were tufted under identical parameters.

increased water weight indicated that during the steaming process, more condensed water was absorbed into the nylon components of the carpet, resulting in more swelling of the structure and lower tuft bind strengths for the six minute steamed carpet.

Once rinsed and dried, the tuft bind strengths of the dyed *C* constructions were measured. Due to the differential swelling of the nylon components in the carpet, this caused a separation of the tufted yarn from the backing when the samples dried. Since nylon 6 had a much higher melting point (218°C) than that of the Elvamide® 8063 (176°C), the saturated steam temperature did not provide enough thermal energy to induce enough flow in the backing's nylon 6 nonwoven veil to counteract the effects of the swelling yarn. However, unlike the bare glass mat carpet with Elvamide® resin, the consolidated, backing *C* carpet did not curl during the dyeing procedures.

5.5.6 Elvamide® 8063 Resin Versus Nylon 6 Resin

Since the Elvamide® resin was initially selected as a substitute for the filled SBR latex to consolidate the final carpet construction due to its melt compatibility with either nylon 6 or 6,6, the concept of using a nylon 6 resin in the final construction was not considered, since earlier research literature treatises indicated the two common polyamides to be immiscible in the melt phase [3, 36]. The melt immiscibility of the two nylons would cause the recycling scheme of the glass carpets with nylon 6,6 face yarns to fail, as injection molded objects produced from an immiscible melt would have unacceptable mechanical properties. However, according to a recent research investigation, nylon 6/6,6 melts are compatible at the melt in micro-domain regions, and when the melt temperature is high enough, slow amide-amide interchange reactions occur

between nylon 6/6,6, eventually producing a random copolymer of the two nylons, i.e., a similar configuration to the Elvamide® line of resins [71]. With this new information, experiments were conducted with using a nylon 6 resin as the carpet consolidation material.

Nylon 6 resin was melt extruded onto the back of tufted (cut loop, un-dyed yarn construction) *original glass mat* backing. Nylon 6 resin was first dried and then slot extruded through a conical, intermeshing, counter rotating twin screw Haake unit with a Brabender drive and a temperature profile of 225, 230, 240, and 240 degrees Celsius from hopper to die. The optimal screw speed was 25 rpm and the take up speed was also 25 rpm, producing a 1.5 in. width thin film (10 oz./yd.²) extruded onto the back of the tufted carpet.

The tuft bind strength of the nylon 6 resin carpet was then measured (Figure 5.15). The carpet was then cut into several pieces and all the previously-described dyeing procedures were conducted with them (Sections 5.2.1 and 5.2.3). Carpet samples were placed in room temperature dye pad baths and then steamed for four and six minutes. The carpet was also carried through the rise to boil and instantaneous boil exhaust batch dyeing procedures for 30 min. hold periods. The tuft bind strengths of all the samples were then determined (Figure 5.15). The carpets were dyed by several procedures, as noted in the abscissa legends. The steamed samples were first padded with a room temperature dye bath.

Compared to the previous carpet samples that were consolidated with the Elvamide® 8063 resin (10 oz./yd.²), the dyeing conditions induced similar tuft bind strength results in the nylon 6 consolidated resin samples (Figure 5.15). The only

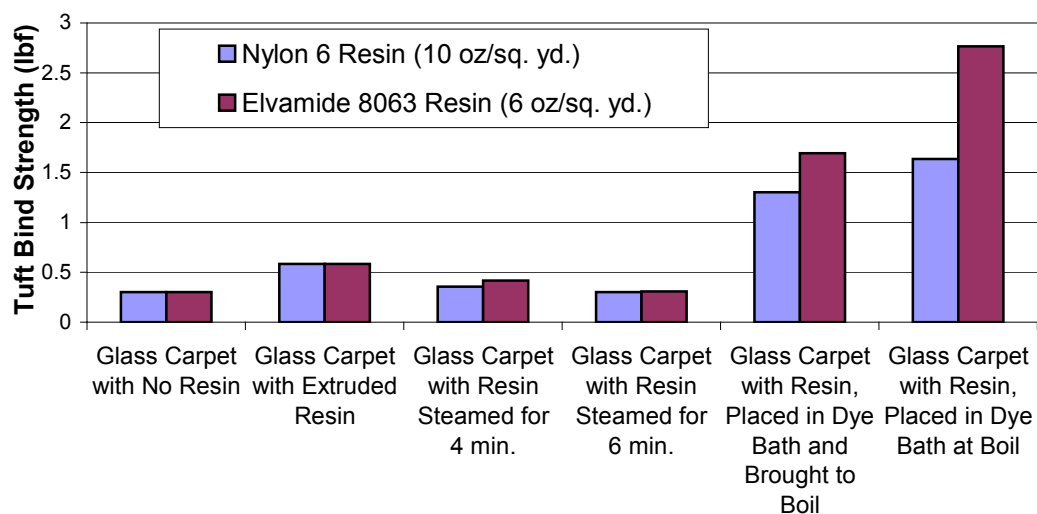


Figure 5.15: Tuft Bind Strengths of Cut Pile, Bare Glass Mat Carpets Consolidated with Applied Nylon 6 and Elvamide® 8063 Nylon Resins.

difference between the two resins was that nylon 6 did not exhibit the thermal instability characteristics of the Elvamide® resin, as the carpet samples consolidated with the former did not curl on dyeing, nor was the glass mat core exposed due to film gap formation (refer back to Section 5.5.3.5).

The thermal instability differences between the resins can be explained through their compositions. The nylon 6 resin film was more thermally stable since it was composed of a highly-crystalline homopolymer, whereas the Elvamide® 8063 resin was a less-crystalline copolymer. With a copolymer composed of components with different glass transition temperatures, each polymer contributes to the overall free volume of the system in proportion to the amount of material present [3]. Overall the mixture of monomers in the Elvamide® copolymer resin caused the material to have a lower crystallinity, lower wet/dry T_g 's and a lower T_m than nylon 6 homopolymer. The dry glass transition temperature of the Elvamide® 8063 resin was 46.5°C vs. 87°C for the nylon 6 resin (Figures 3.1, 4.8 and Table 3.1). Since the Elvamide® resin had a lower glass transition temperature and a lower crystallinity index, the resin layer in the carpet was more susceptible to the onset of water-induced, segmental mobility/plasticized flow at high dyeing temperatures. In summary, bare glass mat backing carpets consolidated with 10 oz./yd.² of applied nylon 6 resin were comparable in tuft binding strength properties to those consolidated with 6 oz./yd.² of applied Elvamide® 8063 resin (Figure 5.5).

CHAPTER 6

Conclusions and Recommendations

6.1 Conclusions of Glass Backing Carpets

6.1.1 Primary Backing Conclusions

Increased glass mat density in the developed glass-based primary carpet backings increased the breaking strength in both the machine and cross machine directions, and also increased the measured tufting needle first penetration and withdrawal forces (Sections 3.4.5 and 4.4.2). However, the density of the glass backing used in the final next generation carpet construction is limited by its cost and the tufting needle penetration forces. Since the developed carpet construction must at least match the current broadloom construction's physical performance on the floor and its overall cost effectiveness, it cannot have the majority of its costs tied to the density of glass mat required to create a viable primary backing. The density of glass mat used cannot be so high that it would cause unreasonable resistance to the tufting process, as signified by high needle force measurements [72]. Higher density glass mats also increase the probability for fractured fiber “fly” generation on machine tufting, even when employing 12 micron, flexible glass fibers to form the mats.

6.1.2 Original Glass Mat Carpet Conclusions

During the tufting of the *original glass mat* primary carpet backing, some fractured fiber “fly” was generated which posed a potential problem for plant workers and indicated the need for entrapment of the glass. Mechanical tests of the developed carpet constructions revealed the highest tuft bind strength obtained was 4.17 lbf. with an application of 6 oz./yd.² of Elvamide® 8063 resin (Table 3.2). The highest delamination strength (separation of the nylon resin layer from the back-tufts of the carpet) obtained for the straight loop pile constructions was 1.06 lb./in., again with an application of 6 oz./yd.² of Elvamide® 8063 resin (Table 3.3). With a conventional, straight-loop pile carpet construction exhibiting a tuft bind strength of 7.6 lbf. and a delamination force (separation of the PP secondary backing from the latex binder) of 4.14 lb./in., the melt resin application process for the glass mat backings must be further optimized to raise the mechanical properties of the new carpet constructions.

Since the critical radiant flux of carpet flammability tests is the minimum energy necessary to sustain flame propagation, the carpet industry uses it to characterize carpet constructions as to what installation areas a carpet can be used where automatic sprinkler protection is not provided [54]. The critical radiant flux for the straight loop pile, glass mat backing carpet was low (Unclassifiable Rating, Table 3.4), and thus the carpet could not be placed in a building area where automatic sprinkler protection is not provided [50]. The cut pile carpet analog exhibited a higher critical radiant flux (Class II Rating), allowing the carpet to be placed in corridors of day care centers, existing detention and correctional facilities, hotels, dormitories, and apartment buildings [54].

Between the two bare glass mat carpet constructions, the use of a cut loop pile instead of a straight loop pile with the same glass mat backing increased the critical heat flux because the former was a 1/10th gauge product with ten stitches per inch and the latter was a 1/8th gauge product with eight stitches per inch (Section 3.4.3.1). While both carpet constructions used 2-ply, 2567 denier yarns, the straight loop pile carpet had a less dense pile, allowing for a higher air-to-fiber ratio. Since the availability of air and its oxygen fraction has a positive effect on sustaining a burn, flame propagation is less in high-density pile carpets, resulting in a higher critical heat flux [55, 56].

The glass mat backing carpets were projected to exhibit better overall flammability results than the PP backing carpets due to the lack of combustibility of the non-carbon glass fiber (E-glass is mainly silica) [42, 57]. Three postulates were developed to explain why the glass mat backing carpets actually gave poorer performances in the flammability tests than the PP backings: the thermal transmittance of glass, the air permeability of the nonwoven mat and the percent binder employed in forming the mat.

With the thermal transmittance, several glass mats of varying densities were studied (Figure 3.13). The data showed that as the mat's density increased, the thermal transmittance decreased. The lower the thermal transmittance of the backing, the lower the amount of heat/energy that will be transferred to the back of the carpet in the employed flammability tests. The thermal transmittance of the bare glass mat backing that was used in the initial tufted carpet was 9.7 W/m.² K, and because E-glass could withstand the thermal heat of the flammability tests without melting, most of the thermal

energy was kept at the surface of the carpet (tuft side facing towards the environment and the heat source of the test), in turn keeping the critical radiant flux low.

The second reason for the test outcomes was that the glass mat backing, unlike the woven PP tape backing, was a highly “open” nonwoven structure that gave easy access to air flows that were drawn in by the flames and fed the fire from the sides of the structure, thus supplying oxygen to sustain the burn. With the addition of more resin, the burn distance was decreased due to a blockage of air supply from underneath the flames provided by the thicker Elvamide® resin layer (Figure 3.9).

Finally, the polymeric acrylic binder used to consolidate the glass mat primary was mainly composed of the elements carbon-hydrogen, and was thus highly combustible in the presence of fire, i.e., it provided a high concentration of hydrogen radicals on thermal degradation to fuel and sustain the fire in the carpet flammability tests. By lowering the amount of binder used to form the glass mat backing (from ~20% by weight to ~10%), a viable fuel source for the test flame was decreased. However, the decreased amount of binder caused a concurrent decrease in the tensile properties of the glass mat backing (Figures 3.16, 3.17). The level of binder employed played the largest role in building the tensile strength of the bare glass mat backings. However, the higher density of binder did not change tufting needle penetration/withdrawal forces with the glass mats (Section 4.4.2), with mat density instead playing the greatest role.

6.1.3 Composite Glass Backing Conclusions

The most obvious benefit of encapsulating the front and back of glass mat cores in composite backings was that the amount of generated fiber “fly” was reduced and plant

worker exposure to the glass core in handling the develop construction was no longer a major concern. The small amount of powdered “fly” generated from tufting thermally-consolidated composite backing *C* (with the glass mat core made from 12 micron, flexible E-glass fiber) was determined to be 78-62% glass and 22-38% nylon 6. The generated, fine particle size powdered “fly” remains a concern for future manufacturing environments, as if not collected in tufting areas by automated vacuum collection systems (e.g., like those used in today in cotton yarn/fabric formation mills), it could be inhaled by humans and potentially lead to lung damage.

The other benefit of adding the nylon veils to the glass mat backings was that as the density of the nylon layer increased, so did the tufting needle penetration/withdrawal forces with the composite backings. The desired needle tufting properties could thus be engineered into the backing by replacing part of the core glass density with nylon veil density (see Section 4.4.1.1). By thermally consolidating the nylon veils of the backings (optimized at 218°C, 40 seconds), an increase in the withdrawal force of the tufting needle was obtained along with an increase in the adhesion of the nylon layer to the glass mat (Sections 4.4.3.1 and 4.4.3.2). If the consolidation temperature or time was increased beyond the optimum conditions, the result was an exposed glass mat core and/or a reduction in the needle penetration/withdrawal forces.

Machine tufting of the *original glass mat* and thermally-consolidated composite glass backings *A* and *C* confirmed that the presence of nylon 6 layers increased the tuft bind strength of the tufted yarn in the latter two backing constructions compared to the former. For example, the *original glass mat* had almost double the density of glass fiber than did composite backing *C*. However, the tuft bind strength for composite backing *C*

was higher than that exhibited by the *original glass mat* backing (0.81 lbf. vs. 0.70 lbf.), confirming that the addition of the nylon veils allowed a concomitant reduction in the density of the core glass mat (Figure 4.16).

6.1.4 Carpet Dyeing Conclusions

In the dyeing studies of carpet produced by tufting the *original glass* mat backing and application of 6 oz./yd.² of melt-applied Elvamide® 8063 nylon copolymer resin, an increase in the tuft bind strength was achieved by water-induced plasticized flow of the film under sufficient dyeing temperature/hold time profiles (Figures 5.8 and 5.9). Plasticized flow of the Elvamide® film was due to the induction/onset of segmental mobility of polymer chains in the amorphous (unordered) regions of the solid-state structure under the employed dyeing conditions [3]. In these aqueous dyeing experiments, the water at the higher hold temperatures entered the amorphous regions of the nylon resin film, breaking the hydrogen bonds between nylon polymer chains and forming water spheres around the participating polymer heteroatoms. The breakage of the polymeric hydrogen bonds caused the free volume of the network to increase and the wet glass transition temperature to decrease. However, the higher the extent of plasticized flow generated in the resin's polymeric structure, the greater the degree of curling/loss of dimensional stability of the carpet samples due to shrinkage of the nylon film as it flowed into the back-tufts of the carpet, generating tension forces within the structure that were manifested visually in the curling phenomenon.

The onset of plasticized flow occurred in dyeing the glass mat/Elvamide® 8063 resin carpets at bath hold temperatures >80°C. The degree of plasticized flow and

concomitant tuft bind strengths were increased by raising the dye bath hold temperature, the hold time at maximum temperature and by thermally “shocking” the carpets by employing an instantaneous boil technique (Figure 5.7). “Shocking” the carpet by entering it at the atmospheric boiling point of the aqueous dyebath (100°C) or dyeing it under pressure to obtain a 115°C temperature produced the greatest increases in tuft bind strength. If the samples were dyed at <80°C hold temperatures, plasticized flow was not generated in the resin layer, and water-induced swelling of the two nylon components instead caused separation of the yarn back tufts from the resin layer, actually resulting in lower tuft bind strengths when compared to that of the un-dyed carpet standard.

With the pad-saturated steam dyeing technique simulating continuous dyeing of carpet, if the dye pad liquor was not heated to at least 65°C, the resulting tuft bind strength of the colored product was less than that of the un-dyed standard (Figure 5.12). The result was credited to both the thermal conductivity of water and the swelling of the nylon yarn and resin layer. If the padded carpets were left in the steam environment too long, any increase in adhesion from plasticized flow of the resin film was offset and lost due to the additional swelling of the nylon components and “ballooning” and physical separation of the Elvamide® resin layer from the yarn back-tufts. For optimal results in continuous dyeing, the carpet should be introduced to a high temperature pad bath ($\geq 65^{\circ}\text{C}$) and then exposed to the saturated steam environment for a minimal amount of time (<4 minutes).

Atmospheric beaker dyeing of the thermally-consolidated composite backing C carpet by either instantaneous or rise to boil methods resulted in a slight increase in the tuft bind strength as the dyebath temperature increased ($>80^{\circ}\text{C}$). The heat of the dyebath

did not cause any curling of the carpet samples or exposure of the glass mat core in the backing system, indicating that the nylon 6 polymer veils used in the composite glass backing constructions were largely stable to water-induced plasticized flow (Figure 5.14). However, in the carpets where nylon 6 resin was substituted for the Elvamide® resins as the extruded layer on the back of the *original glass mat* backing after tufting, dyeing produced the same trends as the dyed Elvamide®-consolidated carpets, albeit with lower dyeing enhancement of the tuft bind strengths. A major advantage of incorporating the nylon 6 resin layer was that the carpets containing it retained their dimensional stability under higher temperature dyeing conditions, i.e., they did not curl or exhibit exposed glass mat after dyeing (Figure 5.15).

Nylon 6 was more stable to water-induced plasticized flow under higher dyeing temperatures since it was composed of a highly-crystalline homopolymer, whereas the Elvamide® 8063 resin was a less-crystalline nylon copolymer. The mixture of monomers in the Elvamide® copolymer resin caused the material to have a lower crystallinity, lower wet/dry T_g 's and a lower T_m than the nylon 6 homopolymer resin. Since the Elvamide® resin had a lower glass transition temperature and a lower crystallinity index, the resin layer in the carpet was more susceptible to the onset of water-induced, segmental mobility/plasticized flow at the higher dyeing temperatures.

6.2 Conclusions of PP Carpet

Since woven PP tape primary carpet backings are currently widely accepted in the broadloom carpet manufacturing industry, nothing in the backing construction needed changing entering the research. With the Elvamide® resins, the same trends for

delamination and tuft bind properties existed with the PP backing carpets were observed for the bare glass mat backing carpets, e.g., the highest breaking strength was exhibited by constructions consolidated with 6 oz./yd.² of applied Elvamide® 8063 resin (Table 3.2 and 3.3). With the Hot Metal Nut Flammability Test, as the mass of resin applied to the PP backing carpet increased, the burn radius increased (Figure 3.9). The burn radius was attributed to the mass of resin, where with more organic material for the flames to consume in the backing system, flame propagation was enhanced. With the radiant panel flammability tests, all of the PP carpet samples achieved a Class I rating. A Class I rating is the highest rating achievable for a carpet and it is therefore allowed to be placed within exits, access to exits (corridors) of health care facilities (hospitals, nursing homes, etc.) and new construction detention and correctional facilities [54].

With both exhaust batch and continuous pad/steam dyeing simulations of PP backing carpets, similar increases in tuft bind strength to those observed with the glass mat backing carpets were achieved, again attributed to water-induced plasticized flow of the resin layer. However, curling of the carpet samples due to the loss of dimensional stability of the Elvamide® resin layer at the higher dyeing temperatures was also evident to approximately the same degree as observed in the glass mat carpet samples.

6.3 Recommendations

6.3.1 Glass Backing Carpets

Based on the research, the ideal glass-based, primary carpet backing should be formed from one inch staple, 12 micron diameter fibers and have a mat weight of ~5.50 oz./yd.² with ~10% by weight of added acrylic binder. This construction should exhibit

optimal mechanical properties for tufting, e.g., breaking strength and resulting tuft bind strength, while minimizing flame propagation tendencies in the standard tests. A single-sample hot metal nut test by British Standard Test Method 470 [52] was conducted on the thermally-consolidated backing **C** carpet showed that the burn radius was minimal (5-6 cm.), comparable to that of the PP backing carpet. Since the non-statistical flammability results showed a benefit to the overall construction of composite backing **C**, the ultimate primary backing construction should resemble a modified version of this backing.

For the core glass mat of the ultimate backing construction, one inch staple fibers of 12 micron diameter should be used, which are more flexible and less susceptible to brittle fracture on handling the backing in the plant and subsequent tufting, and thus minimizing both worker skin irritation and “fly” generation. The core glass mat of ~ 5.50 oz./yd.² should be encapsulated with a nonwoven nylon 6 veil with a weight of 0.86 oz./yd.² on the mat face and 0.58 oz./yd.² on the back. Since recent research found that nylon 6/6,6 are melt-compatible and at the proper melt temperatures can form copolymers via amide interchain reactions [71], nylon 6 veils/extruded layers should replace the Elvamide® resins in the next backing constructions, lowering the costs of production and allowing pre-dyeing applications in composite structures with nylon 6’s superior dimensional stability under commercial dyeing conditions. The composite backing should undergo pre-tufting thermal consolidation at a temperature of 218°C for a period of 40 seconds to improve the tuft bind strength of the carpet and further encase the core glass mat, minimizing powder “fly” generation on tufting. The monofilament chain stitching yarn should be composed of nylon 6 rather than the PET polyester used in the reported research to simplify the recycling schemes with all nylon-glass carpet.

From the described ultimate glass backing descriptions, two more alternative backings should be constructed. One alternative glass composite backing should utilize nylon 6 films instead of veils to encapsulate the nonwoven glass core. The core properties and the same amount of nylon should be applied to the front and back of the glass core as described above, except the nonwoven nylon veils are now films. With the use of a film to encapsulate the glass core, it should further decrease powder release on tufting. Unfortunately at the density, films are more expensive per square yard than nonwoven veils. The other alternative glass composite backing, with either nylon veils or films encapsulating the glass core, should thermally consolidate the nylon layers as they are merged onto the core glass mat at Owens Corning, either by extrusion of the fiber or film hot onto the mat surface and then cooled, or if the nylon 6 structures are preformed, an oven will be inserted in the processing line to heat-consolidate the composite immediately after formation. The advantage of thermally consolidating the backing at this point is that the monofilament stitch bonding operation is eliminated along with its material/process cost.

The same tufting parameters that were used in the tufting of consolidated backing *C* should be followed with the optimized backing. If a post-tufting extruded resin layer is required to reach acceptable tuft bind strengths in the final carpet and/or to consolidate a secondary backing into the structure, nylon 6 melt should be applied in the range of 6-10 oz./yd.². The minimal research conducted for this thesis with extruded nylon 6 resin was done at a 10 oz./yd.² application level, but a lower level may be sufficient to maximize the tuft bind strength of the final carpet, e.g., the optimum level for the Elvamide® resins was 6 oz./yd.².

If a secondary backing of any construction is used in the final carpet, its attachment procedure must be optimized. In the initial trials with the bare glass mat backing/Elvamide® resin carpet, the PP secondary backing's delamination force was extremely weak, requiring only hand force for removal.

If an extruded nylon 6 resin layer is used, the highest tuft bind strengths should be attained after dyeing the carpet under optimized commercial conditions (Figure 5.8). Although this research did not include it, application of a secondary backing in the merge zone with the extruded nylon 6 resin should have no affect on the dyeing behavior, allowing for coloration of the completely-formed carpet. For exhaust batch dyeing, the carpet should be dyed by either the rise to boil method or under pressure at a hold time period of ~30 minutes. Dyeing carpet on an industrial scale with the instantaneous boil technique would be impractical, and hold times at maximum temperature longer than 30 minutes would be costly in terms of additional energy required and lost productivity. For continuous pad/steam dyeing, the dye applied to the carpet should be preheated to at least 65°C, and the padded carpet exposed in a steam chamber for a period of no longer than 4 minutes otherwise “ballooning” will occur resulting in the separation of the yarn from the resin.

6.3.2 PP Carpet

On the PP backing path, since the optimized primary and secondary backing constructions were locked by industry, i.e., woven 15-pick PP tape primary and 5-pick secondary PP tape warp/staple yarn filling backings, no need existed to improve the

constructions. The only recommendation is that the same resin and dyeing choices for the glass carpet should also be used for the PP backing carpet optimization.

6.3.3 Future Work

With the resin application process (Figure 3.3), the main focus should be on optimizing the resin slot melt extrusion variables such as the flow temperature/viscosity, slot distance above the consolidation zone, use of heated versus cooling drums to control melt cooling/solidification rate, etc., to raise the tuft bind strength, breakage strength and other mechanical properties of the final carpet construction to approximately those of the traditional broadloom construction. Since the extruder slot height above the carpet merger zone used in this study was a conservative estimate, a study of the effects of extruder slot height on carpet tuft bind and delamination strengths should be conducted.

Since steaming of an undyed PP backing carpet consolidated with a layer of Elvamide® resin increased the tuft bind strength (Figure 5.12), a study on alternative consolidation process should also be conducted. For example, some carpet constructions are currently steamed before entering the dye application step in continuous dyeing processes to “bloom” the yarn tufts, and this step could be utilized to improve the tuft bind strengths of next-generation carpet constructions.

The strength in the cross machine direction of the glass-based primary backings must be increased avoid separation on tufting by other means other than simply increasing the percent by weight of polymeric acrylic binder. If the backing strength cannot be increased except by increasing the percent binder, then a brominated flame

retardant should be incorporated in the binder to facility carpet performance in the various flammability tests.

Industry acceptance of an E-glass containing carpet backing depends heavily on the demonstrated ability to fully encase the glass components to completely eliminate worker exposure and the release of fractured fiber “fly” on tufting. After both the glass-based and PP backing carpet constructions are fully optimized and sufficient volumes of each product are produced, the various proposed recycling schemes herein should be optimized, demonstrated and fully proven from both technical and economic viewpoints.

REFERENCES

1. Realff, Ammons, and Newton, *Carpet Recycling: Determining the Reverse Production System Design*. Polymer-Plastics Technology and Engineering, 1999. **38**(3): p. 547-567.
2. Realff, M.J., *Personal Communication*, A. Cascio, Editor. 2003, Georgia Tech: Atlanta, Georgia. Carpet Recycling.
3. Rodriguez, F., *Principles Of Polymer Systems*. Fourth ed. 1996: Taylor and Francis. 57-60, 336-337.
4. *History of Carpet* The Carpet and Rug Institute 2006 [cited; Available from: http://www.carpet-rug.org/drill_down_2.cfm?page=10&sub=4&requesttimeout=350].
5. *Erastus Brigham Bigelow*. [cited 2006 March 3]; Available from: <http://www.britannica.com/eb/article-9079166>.
6. *The History of Carpet*. [cited 2006 March 2]; Available from: <http://www.carpetinfo.co.uk/pages/aboutpp/history.htm>.
7. Mohawk. *Mohawk History*. [cited 2006 March 2]; Available from: <http://www.mohawk-flooring.com/history.asp>.
8. Edmiston, K.D. *The Net Economic Impact of Large Firm Openings and Closures in the State of Georgia*. [cited 2006 February 21]; Available from: http://frp.aysps.gsu.edu/frp/frpreports/report_71/rpt71text.htm.
9. *2002 Industry Statistics*. The Carpet and Rug Institute, 2002.
10. *Carpet Talk*. Textile World, 2005. **155**(6): p. 52-55.

11. Warner, S., *Fiber Science*. 1995: Prentice-Hall, Inc. 16-17.
12. M. Braun, A. Levy, and S. Sifniades, *Recycling Nylon 6 Carpet to Caprolactam*. Polymer-Plastics Technology and Engineering, 1999. **38**(3): p. 471-484.
13. Fowler, G., *Personal Communication*, A. Cascio, Editor. 2004, Shaw Industries, Inc.: Dalton, Georgia. Carpet Manufacturing
14. Industries, J., *General Carpet Flooring Terms & Definitions*. 2006.
15. Parachuru, K., *Personal Communication*, A. Cascio, Editor. 2004, Georgia Tech: Atlanta, Georgia. Carpet Backing.
16. Realff, M.L., *Personal Communication*, A. Cascio, Editor. 2004, Georgia Tech: Atlanta, Georgia. Carpet Tufting.
17. Aspland, J.R., *Continuous Nylon Carpet Dyeing*, in *Textile Dyeing and Coloration*. 1997, American Association of Textile Chemists and Colorists. p. 273-282.
18. Cook, F., *PTFE 4100, Chemical Processing of Textile Materials*, A. Cascio, Editor. 2006, Georgia Tech.
19. Tincher, W.C., *Personal Communication*, A. Cascio, Editor. 2005, Georgia Tech: Atlanta, Georgia. Dyeing Parameters.
20. Hurd, F., *Carpet America Recovery Effort*, in *2002 Annual Report*. 2002.
21. Hurd, F., *Carpet America Recovery Effort*, in *2003 Annual Report*. 2003.
22. Hurd, F., *Carpet America Recovery Effort*, in *2004 Annual Report*. 2004.
23. *A Memorandum of Understanding for Carpet Stewardship*. Negotiated Outcomes for Carpet 2002 January 2002. [cited; Available from: <http://www.moea.state.mn.us/carpet/mou.cfm>.

24. Fishbein, B.K., *EPR: What Does it Mean? Where is it Headed?* Pollution Prevention Review, 1998. **8**(4).
25. Organization, R.D. *Partners in Promoting Reuse* 2/20/2006 [cited; Available from: http://www.redo.org/Links/body_links.html].
26. *Collins & Aikman Floorcoverings Inc.* [cited 2006 1/13]; Available from: <http://www.cafloorcoverings.com/product01.html>.
27. Coyler, E., *Closing The Carpet Loop*. Textile World, 2005(April).
28. Mishra, M., *Special Issue on Polymer and Fiber Recycling*. Polymer-Plastics Technology and Engineering, 1999. **38**(3).
29. C. Hagberg. and J. Dickerson, *Recycling Nylon Carpet via Reactive Extrusion*. Plastics Engineering, 1997: p. 41-43.
30. Chen, T., *Recycling Carpet Waste by Reactive Extrusion*, in *School of Polymer, Textile, and Fiber Engineering*. 1996, Georgia Institute of Technology: Atlanta.
31. Morn Jr. and Mckinney, *Conversion of Nylon 6 and/or Nylon 6,6 to Adipic Acid*, in *U.S. Patent 5,468,900*. November 1995.
32. Mckinney, R., *Lewis Acid Catalyzed Ammonolysis of Nylon*, U.S. Patent 5, 974, Editor. March 1995.
33. Hagguist and Hume, *Carpet reclaimer*, in *U.S. Patent 5,230,473*. July 1993.
34. Wang, Y., *Utilization of Recycled Carpet Waste Fibers for Reinforcement of Concrete and Soil*. Polymer-Plastics Technology and Engineering, 1999. **38**(3): p. 533-546.
35. Datta, Polk, and Kumar, *Reactive Extrusion of Polypropylene and Nylon*. Polymer-Plastics Technology and Engineering, 1995. **34**(4): p. 551.
36. Muzzy, J., *Personal Communication*, A. Cascio, Editor. 2004, Georgia Tech: Atlanta, Georgia. Recycling Methods

37. Cooper, S., Atkins, E., Hill, M., *Temperature-Induced Changes in Lamellar Crystals of Monodisperse Nylon 6 and Nylon 6 6 Oligoamides*. *Macromolecules*, 1998. **31**: p. 8947-8956.
38. Hudacek, L., *How to Optimize Adhesion in Hard-Soft Overmolding*, in *Plastics Technology*.
39. Colback. *Premium Carpet Backing*. [cited 2006 February 14]; Available from: <http://www.colback.net/Why2.htm>.
40. Hartmann and Ruzek, *Carpet with non-woven backing*, in *U.S. Patent 4,172,166*. October 1979.
41. Hartmann and Ruzek, *Process for the manufacture of heat shaped automobile carpet*, in *U.S. Patent 4,169,176*. September 1979.
42. Hartman, D., *Personal Communication*, A. Cascio, Editor. 2005, Owens Corning: Columbus, Ohio. Non-Woven Glass Backings.
43. DuPont, *Elvamide, nylon multipolymer resins*, in *Adhesives Guide*. 2000.
44. *Standard Test Method for Breaking Force and Elongation of Textile Fabrics (Strip Method)*, in *ASTM D 5035-95*. 1995: American Society for Testing and Materials.
45. *Standard Practice for Conditioning and Testing Textiles*, in *ASTM D 1776*. 2000: American Society for Testing and Materials.
46. *Standard Test Method for Resistance to Delamination of the Secondary Backing of Pile Yarn Floor Covering*, in *ASTM D 3936-97*. 1997: American Society for Testing and Materials.
47. *Standard Test Method for Air Permeability of Textile Fabrics*, in *ASTM D 737-04*. 2004: American Society for Testing and Materials.
48. *Standard Test Method For Tuft Bind of Pile Yarn Floor Coverings*, in *ASTM D 1335-98*. 2000: American Society for Testing and Materials.

49. *Standard Test Method for Critical Radiant Flux of Floor-Covering Systems Using a Radiant Heat Energy Source*, in *ASTM E 648 – 04*. 2004: American Society for Testing and Materials.
50. Buitenhoff, A., *Personal Communication*, A. Cascio, Editor. 2004, Shaw Industries, Inc.: Dalton, Georgia. Radiant Panel Flammability Test Description.
51. *Standard Test Method for Ignition Characteristics of Finished Textile Floor Covering Materials*, in *ASTM D 2859 – 04*. 2004: American Society for Testing and Materials.
52. *Determination of the Effects of a Small Source of Ignition on Textile Floor Coverings*, in *Hot Metal Nut Method*. 2004: British Standards.
53. *Standard Test Method for Thermal Transmittance of Textile Materials*, in *ASTM D 1518-85*. 2003: American Society for Testing and Materials.
54. *Flammability and Carpet Safety*. CRI Technical Bulletin. 1998: The Carpet and Rug Institute.
55. Ozcan, Dayioglu, and Cevza, *Effect of gray fabric properties on flame resistance of knitted fabric*. Textile Research Journal, 2003(October).
56. Settle, *Assessment of draft ISO radiant panel spread-of-flame test*. Fire and Materials, 1979. **3**(3): p. 171-181.
57. Culimeta, *Safety Data Sheet E-Glass TDB025E*. 2001, Culimeta Textilglas Technologie.
58. Khanna, Y.P., *Dynamic melt rheology. I: Re-examining dynamic viscosity in relationship to the steady shear flow viscosity*. Polymer Engineering & Science, 1991. **31**(6): p. 440-444.
59. Patel and Lee, *Influence of processing and material variables on resin-fiber interface in liquid composite molding*. Polymer Composites, 1993. **14**(2): p. 161-172.

60. Shah and Yazbak, *A study of the effect of the extrusion variables and screw design on the thermal and rheological characteristics of acetal and nylon 66*. Polymer Engineering & Science, 1994. **34**(15): p. 1196-1201.
61. *Selecting Carpet & Rugs*. The Carpet and Rug Institute 2006 [cited 2006; Available from: http://www.carpet-rug.com/drill_down_2.cfm?page=13&sub=3.
62. Watzl, A., *Latex-Free Tufted Carpets*. Textile World, 2004. **154**(11): p. 40-41.
63. Rong, H., Kotra, R. *WET-LAIDNONWOVENS*. [Website] 2004 [cited 2005]; Available from: <http://www.engr.utk.edu/mse/pages/Textiles/Wet%20Laid%20Nonwovens.htm>.
64. Crawshaw, G.H., *Carpet Manufacture*. 2002: Wronz Developments.
65. Aspland, J.R., *Dyeing Nylon with Acid Dyes*, in *Textile Dyeing and Coloration*. 1997, American Association of Textile Chemists and Colorists. p. 258-272.
66. Tincher, W., Beckham, H., Cook, F., Cascio, A., *Textile Chemistry Laboratory Manuel*. 2005, Atlanta: School of Polymer, Textile and Fiber Engineering.
67. *Colortec Small Package, Beam and Loose Fibre Dyeing Machine* [cited 2006 March 22]; Available from: <http://www.roaches.co.uk/package-dyeing.html>.
68. Cook, F., *Personal Communication*, A. Cascio, Editor. 2005, Georgia Tech: Atlanta, Georgia. Pad-Steam dyeing.
69. Odian, G., *Principles Of Polymerization*. 4 ed. 2004, N.J.: Wiley-Interscience. 305-306.
70. Incropera, F., DeWitt, D., *Fundamentals of Heat and Mass Transfer*. Fifth ed. 2002: John Wiley and Sons. 57-58; 924-925.
71. Wallia, Gupta, and Kiang, *Influence of Interchange Reactions on the crystallization and Melting Behavior of Nylon 6,6 Blended With Other Nylons*. Polymer Engineering and Science, 1999. **39**(12): p. 2431-2444.

72. Fowler, G., *Personal Communication*, A. Cascio, Editor. 2005, Shaw Industries, Inc.: Dalton, Georgia. Tufting of Backing ***A***, ***B***, and ***C***.